

**Impacts of Spinal Cord Injury and Formulation on  
Riluzole Pharmacokinetics and  
Pharmacokinetics/Pharmacodynamics (PK/PD)  
Correlation**

A Dissertation Presented to the

Faculty of the Department of Pharmacological and Pharmaceutical Sciences

College of Pharmacy, University of Houston

In Partial Fulfillment of

the Requirements for the Degree of

Doctor of Philosophy

By

Yang (Angela) Teng

December, 2012

## **ACKNOWLEDGEMENTS**

First and foremost, I would like to express my sincere appreciation and gratitude to my advisor, Dr. Diana S-L. Chow, for her guidance, scientific training and mentorship during the pursuit of my Ph.D. degree. Dr. Chow not only offers the scientific guidance and expertise to direct my research work, but also sets up a perfect example as a caring educator and dedicated scientist, which will be an inspiration to me during my life.

I would also like to sincerely thank my committee members, Dr. Robert G. Grossman who gave me many advices on my project, especially the part of PK-PD correlation, Dr. Vincent Tam helped me construct the co-model using Adapt II®, Dr. Douglas Eikenburg and Dr. Dong Liang for their continuous support and valuable advices.

I would like to acknowledge Dr. Keith D. Barau and Dr. Ralph F. Frankowski of University of Texas School of Public Health for providing the information of all the patients enrolled in the Phase I Clinical Trial. My special thanks go to collaborators, Dr. Michael G. Fehlings from University of Toronto for providing preclinical samples of control uninjured and acute spinal cord injured rats, as well the collaborators from six clinical sites for providing clinical patients' samples in time.

I have the pleasure to express my deepest appreciation to my husband, Zhen Yang for his advice, support, and love during the long journey. I am especially grateful to my

parents, Weiguang Teng and Ying Yang, for their encouragement and support of my pursuit for the highest education.

Finally, I would like to thank all the members of Dr. Diana Chow's lab for their helps of my study, especially to Dong Dong, Tanay Samant, Lei Wu, Lili Cui, Stanley Hsiao, and Jie He. I must also thank all the members of PPS Department at the University of Houston for providing me with the opportunity and environment to pursue my studies.

## **ABSTRACT**

Acute Spinal Cord injury (SCI) is a complex disorder involving a sudden traumatic insult to the cord resulting in deficits to ambulatory, sensory and autonomic function. At present, no effective acute treatment or rehabilitative therapy exists. Recently, several studies show that Riluzole has neuroprotective effect and promotes functional and neurological recoveries in animal models of brain and spinal cord ischemic and traumatic injuries; however, hepatotoxicity is a significant side effect concern for this therapy. Therefore, pharmacokinetic (PK) and pharmacodynamic (PD) study of Riluzole is of great importance for us to understand its toxicity and efficacy in acute SCI patients.

We hypothesize that spinal cord injury and formulation/administration alteration would affect the pharmacokinetics of Riluzole, and PK/PD studies would enable us to establish the correlation of Riluzole concentration/exposure with its toxicity and efficacy outcomes. Our project has three specific aims: 1) To investigate whether the change of formulation/administration would alter the PK of Riluzole. The rat model was used and different formulations of Riluzole were administered (oral: crushed tablet, crushed paste, crushed paste with glycerin, suspension and solution; i.v.: solution). The PK of Riluzole in different treatment groups would be characterized and compared. 2) To explore the impact of SCI on Riluzole PK. Spinal cord injured and non-injured control rats were used to establish the impacts of acute SCI on Riluzole PK by monitoring PK profiles of Riluzole in plasma, brain and spinal cord after single and multiple doses. 3) To characterize individual and population PK of Riluzole and establish PK/PD correlation of

Riluzole in terms of concentration/exposure with its toxicity and efficacy in acute SCI patients. Thirty-five individuals with acute SCI, American Spinal Injury Association (ASIA) Impairment Scale (AIS) Grades A-C, neurological levels from C-4 to T-12, who were enrolled in the Phase 1 clinical trial sponsored by the North American Clinical Trial Network (NACTN) for the treatment of SCI, received 50 mg Riluzole twice daily for 28 doses. The first dose was administered at a mean of  $8.7 \pm 2.2$  hours post-injury. Trough plasma samples were collected within 1 hour pre-dose, and peak plasma samples were collected 2 hours post-dose on Day 3 and 14 of treatment. The data were analyzed for individual and population PK using basic structural and covariate models. The PK measures studied were the peak concentration ( $C_{max}$ ), trough concentration ( $C_{min}$ ), systemic exposure ( $AUC_{0-12}$ ), clearance (CL/F), and volume of distribution (V/F) normalized by the bioavailability (F). Linear and logistic regressions were used to establish the PK/PD correlations of Riluzole in acute SCI patients. Riluzole concentrations were quantified by a validated high-performance liquid chromatographic with UV detection assay.

In animal models, the alteration of formulation from crushed tablet to liquid increased the bioavailability of Riluzole, but did not affect its intrinsic PK characteristics; Acute SCI resulted in higher plasma, brain and spinal cord concentrations in acute phase of SCI after multiple I.P. doses, which was due to a slower elimination caused by an impaired hepatic clearance.

In acute SCI patients, the  $C_{max}$  and  $AUC_{0-12}$  of Riluzole were lower than those in ALS patients on the same dose basis, due to a higher CL and a larger V. The PK of Riluzole ( $C_{max}$ ,  $C_{min}$ ,  $AUC_{0-12}$ , CL/F, and V/F) changed during the acute and subacute phases of SCI in the 14 days of therapy. It was consistently observed in patients at all clinical sites that  $C_{max}$ ,  $C_{min}$ , and  $AUC_{0-12}$  (128.9 ng/ml, 45.6 ng/ml, and 982.0 ng\*hr/ml, respectively) were significantly higher on Day 3 than on Day 14 (76.5 ng/ml, 19.1 ng/ml, and 521.0 ng\*hr/ml, respectively). These changes resulted from a lower CL (49.5 vs 106.2 L/hour) and a smaller V (557.1 vs 1297.9 L) on Day 3. Neither fluid imbalance nor cytochrome P 1A2 induction due to concomitant medications was identified during the treatment course to account for such increases in V and CL on Day 14, respectively. Possible mechanisms underlying these changes are discussed. The changes of motor and sensory scores at 3-month follow-up had good correlation with Day 3 AUC/kg. The establishments of PK-PD correlation could be used to predict the PD outcomes in the future clinical trial.

## List of Tables

Table 1	Spinal Cord Injury Phases and Key Pathological Events.....	9
Table 2	Key Muscles Used for ASIA Motor Score Assessment, with Muscle Grades Categorizing Functional Assessment of Each Muscle's Contraction.....	29
Table 3	Classification of ASIA Impairment Scale (AIS).....	33
Table 4	Accuracy, Precision and Recovery of Riluzole HPLC Assay at Levels of 15.6, 125 and 1,000 ng/ml for Rat Plasma Samples and at Levels of 62.5, 500 and 4,000 ng/g for Rat Brain and Spinal Cord Samples (N = 15) .....	89
Table 5	Accuracy, Precision and Recovery of Riluzole HPLC Assay at Levels of 15.6, 125 and 1,000 ng/ml for Human Plasma Samples and at Two Concentration Levels (62.5 and 1,000 ng/ml) Levels for Human CSF Samples (N = 15 for Plasma Samples; N = 18 for CSF Samples) .....	90
Table 6	Stability (% Remaining) of Riluzole in Human Plasma and CSF Samples, at Room Temperature, after Repeated Freeze-thaw and Long-term Storage (N = 3 for Each Condition).....	92
Table 7	Calibration Curves of Riluzole of CSF with Different Protein Concentrations [LP Samples (53.9 mg/dl, IP Samples (142.2 mg/dl and HP Samples (348.2 mg/dl)] (N = 2 for IP Group; N = 5 for LP and HP Groups).....	94
Table 8	Comparisons of Accuracies and Precisions Using Individual and Pooled Calibration Curves (N = 6 for Individual Curve; N = 18 for Pooled Curve) .....	95
Table 9	Pharmacokinetic Parameters of Riluzole After Oral Administrations (10 mg/kg) of Crushed Tablet, Crushed Paste, Suspension and Solution, and I.V. Administration (5 mg/kg) of Riluzole Solution in Sprague-Dawley Rats (N = 3-5 for Each Group; * indicates $p < 0.05$ ) .....	98
Table 10	Pharmacokinetic Parameters of Riluzole in Plasma, Brain and Spinal Cord Samples between Uninjured Control Group and Cervical Spinal Cord Injured (SCI) Group after Single I.P. Administration of 8 mg/kg.....	102
Table 11	Pharmacokinetic Parameters of Riluzole Derived by ADAPT II Model between Uninjured Control and Cervical Spinal Cord Injured (SCI) Rats after Single I.P. Administration of 8 mg/kg .....	113
Table 12	Comparisons of Observed Riluzole Concentrations vs. Predicted Riluzole Concentrations by Simulation in Plasma, Brain and Spinal Cord of Uninjured Control Group after 2 and 6 I.P. Doses.....	120
Table 13	Comparisons of Observed Riluzole Concentrations vs. Predicted Riluzole Concentrations by Simulation in Plasma, Brain and Spinal Cord of Cervical SCI Group after 2 and 6 I.P. Doses.....	123

Table 14	Comparisons of Observed Riluzole Concentrations vs. Predicted Riluzole Concentrations by Simulation in Plasma, Brain and Spinal Cord in Cervical SCI Group after 2 and 6 I.P. Doses after Decreased Elimination Rate Constant to Half Value ( $k_{20}=0.33/2=0.17$ ) .....	127
Table 15	Demographics of Patients .....	132
Table 16	Pharmacokinetic Parameters of Riluzole in Spinal Cord Injured Patients and Healthy Volunteers* (*: Mean Values are $\pm$ SE).....	138
Table 17	Comparison of Population and Individual Pharmacokinetic Parameters of Riluzole on Day 3 and Day 14* (*: Mean Values are $\pm$ SE).....	140
Table 18	Forward and Backward Steps for Covariate Model of Riluzole .....	142
Table 19	Pharmacokinetic Parameters of Riluzole in Acute SCI Patients on Day 3 and Day 14 .....	143
Table 20	Attempts of PK-PD Correlations ( $p < 0.05$ indicates correlation established).....	153
Table 21	Comparisons of Riluzole Exposures ( $AUC_{0-12}$ ) for the Patients Taking Oral Tablet, Nasogastric Paste and Mixture of Tablet and Paste .....	165
Table 22	Comparisons of Riluzole Exposures ( $AUC_{0-\infty}$ ) for the Patients Taking Oral Tablet, Nasogastric Paste and Mixture of Tablet and Paste .....	166
Table 23	Morphological and Physiological Differences between the BBB and BSCB .....	171
Table 24	Comparison of Population Pharmacokinetic Parameters in Acute Spinal Cord Injured Patients versus Patients with Amyotrophic Lateral Sclerosis (ALS) and Spinal Muscular Atrophy (SMA) .....	177

## List of Figures

Figure 1	Anatomy of Spinal Cord .....	3
Figure 2	Spinal Cord Nerve Levels .....	5
Figure 3	Chemical Structure and Physical-chemical Properties of Riluzole.....	15
Figure 4	Metabolic Pathways Involved in Phase I Biotransformation of Riluzole.....	19
Figure 5	Assessments of ASIA Sensory Score .....	31
Figure 6	Chemical Structures of Riluzole and 5-Methoxypsoralen (5-MOP, Internal Standard).....	47
Figure 7	Final Model Structure of Riluzole in Plasma, Brain and Spinal Cord Built by ADAPT II. ....	62
Figure 8	3D Diagram of the UV Absorbance of Riluzole from 200 to 400 nm.....	78
Figure 9	2D Diagram of the UV Absorbance of Riluzole from 200 to 400 nm.....	79
Figure 10	Authentic HPLC Chromatograms of Extracts from (A) Blank Human Plasma, (B) Spiked Plasma Sample, (C) Blank Human CSF, and (D) Spiked CSF Sample .....	81
Figure 11	Authentic HPLC Chromatograms of Extracts of (A) Blank Spinal Cord, (B) Spiked Spinal Cord Sample at LLOQ (31.25 ng/g) and (C) Spiked Spinal Cord Sample at 4,000 ng/g .....	84
Figure 12	Authentic HPLC Chromatograms of Extracts of (A) Blank Brain, (B) Spiked Brain Sample at LLOQ (31.25 ng/g) and (C) Spiked Brain Sample at 4,000 ng/g .....	84
Figure 13	Authentic HPLC Chromatograms of Extracts of (A) Blank Plasma, (B) Spiked Plasma Sample at LLOQ (7.8 ng/g) and (C) Spiked Plasma Sample at 1,000 ng/g .....	84
Figure 14	HPLC Chromatogram of Riluzole and Internal Standard (I.S.) for Samples with Concomitant Medications of Acetaminophen, Baclofen, Hydrocortisone, Methylprednisolone (MPSS) and Midazolam .....	85
Figure 15	Calibration Curves of Riluzole for Rat (A) Spinal Cord, (B) Brain and (C) Plasma Samples .....	87
Figure 16	Representative HPLC Calibration Curve of Riluzole in Human Plasma .....	88
Figure 17	Mean Plasma Concentrations/Dose-time Profiles of Riluzole after Oral and I.V. Administrations in Rats (N =3-5 for Each Group).....	97
Figure 18	Pharmacokinetic Profiles of Riluzole in Rat Plasma, Brain and Spinal Cords (Cervical and Thoracic Segments) after Single I.P. Administration (8 mg/kg)	

	(A) Uninjured Control and (B) Cervical Spinal Cord Injured (SCI) Rats (N = 4 for Each Time Point, Mean $\pm$ SD) (a indicates significantly lower than those in cervical and thoracic spinal cord; b indicates significantly lower than those in cervical, thoracic spinal cord and brain; c indicates lower than those in cervical and thoracic spinal cord, but higher than that in plasma)..	101
Figure 19	Comparisons of Riluzole Pharmacokinetic Profiles between SCI and Uninjured Rats after Single I.P. Dose of 8 mg/kg (A) Plasma, (B) Brain, (C) Cervical Spinal Cord and (D) Thoracic Spinal Cord (n=4 for at Each Time Point, Mean $\pm$ SD; * indicates $p < 0.05$ ) .....	103
Figure 20	Comparisons of Riluzole Concentrations between Uninjured Control and Cervical SCI Rats in Plasma, Brain, Cervical and Thoracic Spinal Cords after Two I.P. Doses Every 12 Hours (n=4 for Each Group, Mean $\pm$ SD; * indicates $p < 0.05$ ) .....	104
Figure 21	Comparisons of Riluzole Concentrations between Uninjured Control and Cervical SCI Rats in Plasma, Brain, Cervical and Thoracic Spinal Cords after Six I.P. Doses Every 12 Hours for 3-day Treatment (n=4 for Each Group, Mean $\pm$ SD; * indicates $p < 0.05$ ) .....	105
Figure 22	Profiles of Partition Coefficients (Kp) of Riluzole from Plasma to Brain and Spinal Cords for Uninjured Control and Cervical SCI Rats .....	109
Figure 23	Model Fitting of Riluzole Concentration vs. Time Profiles in Plasma, Brain and Spinal Cord after Single I.P. Dose of 8 mg/kg for Uninjured Control Group .....	115
Figure 24	Model Fitting of Riluzole Concentration vs. Time Profiles in Plasma, Brain and Spinal Cord after Single I.P. Dose of 8 mg/kg for Cervical SCI Group..	116
Figure 25	Predicted Riluzole Concentration Profiles in Plasma, Brain and Spinal Cord after 2 I.P. Doses (8 mg/kg+ 6 mg/kg, q 12 hr) for Uninjured Control Group (N = 4 at Each Time Point for Observed Concentrations) .....	118
Figure 26	Predicted Riluzole Concentration Profiles in Plasma, Brain and Spinal Cord after 6 I.P. Doses (First Loading Dose of 8 mg/kg, Followed by 6 mg/kg, q 12 hr) for Uninjured Control Group (N = 4 at Each Time Point for Observed Concentrations) .....	119
Figure 27	Predicted Riluzole Concentration Profiles in Plasma, Brain and Spinal Cord after 2 I.P. Doses (8 mg/kg+ 6 mg/kg, q 12 hr) for Cervical SCI Group (N = 4 at Each Time Point for Observed Concentrations) .....	121
Figure 28	Predicted Riluzole Concentration Profiles in Plasma, Brain and Spinal Cord after 6 I.P. Doses (First Dose Loading of 8 mg/kg, Followed by 6 mg/kg, q 12 hr) for Cervical SCI Group (N = 4 at Each Time Point for Observed Concentrations) .....	122
Figure 29	Predicted Riluzole Concentration Profiles in Plasma, Brain and Spinal Cord after 2 I.P. Doses (8 mg/kg+ 6 mg/kg, q 12 hr) for Cervical SCI Group after	

	Decreased Elimination Rate Constant to Half of the Value ( $k_{20} = 0.33/2 = 0.17$ ) (N = 4 at Each Time Point for Observed Concentrations).....	125
Figure 30	Predicted Riluzole Concentration Profiles in Plasma, Brain and Spinal Cord after 6 I.P. Doses (First Loading Dose of 8 mg/kg, Followed by 6 mg/kg, q 12 hr) for Cervical SCI Group after Decreased Elimination Rate Constant to Half of the Value ( $k_{20} = 0.33/2 = 0.17$ ) (N = 4 at Each Time Point for Observed Concentrations) .....	126
Figure 31	Correlations of Riluzole Concentrations in Brain and Spinal Cord vs. Plasma Concentrations. for both Control and Injured Groups after Single I.P. Dose of 8 mg/kg.....	129
Figure 32	Correlations of Riluzole Concentrations in Brain and Spinal Cord vs that in Plasma for Both Control and Injured Groups after Multiple I.P. Doses .....	130
Figure 33	Typical Pharmacokinetic Profiles of Riluzole in Human Plasma Samples on Day 3 and Day 14.....	134
Figure 34	Spaghetti Plots of (A) $C_{max}$ , (B) $C_{min}$ and (C) $AUC_{0-12}$ on Day 3 and Day 14	135
Figure 35	Spaghetti Plots of (A) Clearance (CL/F) and (B) Volume of Distribution (V/F) on Day 3 and Day 14.....	137
Figure 36	Goodness Fit of Plots. Population PK Predicted and Individual PK Predicted Riluzole Concentrations vs. Observed Riluzole Concentrations on (a) Day 3 and (b) Day 14.....	144
Figure 37	Scatter Plots of Motor and Sensory Scores vs. Follow-up Examinations (* indicates $p < 0.05$ ).....	147
Figure 38	Scatter Plots of the Changes of Motor and Sensory Scores at the Last Follow-up Examination (3-month or 6-month follow-ups) vs. First Dosing Time .....	148
Figure 39	Scatter Plots of the Changes of Motor and Sensory Scores at the Last Follow-up Examination (3-month or 6-month follow-ups) vs. ASIA Impairment Scale (AIS) (* indicates $p < 0.05$ ) .....	150
Figure 40	Scatter Plots of the Changes of Motor and Sensory Scores at the Last Follow-up Examination (3-month or 6-month follow-ups) vs. Position of Spinal Cord Injury (* indicates $p < 0.05$ ).....	151
Figure 41	PK-PD Correlations of Changes of Motor and Sensory Scores at 3-month Follow-up with Riluzole Day 3 $AUC_{0-12}/kg$ (N = 16 for Correlation of Change of Motor Score; N = 20 for Correlation of Change of Sensory Score).....	154
Figure 42	Correlations of Day 3 ULN Ratios of ALT and AST with Riluzole Day 3 $AUC_{0-12}/kg$ (N =20) .....	155
Figure 43	Plasma and Brain Pharmacokinetic Profiles of Riluzole Given by I.P. Route to CF1 <i>mdr1a</i> (+/+) Mice (10 mg/kg; n=3 mice per time point, Mean $\pm$ SD). 168	

Figure 44 Brain and Plasma AUC<sub>0-∞</sub> Achieved After Administration of Riluzole (5, 10, 20 mg/kg) by I.P. Route to CF1 mdr1a (+/+) Mice and at 10 mg/kg by I.P. Route to CF1 mdr1a (-/-) Mice (n=27 mice/dose)..... 169

## List of Abbreviations

ALT	Alanine Aminotransferase
AST	Aspartate Aminotransferase
AIC	Akaike's Information Criterion
AIS	ASIA Impairment Scale
ALS	Amyotrophic Lateral Sclerosis
ASIA	American Spinal Injury Association
AUC	Area Under the Curve
BBB	Blood-Brain Barrier
BSCB	Blood-Spinal Cord Barrier
C <sub>max</sub>	Peak Plasma Concentration
CL	Clearance
CL/F	Clearance Normalized by Bioavailability
CL <sub>H</sub>	Hepatic Clearance
CNS	Central Nervous System
CSF	Cerebral Spinal Fluid
CYP	Cytochrome P (CYP) 450
F	Bioavailability
FOCEI	First-Order Conditional Estimation Method with $\eta$ - $\epsilon$ Interaction
f <sub>u</sub>	Fraction Unbound
GGT	Gamma Glutamyl Transpeptidase
HBV	Hepatitis B Virus

HCV	Hepatitis C Virus
HED	Human Equivalent Dose
HP	High Protein Level
HP- $\beta$ -CD	2-Hydroxypropyl- $\beta$ -Cyclodextrin
HPLC	High Performance Liquid Chromatography
HPLC-UV	High Performance Liquid Chromatography with Ultraviolet Detector
INR	International Normalized Ratio
I.P.	Intraperitoneal
IP	Intermediate Protein Level
I.S.	Internal Standard
i.v.	Intravenous
k	Elimination Rate Constant
ka	Absorption Rate Constant
kp	Tissue/Plasma Partition Coefficient
LC/MS/MS	Liquid Chromatography-Mass Spectroscopy
LEMS	Lower Extremity Motor Score
LLOQ	Lower Limit of Quantification
LP	Low Protein Level
5-MOP	5-Methoxypsoralen
MPSS	Methylprednisolone
MVBF	Microvascular Blood Flow
NACTN	North American Clinical Trial Network
NG	Nasogastric Tubing

NMDA	N-Methyl-D-Aspartate
PK	Pharmacokinetics
PK/PD	Pharmacokinetic/Pharmacodynamic
P.O.	Oral
PT	Prothrombin Time
ROS	Reactive O <sub>2</sub> Species
SCI	Spinal Cord Injury
SD	Sprague-Dawley
T <sub>1/2</sub>	Half-Life
T <sub>max</sub>	Time to Reach Peak Concentration
UEMS	Upper Extremity Motor Score
ULN	Upper Limit of Normal Range
V	Volume of Distribution
V/F	Volume of Distribution Normalized by Bioavailability

# CONTENTS

ACKNOWLEDGEMENTS .....	i
ABSTRACT .....	iii
List of Tables .....	vi
List of Figures .....	viii
List of Abbreviations .....	xii
CHAPTER 1. LITERATURES .....	1
1.1 Spinal Cord Injury (SCI) .....	1
1.1.1 Spinal Cord Anatomy .....	1
1.1.2 Spinal Nerves .....	2
1.1.3 Spinal Cord Nerve Levels .....	4
1.1.4 Epidemiology of SCI .....	6
1.1.5 Pathophysiology of SCI .....	6
1.2 Riluzole .....	14
1.2.1 Mechanism of Action of Riluzole .....	14
1.2.2 Pharmacokinetics of Riluzole .....	17
1.2.3 Toxicity of Riluzole .....	21
1.2.4 Alterations of Pharmacokinetics of Drugs in SCI .....	21
1.2.5 Phase I Clinical Trial of Riluzole in SCI Patients .....	24
1.2.6 Rationale of Dose Selected and Treatment Duration of Riluzole for SCI Patients .....	26
1.3 Safety and Efficacy Evaluations of Riluzole Phase I Clinical Trial .....	27

1.3.1 Safety.....	27
1.3.2 Efficacy .....	27
1.3.2.1 ASIA Motor Score.....	28
1.3.2.2 ASIA Sensory Score.....	30
1.3.2.3 ASIA Impairment Scale (AIS) .....	32
CHAPTER 2. OBJECTIVES AND SPECIFIC AIMS.....	34
2.1 Hypothesis.....	34
2.2 Objectives.....	34
2.3 Specific Aims .....	35
CHAPTER 3. MATERIALS AND METHODS.....	38
3.1 Materials .....	38
3.1.1 Chemicals and Materials.....	38
3.1.2 Supplies .....	40
3.1.3 Equipment, Apparati and Softwares .....	42
3.2 Methods.....	44
3.2.1 HPLC Assay.....	44
3.2.1.1 Rationale .....	44
3.2.1.2 Stock Solutions and Standards .....	45
3.2.1.3 Chromatographic Apparatus and Conditions .....	48
3.2.1.4 Sample Preparations.....	48
3.2.1.5 Effects of Different CSF Protein Concentrations on Recovery and Accuracy of Quantification of CSF Samples .....	50
3.2.1.6 Validation Process.....	50
3.2.2 Pharmacokinetics of Different Formulations in Rats .....	54
3.2.2.1 Rationale .....	54
3.2.2.2 Dosing of Riluzole of Different Formulations .....	54
3.2.2.3 Pharmacokinetic Analysis .....	55
3.2.2.4 Statistical Analysis.....	58
3.2.3 Impacts of Acute Spinal Cord Injury on Riluzole Pharmacokinetics in Rats ...	58

3.2.3.1 Rationale .....	58
3.2.3.2 Pharmacokinetic Studies .....	59
3.2.3.3 Pharmacokinetic Analysis .....	60
3.2.3.4 Statistical Analysis.....	64
3.2.4 Phase I Clinical Trial of Riluzole in Acute Spinal Cord Injured Patients.....	65
3.2.4.1 Rationale .....	65
3.2.4.2 Criteria of Patient Selection.....	65
3.2.4.3 Treatment with Riluzole (Rilutek®).....	67
3.2.4.4 Plasma Protein Binding .....	67
3.2.4.5 Pharmacokinetic Analysis .....	67
3.2.4.6 Monitoring of Potential Hepatotoxicity and Metabolic Status .....	74
3.2.4.7 Monitoring of Efficacy .....	75
3.2.4.8 Pharmacokinetic/Pharmacodynamic (PK/PD) Correlations.....	76
CHAPTER 4. RESULTS .....	77
4.1 HPLC Assay .....	77
4.1.1 UV Spectrum.....	77
4.1.2 HPLC Assay Validation.....	80
4.1.2.1 HPLC Chromatogram.....	80
4.1.2.2 Linearity.....	80
4.1.2.3 Recovery, Accuracy and Precision.....	87
4.1.2.4 Stability.....	91
4.1.3 Effects of CSF Protein on Recovery and Accuracy of the Quantification of CSF Samples.....	93
4.2 Pharmacokinetics of Riluzole from Different Formulations in Rats.....	96
4.3 Impacts of Acute Spinal Cord Injury on Riluzole Pharmacokinetics in Rats .....	100
4.3.1 Single-Dose Treatment of Riluzole .....	100
4.3.1.1. Uninjured Control Group .....	100
4.3.1.2. Cervical Spinal Cord Injured Group.....	106
4.3.1.3. Comparative Tissue/Plasma Partition Coefficients of Riluzole.....	108
4.3.2 Multiple-Dose Treatment of Riluzole.....	108
4.3.2.1. Uninjured Control Group .....	108
4.3.2.2. Cervical Spinal Cord Injured Group.....	110

4.3.3 Three-compartment Model of Riluzole by ADAPT II After Single Dose .....	112
4.3.4 Evaluations of ADAPT II Model.....	117
4.3.5 Correlations of Riluzole Concentrations in Brain and Spinal Cord with Concentrations in Plasma .....	128
4.4 Phase I Clinical Trial of Riluzole in Acute Spinal Cord Injured Patients .....	131
4.4.1 Patient Demographics.....	131
4.4.2 Distinct Alterations of Riluzole Pharmacokinetics in SCI Patients during Two- week Period Post-injury .....	133
4.4.3 Individual and Population Pharmacokinetic Parameters.....	139
4.4.4 Plasma Protein Binding.....	141
4.4.5 Safety Data .....	145
4.4.6 Efficacy Evaluations.....	146
4.4.7 Pharmacokinetic/pharmacodynamic (PK/PD) Correlations .....	152
DISCUSSION .....	156
5.1 HPLC Assay .....	161
5.2 Different Formulations of Riluzole in Rats .....	163
5.3 Impacts of SCI on Riluzole Pharmacokinetics in Rats.....	167
5.3.1 Single I.P. Dose of Riluzole .....	167
5.3.2 Multiple I.P. Doses of Riluzole .....	173
5.3.3 Correlations of Riluzole Concentrations in Central Nervous Tissues with Those in Plasma .....	175
5.4 Phase I Clinical Trial of Riluzole in Acute SCI Patients .....	176
5.4.1 Distinct Alterations of Riluzole Pharmacokinetics in Acute SCI Patients .....	176

5.4.2 Pharmacodynamics of Riluzole.....	180
5.4.3 PK/PD Correlations of Riluzole .....	181
SUMMARY .....	183
6.1 HPLC Assay .....	183
6.2 Pharmacokinetics of Different Formulations in Rats.....	183
6.3 Impacts of SCI on Riluzole Pharmacokinetics in Rats.....	184
6.4 Phase I Clinical Trial of Riluzole in Acute SCI Patients .....	185
6.4.1 Distinct Alterations of Riluzole Pharmacokinetics in SCI Patients .....	185
6.4.2 Individual and Population Pharmacokinetic Parameters.....	186
6.4.3 Safety.....	187
6.4.4 Efficacy Outcomes .....	187
6.4.5 PK/PD Correlations.....	188
Bibliography .....	189

# **CHAPTER 1. LITERATURES**

## **1.1 Spinal Cord Injury (SCI)**

### **1.1.1 Spinal Cord Anatomy**

The spinal cord has a core of tissue containing nerve cells that extends from the brain (the medulla oblongata specifically), surrounded by long tracts of nerve fibers consisting of axons and protected by the bony vertebral column (Figure 1). The spinal cord is also surrounded by a clear fluid called Cerebral Spinal Fluid (CSF), that acts as a cushion to protect the delicate nerve tissues against damage from banging against the inside of the vertebrae.

The anatomy of the spinal cord itself, consists of millions of nerve fibers which transmit electrical information to and from the limbs, trunk and organs of the body, from and back to the brain. The nerves which exit the spinal cord in the upper section, the neck, control breathing and the arms. The nerves which exit the spinal cord in the mid and lower section of the back, control the trunk and legs, as well as bladder, bowel and sexual function.

The nerves which carry information from the brain to muscles are called Motor Neurons. The nerves which carry information from the body back to the brain are called Sensory Neurons. Sensory Neurons carry information to the brain about skin temperature, touch, pain and joint position.

The brain and spinal cord are referred to as the Central Nervous System (CNS), whilst the nerves connecting the spinal cord to the body are referred to as the Peripheral Nervous System. The spinal cord is the main pathway for information connecting the brain and peripheral nervous system.

### **1.1.2 Spinal Nerves**

Spinal nerves branch off the spinal cord and pass out through a hole in each of the vertebrae called the Foramen. These nerves carry information from the spinal cord to the rest of the body and from the body back up to the brain.

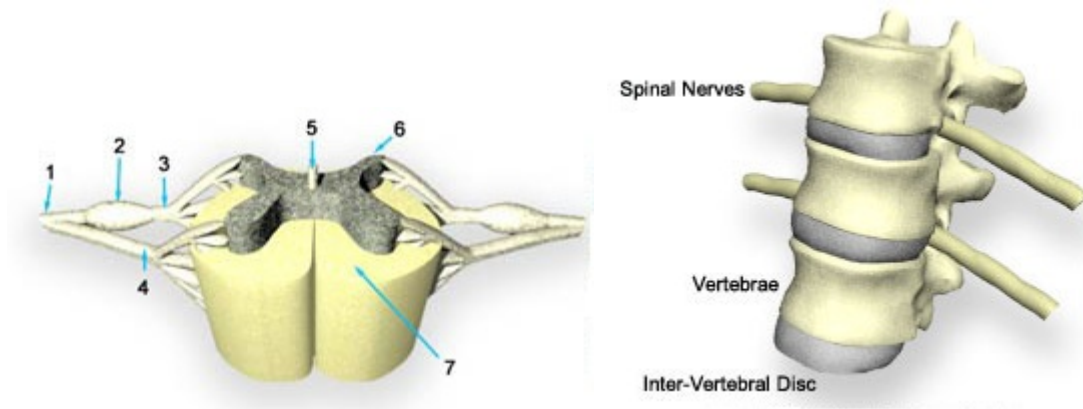
There are four main groups of spinal nerves, which exit from different levels of segments of the spinal cord.

These are in descending order down the vertebral column:

Cervical Nerves "C" : (nerves in the neck) supply movement and feeling of the arms, neck and upper trunk, as well as control breathing.

Thoracic Nerves "T" : (nerves in the upper back) supply movement and feeling of the trunk and abdomen.

Lumbar Nerves "L" and Sacral Nerves "S" : (nerves in the lower back) supply movement and feeling of the legs, the bladder, bowel and sexual organs.



- |                         |                            |
|-------------------------|----------------------------|
| 1. Spinal Nerve         | 5. Central Canal (Sensory) |
| 2. Dorsal Root Ganglion | 6. Grey Matter             |
| 3. Dorsal Root          | 7. White Matter            |
| 4. Ventral Root (Motor) |                            |

**Figure 1 Anatomy of Spinal Cord**

### **1.1.3 Spinal Cord Nerve Levels**

The spinal nerves carry information to and from different levels (segments) in the spinal cord. Both the nerves and segments in the spinal cord are numbered in a similar way to the vertebrae. The point at which the spinal cord ends is called the conus medullaris, and is the terminal end of the spinal cord. It occurs near lumbar nerves L1 and L2. After the spinal cord terminates, the spinal nerves continue as a bundle of nerves called the cauda equina. The upper end of the conus medullaris is usually not well defined.

There are 31 pairs of spinal nerves which branch off from the spinal cord (Figure 2). In the cervical region of the spinal cord, the spinal nerves exit above the vertebrae. A change occurs with the C7 vertebra however, where the C8 spinal nerve exits the vertebra below the C7 vertebra. Therefore, there is an 8th cervical spinal nerve even though there is no 8th cervical vertebra. From the 1st thoracic vertebra downwards, all spinal nerves exit below their equivalent numbered vertebrae.

The spinal nerves which leave the spinal cord are numbered according to the vertebra at which they exit the spinal column. So, the spinal nerve T4, exits the spinal column through the foramen in the 4th thoracic vertebra. The spinal nerve L5 leaves the spinal cord from the conus medullaris, and travels along the cauda equina until it exits the 5th lumbar vertebra.

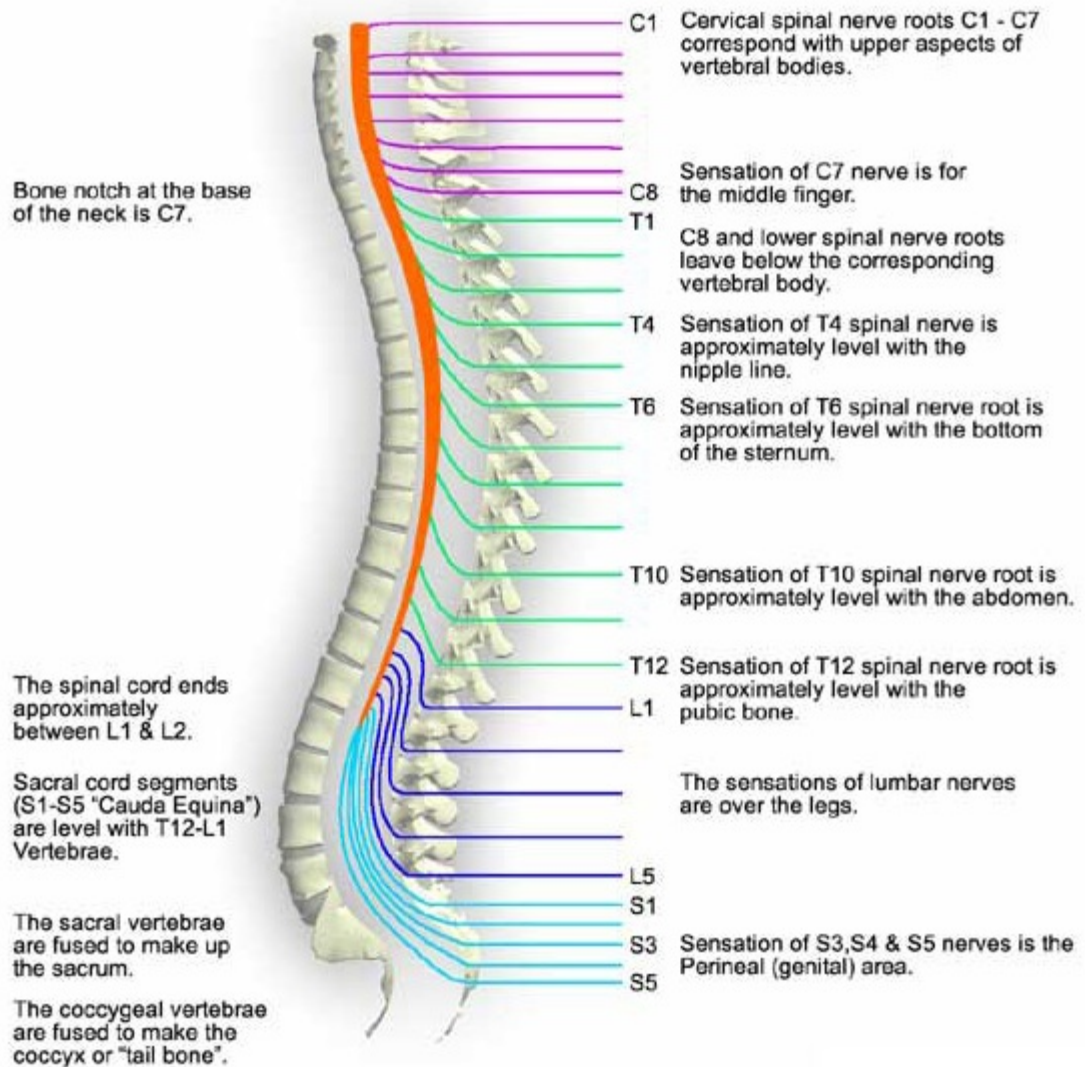


**Figure 2 Spinal Cord Nerve Levels**

The level of the spinal cord segments do not relate exactly to the level of the vertebral bodies i.e. damage to the bone at a particular level e.g. L5 vertebrae does not necessarily mean damage to the spinal cord at the same spinal nerve level.

#### **1.1.4 Epidemiology of SCI**

Acute traumatic spinal cord injury (SCI) occurs worldwide with an estimated annual incidence of 15-40 cases per million (Sekhon LH and Fehlings MG, 2001) and is associated with severe physical, psychological, social, and economic burdens on patients and their families. Common causes of SCI are motor vehicle accidents (44%), falls and work-related injuries (18%), violent crime (17%), and sports-related injuries (13%) and other causes (8%) (Ho CH et al., 2007). Flexible regions of the spinal column are most susceptible to injury and accordingly, injuries most commonly occur in the cervical spine where they are associated with the most devastating neurological impairments. A recent report from the US National Spinal Cord Injury Database found that 56% of all SCI cases occur in the cervical spine (Rowland JW et al., 2008).

#### **1.1.5 Pathophysiology of SCI**

Although the hard bones of the spinal column protect the soft tissues of the spinal cord, vertebrae can still be broken or dislocated in a variety of ways and cause traumatic injury to the spinal cord. Injuries can occur at any level of the spinal cord. The segment of the cord that is injured, and the severity of the injury, will determine which body functions are

compromised or lost. Because the spinal cord acts as the main information pathway between the brain and the rest of the body, a spinal cord injury can have significant physiological consequences.

The pathophysiology of SCI is best described as biphasic, consisting of primary and secondary phases of injury. The primary phase involves the initial mechanical compressive-contusive-type injury during which failure of the spinal column (fracture and/or dislocation) directly imparts force to the spinal cord, disrupting axons, blood vessels, and cell membranes. This is followed by a delayed onset of a secondary injury phase, which ultimately causes progressive degeneration of the spinal cord. These secondary events include vascular abnormalities, edema, ischemia-reperfusion injury, glutamate excitotoxicity, disturbances in ionic homeostasis, free radical production, an extensive inflammatory response, and delayed apoptotic cell death. These events of the secondary injury process are divided temporally into multiple continuous phases: the immediate, acute (early acute and subacute), intermediate, and chronic stages of SCI (Table 1) (Rowland JW et al., 2008).

**Immediate phase (0-2 hours):** The immediate phase begins at the time of injury, lasting for ~2 hours, and represents the primary phase of injury in the biphasic SCI model (Norenberg MD et al., 2004). This phase is dominated by the immediate results of the injurious events. The traumatic severing of axons, the immediate death of neurons and glia, and the accompanying (poorly understood) phenomena of spinal shock (Ditunno JF

et al., 2004) result in instantaneous loss of function at and below the level of injury for complete injuries.

The pathological changes include swelling of the spinal cord in the central gray matter, disruption of the microvasculature leading to hemorrhage in the surrounding white matter (Kakulas BA, 2004; Tator CH and Koyanagi I, 1997) and upregulation of the proinflammatory cytokines TNF $\alpha$  and IL- $\beta$ .

**Table 1 Spinal Cord Injury Phases and Key Pathological Events** (Rowland JW et al., 2008)

Phase and Key Events	Time after SCI				
	≤ 2 hours	≤ 48 hours	≤ 14 days	≤ 6 months	≥ 6 months
Injury Phase	Primary Immediate	Early Acute	Secondary Subacute	Intermediate	Chronic/Late
Key Processes and Events	Primary mechanical injury Traumatic severing of axons Grey matter Hemorrhage Hemorrhagic necrosis microglial activation Released factors: IL-1 $\beta$ , TNF $\alpha$ , IL-6, & others	Vasogenic & cytotoxic edema ROS production: lipid peroxidation Glutamate-mediated excitotoxicity Continued hemorrhage & necrosis Neutrophil invasion Peak BBB permeability Early demyelination (oligodendrocyte death) Neuronal death Axonal swelling Systemic events (systemic shock, spinal shock, hypotension, hypoxia)	Macrophage infiltration Initiation of astroglial scar (reactive astrocytosis) BBB repair & resolution of edema	Continued formation of glial scar Cyst formation Lesion stabilization	Prolonged Wallerian degeneration Persistence of spared Demyelinated axons Potential structural & functional plasticity of spared spinal cord tissue
Therapeutic Aims	Neuroprotection	Neuroprotection Immune modulation Cell-based remyelination approaches Glial scar degradation		Glial scar degradation	Rehabilitation Neuroprostheses

**Acute phase:** The acute phase is the period in which the secondary injury processes become dominant. For clinically practical reasons, it is the SCI phase likely to be most amenable to neuroprotective interventions. The acute phase is divided into early acute and subacute stages.

**Early acute phase (2-48 hours):** The early acute phase of SCI lasts from 2 to 48 hours following injury. This phase is characterized by continuing hemorrhage, increasing edema, and inflammation, and marks the onset of additional secondary injury processes including free radical production, ionic dysregulation, glutamate-mediated excitotoxicity, and immune-associated neurotoxicity leading to further axonal injury and cell death. Vascular disruption, hemorrhage, and the resulting ischemia are central events of this secondary injury phase (Tator CH and Koyanagi I, 1997; Tator CH and Fehlings MG, 1991).

**Ionic Dysregulation and Excitotoxicity:** The loss of appropriate ionic homeostasis is the central feature of both necrotic and apoptotic cell death following injury. Specifically, the dysregulation of  $\text{Ca}^{2+}$  ion concentration is a common element in cell death and initiates a number of damaging processes including the activation of calpains, mitochondrial dysfunction, and free radical production culminating in cell death (Schanne FA et al., 1979).

Excitotoxicity is a result of the excessive activation of glutamate receptors leading to the influx of  $\text{Na}^+$  and  $\text{Ca}^{2+}$  through the N-Methyl-D-Aspartate (NMDA) and alpha-amino-3-

hydroxy-5-methyl-isoxazolepropionate/kainate receptors. It is believed to play a role in the death of both neurons and glia following many forms of neurotrauma, including SCI (Park E et al., 1979).

**Free Radical Mediated Injury:** Free radical mediated injury is an important contributor to the secondary damage following SCI with radical-mediated lipid peroxidation contributing to axonal disruption and the death of both neurons and glia. The detection of reactive O<sub>2</sub> species (ROS) peaks at roughly 12 hours following injury and remains elevated for ~1 week, returning to basal, pre-injury levels 4-5 weeks after injury (Donnelly DJ and Popovich PG, 2008; Xiong Y et al., 2007).

Permeability of the blood-brain barrier (BBB): In the uninjured CNS, the BBB functions as a highly selective filter limiting the transport of compounds both into and out of the CNS parenchyma. Following SCI there is a marked increase in BBB permeability due to both direct mechanical disruption by the primary injury and the effects on endothelial cells by numerous inflammatory mediators and other compounds. On the other hand, P-gp efflux transporter is also demonstrated to be upregulated after acute SCI (Grill and Dulin, personal communication, 2011) that may exhibit high efflux of the drug out of CNS.

**Inflammatory Mediators and the Cellular Immune Response:** The early acute stage involves infiltration by inflammatory cells and continuing activation of resident microglia. The inflammatory process following SCI is highly complex and involves numerous cellular populations, including astrocytes, microglia, T cells, neutrophils, and invading

monocytes. A multitude of noncellular mediators, including TNF $\alpha$ , interferons, and ILs also play important roles (Donnelly DJ and Popovich PG, 2008; Filippi M and Rocca MA, 2007; Popovich PG et al., 1997).

**Cell Death and Demyelination:** Cell death after SCI may occur by necrosis or apoptosis. Death of neurons at all stages of injury occurs mainly through necrosis, with little evidence to date that apoptosis plays an important role in neuronal death after human SCI (Emery E et al., 1998; Keane RW et al., 2001), although it has been observed in animal SCI (Lou J et al., 1998; Yong C et al., 1998).

**Subacute phase (2 days to 2 weeks):** The subacute phase is considered to last from ~2 days to 2 weeks following injury and importantly is the time period in which future cell-based therapeutic strategies are most likely to be applied. The phagocytic response is maximal during the subacute phase and is likely beneficial in removing cell debris from the lesion area and may promote axon growth to some degree through the removal of growth-inhibitory components of myelin debris (Donnelly DJ and Popovich PG, 2008).

**Intermediate Phase (2 Weeks to 6 Months):** The intermediate phase is characterized by the continued maturation of the astrocytic scar and by regenerative axonal sprouting (Hill CE et al., 2001). In rat models of contusive SCI, corticospinal tract axons display sprouting from 3 weeks to 3 months following injury, whereas sprouting reticulospinal fibers are observed to sprout from 3 to 8 months post-injury (Hill CE et al., 2001).The

follow-up of the reporting trial was scheduled for up to 6 months, through the intermediate phase.

**Chronic phase (>6 months):** The chronic phase begins in 6 months following an injury and continues throughout the lifetime of the patient with SCI. The chronic phase is characterized by the maturation/stabilization of the lesion including continued scar formation and the development of cysts and/or syrinxes. The process of Wallerian degeneration of injured or severed axons is ongoing and it may take years for severed axons and their cell bodies to be fully removed (Beattie MS et al., 2002; Coleman MP and Perry VH, 2002; Ehlers MD, 2004). Despite some instances of improved neurological function many years following injury (McDonald JW et al., 2002), it can be considered that at ~1-2 years post-injury, the neurological deficits have stabilized and the lesion has fully matured. The lesion itself is characterized by cystic cavitation and myelomalacia, representing the final stage of necrotic death after SCI.

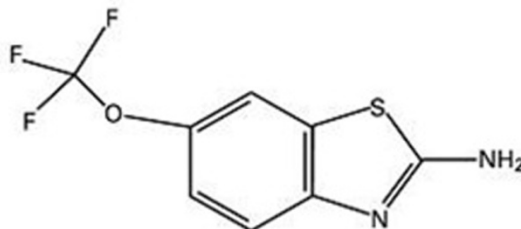
## 1.2 Riluzole

### 1.2.1 Mechanism of Action of Riluzole

Riluzole (Figure 3), a benzothiazole anticonvulsant Na<sup>+</sup> channel blocker, received FDA approval in 1995 for the treatment of patients with amyotrophic lateral sclerosis (ALS), a progressive neurodegenerative disorder characterized by motoneuron and corticospinal tract degeneration (Lacomblez L et al., 1996; Hugon J, 1996; Bensimon G et al., 1994). The standard regimen is of fixed oral doses of 50 mg BID.

There are potential merits of Riluzole, as a Na<sup>+</sup> channel blocker, to offer neuroprotective activity in primary immediate ( $\leq 2$  hr) and early acute ( $\leq 48$  hr) injury phases of SCI. SCI results in a deleterious accumulation of intracellular sodium [Na<sup>+</sup>]<sub>i</sub> within neurons (Stys PK, 2004); the resulting membrane depolarization associated with cellular inability to remove [Na<sup>+</sup>]<sub>i</sub> favors further Na<sup>+</sup> influx via non-inactivating Na<sup>+</sup> channels.

The neuroprotective effects of Na<sup>+</sup> channel blockade are likely exerted on neurons and spinal cord axons to reduce intra-cellular increases in [Na<sup>+</sup>]<sub>i</sub> and to reverse the operation of axonal Na<sup>+</sup>/Ca<sup>2+</sup> exchangers. In addition, Na<sup>+</sup> channel blockade may preserve spinal cord white matter by preventing the disruption of the axonal Na<sup>+</sup>/H<sup>+</sup> antiporter system, as shown in tetrodotoxin damage (Rosenberg LJ et al., 1999) to maintain compound action potentials following acute compression in an *ex vivo* model of SCI (Agrawal SK and Fehlings MG, 1996). Riluzole is also known to inhibit presynaptic Ca<sup>2+</sup>-dependent glutamate release (Wang SJ et al., 2004).



**Physical-Chemical Properties:**

**Chemical name:** 2-amino-6-(trifluoromethoxy) benzothiazole

**Molecular mass:** 234.2

**Description:** Riluzole is a white to slightly yellow powder

**Solubility:** Riluzole is highly soluble in dimethylformamide, dimethylsulfoxide (DMSO) and methanol, freely soluble in dichloromethane, sparingly soluble in 0.1 N HCl and very slightly soluble in water and in 0.1 N NaOH.

**pKa:** 3.8

**Partition Coefficient:** Octanol/Water is about 3000

**Log P:** 3.5

**Melting Point:** Between 117°C and 120°C.

**Figure 3 Chemical Structure and Physical-chemical Properties of Riluzole**

Studies have demonstrated that Riluzole is neuroprotective and promotes functional neurological recovery in various species of animal models of brain and spinal cord ischemic and traumatic injury (Heurteaux C et al., 2006; Ates O et al., 2007; Lang-Lazdunski L et al., 1999; Schwartz G et al., 2001). Other authors have reported that the effects of Riluzole are synergistic with those of methylprednisolone, which is the only drug used in routine clinical practices to attempt attenuating secondary injury effects after SCI (Mu X et al., 2000).

### **1.2.2 Pharmacokinetics of Riluzole**

The pharmacokinetics of Riluzole have been established in healthy subjects (Le Liboux A et al., 1997; Le Liboux A et al., 1999), young and old, as well as in patients with ALS (Bruno R et al., 1997; Groeneveld GJ et al., 2003) and pediatric patients with spinal muscular atrophy (SMA) (Abbara C et al., 2011). In humans, Riluzole has been administered orally at a dose of 50 mg BID, or 50 mg QD in SMA patients (Abbara C et al., 2011). The half-life of Riluzole is 12 hours. Most drugs reach steady state plasma concentrations in 4-5 half-lives and the same is assumed for Riluzole at 48-60 hr post dose.

Riluzole is highly protein bound to serum albumin and lipoproteins, 96%, like phenytoin, and thus poses potential concerns for drug-drug interactions with other concomitant medications that compete for protein binding. In patients taking such concomitant medications, a higher concentration of free Riluzole in the plasma, resulting from the competition, will be anticipated to exert a greater therapeutic activity.

Riluzole is extensively metabolized to five major and a number of minor metabolites, not all of which have been identified. The metabolism of Riluzole is mostly hepatic and consists of cytochrome P (CYP) 450 (multiple CYP isozymes)-dependent hydroxylation and glucuronidation (Figure 4).

Most of the drugs metabolizing enzymes are in the CYP 1, 2 & 3 families. Riluzole is specifically metabolized by CYP 1A2 subfamily extensively, with only 2% of the dose recovered unchanged in the urine. Smoking is known to induce CYP 1A2. In addition, the care of SCI patients may include the administration of methylprednisolone (MPSS) which is a substrate and inducer of CYP 3A4 and 2C19, and may indirectly affect the hepatic clearance of Riluzole. Therefore, smoking history and other concomitant medications of CYP 1A2 substrates, inhibitors or inducers may affect Riluzole blood concentrations.

The substrates of CYP1A2 include acetaminophen, caffeine, theophylline and warfarin. The inhibitors include tacrine (Cognex), omeprazole (Prilosec), quinolone antibiotics, erythromycin, and oral contraceptives. Co-administration of Riluzole with these drugs can increase riluzole blood concentrations (Abbara C et al., 2011). The inducers, including carbamazepine, phenobarbital, phenytoin, St John's wort, ritonavir and smoking, can decrease Riluzole blood concentrations.

The activity of the CYP 1A2 enzyme is lower in women than in men, as well as in the Japanese population, and possibly in other Asian populations (no data available). Presumably in these populations the activity of the drug would be greater, although no sex differences were noted in the ALS studies with Riluzole.

A high inter-subject variability of Riluzole blood concentrations has been documented among ALS (Bruno R et al., 1997; Groeneveld GJ et al., 2003) and SMA patients

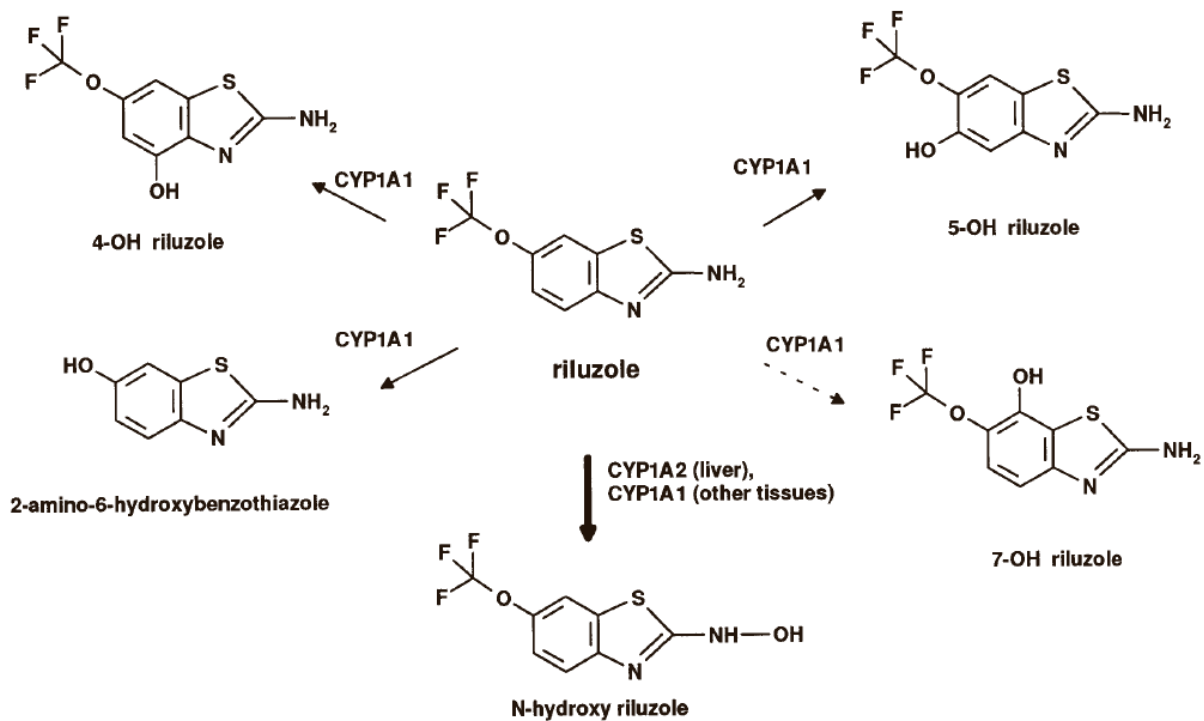


Figure 4 Metabolic Pathways Involved in Phase I Biotransformation of Riluzole.

(Abbara C et al., 2011), which is probably attributable to the variability of CYP 1A2 activity, the principal isozyme involved in N-hydroxylation.

Riluzole blood concentrations in patients with ALS are associated with the observed side effects and the symptom modifications of ALS (Groeneveld GJ et al., 2003).

### **1.2.3 Toxicity of Riluzole**

In a recent study of prolonged administration of Riluzole in Huntington's disease, no benefit was found in slowing disease progression, but Riluzole was well tolerated.

Adverse effects were virtually similar in 357 patients treated with Riluzole, and in 180 placebo patients. Thirteen patients had elevations of liver enzymes and five patients discontinued the treatment due to the elevations (Landwehrmeyer GB et al., 2007).

Notably, Riluzole is without potent neurotoxic and cardiotoxic adverse effects (Bensimon G and Doble A, 2004), even though potential hepatotoxicity has been noted (Lacomblez L et al., 1996).

### **1.2.4 Alterations of Pharmacokinetics of Drugs in SCI**

The SCI population is heterogeneous, and possible changes in pharmacokinetics may depend on the variables of injury characteristics (intensity, level and time elapsed after injury), pharmacological properties of the drug and the route of administration (Rowland JW et al., 2008; Garcia-Lopez P et al., 2007; Fuentes-Lara G et al., 1999). Based on the knowledge of SCI effects on the pharmacokinetics of drugs reported in the past 26 years, 1985-2011 (Fuentes-Lara G et al., 1999; Hayes KC et al., 2004; Mestre H et al., 2011; Vertiz-Hernandez A et al., 2007; Reihani-Kermani H et al., 2006; Segal JL et al., 2000; Gilman TM et al., 1996; Ibarra A et al., 1996; Aisen ML et al., 1992; Segal JL and Brunnemann SR, 1989; Segal JL et al., 1986; Segal JL et al., 1985), we may anticipate the following alterations of pharmacokinetics of Riluzole in acute SCI patients from those in normal subjects:

Absorption: In SCI, there may be reduced bioavailability (F) and prolonged peak time ( $t_{max}$ ) of oral medications that are commonly prescribed for SCI patients, such as acetaminophen, theophylline (Segal JL et al., 1986), dantrolene (Gilman TM et al., 1996), carbamazepine (Reihani-Kermani H et al., 2006), 4-aminopyridine (Hayes KC et al., 2004), cyclosporine A (Ibarra A et al., 1996) and baclofen (Aisen ML et al., 1992). The underlying causes are impaired gastric emptying and intestinal motility, as well as reduced microvascular gastrointestinal blood flow (MVBF) (Segal JL et al., 1986; Guizar-Sahagun G et al., 2004; Stone JM et al., 1990; Fealey RD et al., 1984). Moreover, it is also recognized that injury above T6 induces significant reduction in MVBF to GI and liver, more than that in injury below T6 (Mathias CJ et al., 1983; Cruz-Antonio L et al., 2006).

Distribution: Distribution implies transporting the drug to tissues and ultimately to cells throughout the bloodstream. This process depends on several factors, including cardiac output, systemic macro- and micro-circulation, and drug-protein binding (Segal JL et al., 2000; Shargel L W-PS and Yu A, 2005).

Population-specific alterations in drug distribution kinetics are unavailable. However, SCI patients commonly have hypoalbuminemia that alters the plasma protein binding of highly bound drugs and results in increase of distribution ranging from 20% (amikacin) to 70% (cefotiam) (Segal JL and Brunnemann SR, 1989), as known with ketamine (Hijazi Y et al., 2003), lorazepam (Segal JL et al., 1991), amikacin and cefotiam.

Riluzole is a highly plasma protein binding drug (96% bound;  $f_u=0.04$ ) and will be sensitive to a change of fraction unbound ( $f_u$ ), since only the free drug molecules are transported to interstitial fluid.

Metabolism: Hepatic clearance ( $CL_H$ ) that relates to drug metabolism has been reported to decrease in SCI patients for phenacetin (Vertiz-Hernandez A et al., 2007), methylprednisolone (Segal JL et al., 1998) and cyclosporine A (Garcia-Lopez P et al., 2007; Ibarra A et al., 1996). The underlying causes can be a reduced MVBF in liver (Cruz-Antonio L et al., 2006), enzyme synthesis or protein binding (Shargel L W-PS and Yu A, 2005), singly and in combination.

In SCI, reductions in the MVBF in the liver, spleen and skeletal muscle occur in the acute phase of SCI and peaks at ~24 h after the injury. The reduction is more pronounced after a high thoracic complete (above T6) lesion than a low one. These alterations are likely due to a redirection of blood flow to maintain an adequate perfusion of the brain and heart (Cruz-Antonio L et al., 2006).

The decrease of hepatic blood flow ( $Q$ ) due to SCI will reduce the hepatic metabolism clearance ( $CL_H$ ) of drugs with high hepatic extraction ratios (high  $E = CL_H/Q \geq 0.7$ ), such as phenacetin, methylprednisolone and cyclosporine A. In contrast, biotransformation of low-extraction drugs ( $E \leq 0.3$ ), such as most non-steroidal anti-inflammatory drugs, does not depend on liver blood flow, but on liver intrinsic enzymatic activity ( $CL_{int}$ ) (Rowland M

TT, 1989; GM W, 1992; Tietze KJ and Putcha L, 1994) and plasma protein binding ( $f_u$ , fraction unbound) (Shargel L W-PS and Yu A, 2005). The  $CL_H$  of drugs of intermediate hepatic extraction ratio ( $0.7 > E > 0.3$ ), such as Riluzole whose  $E = 0.67$ , will be affected by all the three factors,  $Q$ ,  $CL_{int}$  and  $f_u$ .

Elimination (excretion): Decreased renal clearance ( $CL_R$ ) and prolonged  $t_{1/2}$  in SCI have been reported with amikacin (Brunnemann SR and Segal JL, 1991), cefotiam, doxycycline, ketamine (Hijazi Y et al., 2003), diclofenac (Garcia-Lopez P and Salas R, 1999), vancomycin (Lavezo LA and Davis RL, 1995) and lorazepam (Segal JL et al., 1991), due to the decrease in renal function. Riluzole is excreted unchanged in urine at only 2% of the dose, and thus urinary excretion may not be significantly affected by SCI.

### **1.2.5 Phase I Clinical Trial of Riluzole in SCI Patients**

Clinical guidelines for the management of SCI have been established and widely accepted by physicians who treat patients with SCI (Hadley MN et al., 2002). These guidelines include stabilization of the vertebrae, and cardiopulmonary and metabolic support of the patient. However, beyond supportive care there are no medical or surgical treatments that have been clearly demonstrated to improve functional outcomes in human SCI. Clinical trials with methylprednisolone (NASCIS II and III) (Bracken MB et al., 1990; Bracken MB et al., 1997), GM-1 ganglioside (Geisler FH et al., 2001), fampridine (4-aminopyridine) (Hayes KC et al., 2004; Hayes KC et al., 2003; Potter PJ et

al., 1998) and lithium carbonate (Miller RG et al., 2007; Yang ML et al., 2012) have provided suggestive but equivocal evidence of benefits.

In light of the overwhelming impact of SCI on the individuals, new therapeutic interventions are urgently needed. Compelling evidence exists that Riluzole, a sodium channel blocking agent with anti-glutamatergic activity with putative neuroprotective properties gleaned from the preclinical literature, offers promise for improving the outcomes of SCI. Therefore, the use of Riluzole as a therapy for SCI is potentially feasible.

A phase I trial of Riluzole was conducted as a multi-site, single arm active treatment pilot study with an enrollment goal of 36 patients by the North American Clinical Trial Network (NACTN). The clinical trial performed for two weeks post-injury, dosing of Riluzole started within 12 hours post-injury and through the early acute and subacute phases. The blood sampling for pharmacokinetic monitoring was on Day 3 and Day 14, both in the subacute phase. The pathophysiological conditions vary during the various phases of SCI and thus the pharmacokinetics (absorption, distribution, metabolism and excretion) of Riluzole may be affected differently, specific with individual stages of the phases.

The primary aim of the trial was to obtain data on safety, pharmacokinetics (PK) and preliminary pharmacodynamics of Riluzole in patients who had sustained an acute traumatic SCI.

## 1.2.6 Rationale of Dose and Treatment Duration Selected of Riluzole for SCI Patients

Riluzole is an FDA approved agent for ALS (Miller RG et al., 2007) at a dose of 100 mg/day. The dose for the current phase I trial was selected using human data and scaling from animal data. From the human data the most conservative approach based on the FDA approved dose for ALS patients was used in confirmatory dose-ranging (50, 100, 200 mg/day) studies of Riluzole in ALS (Lacomblez L et al., 1996), a daily dose of 100 mg (50 mg bid) of Riluzole was confirmed to have the best benefit-to-risk ratio.

From animal data, the human equivalent dose (HED) for SCI patients was allometrically scaled from the animal dose (6 mg/kg bid) in SCI female Wistar rats, weight of 250-300 gm (Schwartz G and Fehlings MG, 2001) based on the power equation:  $HED = \text{Animal Dose (mg/kg)} \times (\text{animal wt/human wt in kg})^{0.33} = (6 \text{ mg/kg bid}) \times (0.25 \text{ kg}/70 \text{ kg})^{0.33} = 0.92 \text{ mg/kg bid} = 64.2 \text{ mg}/70 \text{ kg bid}$ . The trial dose of 50 mg/ bid is within the HED, 64.2 mg bid, scaled from the tolerable dose in rats.

Riluzole has been administered for prolonged periods of time in patients with ALS. The duration of Riluzole treatment of the reporting trial was selected, based upon the current understanding of the duration of sodium and glutamate mediated secondary injury after SCI that encompass a period of 14 days after injury (Rowland JW et al., 2008).

## **1.3 Safety and Efficacy Evaluations of Riluzole Phase I**

### **Clinical Trial**

#### **1.3.1 Safety**

Appropriate laboratory monitoring would be carried out to detect liver damage and/or neutropenia, and other disturbances of body chemistry and hematology. Baseline testing of liver function would be performed to rule out preexisting liver disease. Baseline testing would include Hepatitis B Virus (HBV) and Hepatitis C Virus (HCV). Besides, the baseline testing would include alanine aminotransferase (ALT), aspartate aminotransferase (AST), alkaline phosphatase (ALP), gamma glutamyl transpeptidase (GGT), bilirubin, prothrombin time (PT), international normalized ratio (INR), and hemogram as well. These tests would be also conducted at 3, 7, 10 and 14 days after the start of Riluzole treatment, as well as at 3-month and 6-month follow-ups.

#### **1.3.2 Efficacy**

The American Spinal Injury Association (ASIA) protocols (or equivalents) are the most frequently used assessment tool in SCI clinical trials and survey studies to measure the neurological recovery. Two types of measures are included. The completeness of the SCI is graded by the ASIA impairment scale (AIS grades A-E). The motor and sensory abilities of patients are described by the ASIA motor and sensory scores that constitute the International Standards for Classification of SCI. Recovery can be measured by conversions in the AIS and/or by changes in the ASIA motor and sensory scores. By

repeated measures over the continuum from the acute to chronic stage of SCI, the time profile of changes, as well as the absolute amount of neurologic recovery, can be determined (Fawcett JW et al., 2007).

#### **1.3.2.1 ASIA Motor Score**

In many respects, the ASIA motor score is considered more reliable than the ASIA sensory score in predicting functional outcomes after SCI (Marino RJ and Graves DE, 2004). The upper and lower limb motor scores should be compiled separately as the upper-extremity motor score (UEMS) and lower-extremity motor score (LEMS). This enables a change in motor function to be more clearly tracked and recorded as specific to either the cervical or lumbar levels (Table 2). In addition, the separation of the motor scores into UEMS and LEMS reduces the misinterpretation of therapeutic benefit resulting from the influence of a significant change of the functional strength from only one or limited muscles. The range of the score is from 0 to 100 (normal motor function in all 10 muscles examined bilaterally).

**Table 2 Key Muscles Used for ASIA Motor Score Assessment, with Muscle Grades Categorizing Functional Assessment of Each Muscle's Contraction**

Left side (max. grade)	Key muscles for ASIA motor score assessment and primary level of spinal innervation	Right side (max. grade)
5	Elbow flexors (biceps brachialis)-C5	5
5	Wrist extensors (extensor carpi radialis longus and brevis)-C6	5
5	Elbow extensor (triceps)-C7	5
5	Finger flexors (flexor digitorum profundus, middle finger)-C8	5
5	Finger abductors (abductor digiti, little finger)-T1	5
<b>25</b>	<b>Upper Extremity Motor Score (UEMS)</b>	<b>25</b>
5	Hip flexors (iliopsoas)-L2	5
5	Knee extensors (quadriceps)-L3	5
5	Ankle dorsiflexors (tibialis anterior)-L4	5
5	Long toe extensors (extensor hallucis longus)-L5	5
5	Ankle plantar flexors (gastrocnemius, soleus)-S1	5
<b>25</b>	<b>Lower Extremity Motor Score (LEMS)</b>	<b>25</b>
<b>50</b>	<b>Total ASIA motor score (=100 for both sides)</b>	<b>50</b>

ASIA muscle grades: 0=total paralysis; 1=palpable or visible contraction; 2=active movement, gravity eliminated; 3=active movement, against gravity; 4=active movement, against some resistance; 5=active movement

### **1.3.2.2 ASIA Sensory Score**

The lack of sophistication of the ASIA sensory score has long been recognized for an accurate description of the preserved sensory levels after SCI or as a valid outcome measurement. The ordinal 3-point scales for light touch, normal, abnormal, or absent (Figure 5) is highly variable at different assessment times and between ASIA assessors. The ASIA pin-prick score appears to be a more useful clinical measure of the preserved spinal sensory function (e.g. sacral sparing in people with an ASIA B classification), and a predictor for future recovery (Crozier KS et al., 1991; Katoh S and Masry WS, 1995). The range of the score is from 0 (absence of sensory function) to 224 (no sensory disturbances) based on 28 key points examined bilaterally.

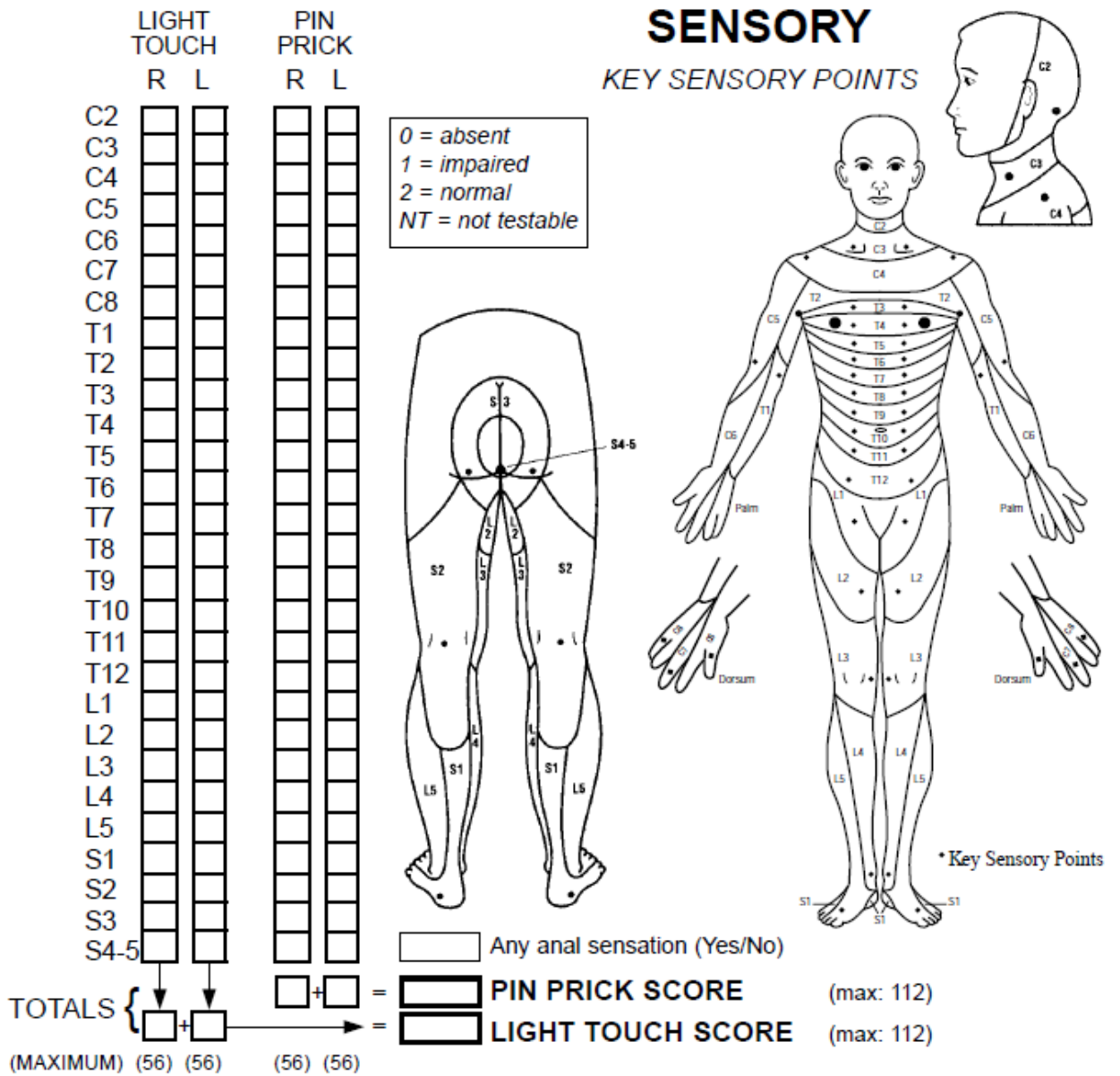


**Figure 5 Assessments of ASIA Sensory Score**

### **1.3.2.3 ASIA Impairment Scale (AIS)**

The ASIA Impairment Scale has become a standardized and routinely adopted classification for the patients suspected of suffering a SCI (Marino RJ et al., 2003). It is especially useful for classification of motor-complete and sensory-complete SCI (AIS A) as well as motor complete, sensory-incomplete SCI (AIS B) (Table 3).

**Table 3 Classification of ASIA Impairment Scale (AIS)**

AIS Grades	Clinical State (below the level of injury)
Grade A	No motor or sensory function is preserved in the sacral segments S4-S5
Grade B	Sensory but not motor function is preserved below the neurological level and includes the sacral segments S4-S5
Grade C	Motor function is preserved below the neurological level and more than half of key muscles below the neurological level have a muscle grade of less than 3
Grade D	Motor function is preserved below the neurological level and at least half of the key muscles below the neurological level have a muscle grade of 3 or more
Grade E	Motor and sensory scores are normal

## **CHAPTER 2. OBJECTIVES AND SPECIFIC AIMS**

### **2.1 Hypothesis**

Spinal cord injury and formulation alteration will affect the pharmacokinetics of Riluzole, and pharmacokinetic/pharmacodynamic (PK/PD) studies will enable us to establish the correlation of Riluzole concentration/exposure with its toxicity and efficacy outcomes.

### **2.2 Objectives**

The overall objective is to evaluate the safety and preliminary efficacy of Riluzole in patients with acute spinal cord injury. The ultimate goal of the study is to set the stage of a Phase II/III randomized controlled trials.

1. To establish potential impacts of changes of formulation/administration on bioavailability of Riluzole in an animal (rat) model.
2. To characterize the impacts of acute SCI on Riluzole pharmacokinetics in animal (rat) models.
3. To characterize the population pharmacokinetics of Riluzole, and to attempt correlating plasma PK/PD (efficacy and toxicity) of Riluzole in acute SCI patients.

## 2.3 Specific Aims

### ***Aim 1***

**To establish potential impacts of changes of formulation/administration on bioavailability of Riluzole in an animal (rat) model.** The healthy Sprague-Dawley (SD) rats will be used and different formulations (oral crushed tablet, oral crushed paste, oral suspension and solution, as well as intravenous solutions) of Riluzole will be administered to the animals. The pharmacokinetics of Riluzole in different treatment groups will be characterized and compared. The *hypothesis for this aim* is that the alteration of formulation/administration will change the pharmacokinetics of Riluzole and the formulated oral suspension and solution may improve the bioavailability and compliance of Riluzole. Riluzole concentrations in rat plasma will be measured as an outcome variable.

### ***Aim 2***

**To characterize the impacts of acute SCI on Riluzole pharmacokinetics in animal (rat) models.** A cervical spinal cord injured rat model and an uninjured control model will be used to establish the impacts of acute SCI on Riluzole pharmacokinetics by monitoring pharmacokinetic profiles of Riluzole in plasma, brain and spinal cords of different segments (cervical and thoracic segments). The *hypothesis of this aim* is that acute spinal cord injury will affect the Riluzole pharmacokinetics in the rat model. Riluzole concentrations in plasma, brain and spinal cords of different segments are the primary outcome variables for this aim.

### ***Aim 3***

**To characterize the population pharmacokinetics of Riluzole, and to attempt correlating plasma PK/PD (efficacy and toxicity) of Riluzole in acute SCI patients.**

Thirty-six acute SCI patients will be enrolled in this phase I clinical trial, who will receive Riluzole 50 mg orally or by nasogastric tubes (NG) every 12 hours, starting within 12 hours of injury and lasting for 14 days.

#### ***Aim 3-1***

The plasma concentrations of Riluzole in 36 acute SCI patients will be monitored during the treatment course of Riluzole. The individual and population pharmacokinetics ( $C_{max}$ , AUC, CL/F, and half-life) will be derived in the acute SCI patients of current trial by two concentration-time data method and Non-linear Mixed Effects Model (NONMEM), respectively. The *hypothesis* is that the pharmacokinetic parameters can be characterized, and plasma concentrations ( $C_{max}$ ) and/or systemic exposures (AUC) can be used for PK-PD correlations. The plasma concentrations of Riluzole in acute SCI patients will be measured as an outcome variable.

#### ***Aim 3-2***

The liver enzymes (mainly ALT and AST) will be monitored and recorded at baseline, 3, 7, 10 and 14 days, 3 months and 6 months. The ASIA motor, sensory, impairment scores will be examined and recorded on day 1 as the baseline, Day 3, Day 14,

discharge, as well as at 6-week, 3-month and 6-month follow-ups. The *hypothesis* is that 14-day Riluzole treatment is tolerated, and the elevated enzyme levels will be less than 3 times of normal limits; the ASIA motor, sensory and impairment scores will be improved after the Riluzole treatment. The primary outcomes are (a) Day-3, Day-14 and maximal enzyme levels after the start of Riluzole treatment, (b) 3-month and 6-month follow-up changes of ASIA motor and sensory scores and (c) maximal changes of ASIA motor and sensory scores during the 6-month follow-up.

### ***Aim 3-3***

We will attempt to correlate our PK results with the clinical treatment outcomes (enzyme levels, changes of ASIA motor and sensory scores). The *hypothesis of this aim* is that the plasma concentrations and/or systemic exposures of Riluzole can be used to correlate with its toxicity and efficacy. The primary outcome variables will be the correlations of PK parameters ( $C_{max}$  and/or AUC) of Riluzole with toxicity (day-3, day-14 and maximal enzyme levels after the start of Riluzole treatment) and efficacy (3-month and 6-month follow-up changes of ASIA motor and sensory scores, and maximal changes of ASIA motor and sensory scores during the 6-month follow-up).

# CHAPTER 3. MATERIALS AND METHODS

## 3.1 Materials

### 3.1.1 Chemicals and Materials

- Acepromazine used in combination with ketamine and xylazine (all from Sigma Chemical Co., St. Louis, MO, USA) as the anesthetic combo used in the pharmacokinetic studies.
- Acetonitrile OMNISOLV (EMD, Gibbstown, NJ, USA) was used in the preparation of the mobile phase for routine HPLC assay.
- Ammonium acetate (J.T. Baker Co, Phillipsburg NJ, USA) was used in the preparation of the mobile phase for the routine HPLC assay.
- Double distilled water (DDW), was used for the preparation of all the buffers and the mobile phase for HPLC analysis.
- Drug-free blank human plasma was kindly donated by the Methodist Hospital, Houston, USA, used to prepare the calibration curves for the analysis of human samples.
- Drug-free blank human cerebrospinal fluid (CSF) was kindly donated by the Methodist Hospital, Houston, USA, used to prepare of the standard curves and spiked samples.
- Ethyl acetate (EMD, Gibbstown, NJ, USA) was used for liquid-liquid extraction of Riluzole from biomatric samples.

- Glacial acetic acid (J.T. Baker Co, Phillipsburg NJ, USA) was used to adjust the pH of the mobile phase to 6.5.
- Heparin sodium salt (Sigma Chemical Co., St. Louis, MO, USA) was dissolved in normal saline (0.9% sodium chloride) and used to prepare heparinized micro-tubes for blood collection in the pharmacokinetic studies.
- 5-methoxypsoralen (5-MOP) (Sigma Chemical Co., St. Louis, MO, USA) was used as the internal standard (I.S.) of the HPLC assay for Riluzole.
- Methanol OMNISOLV (EMD, Gibbstown, NJ, USA) was used in the preparation of the mobile phase for routine HPLC assay and as a solvent (mixed with D.D.W. at a ratio of 1:1) of Riluzole stock solution.
- Methylprednisolone (MPSS), hydrocortisone, midazolam, baclofen, acetaminophen (Sigma Chemical Co., St. Louis, MO, USA) were used to validate the HPLC methods and exclude the potential assay interferences of concomitant medications.
- Oral suspension vehicle was purchased from Professional Compounding Centers of America (PPCA, Houston, TX) for the preparation of Riluzole liquid formulation in Aim 1.
- Propylene glycol (J.T. Baker Co, Phillipsburg NJ, USA) was used in the preparation of Riluzole liquid formulation in Aim 1.
- Riluzole film-coated tablets (Rilutek<sup>®</sup>, Sanofi-Aventis, USA) was supplied by the hospital pharmacy at each clinical site. The acute SCI patients enrolled in phase I clinical trial received Rilutek<sup>®</sup> throughout the project.

- Riluzole powder (Sigma Chemical Co., St. Louis, MO, USA) was the drug used throughout the preclinical studies and for high performance liquid chromatographic (HPLC) assay development and validation.
- Sprague-Dawley rats (males, 250-300 gm) were purchased from Charles River (Houston, TX, USA) and were used for the pharmacokinetic studies.
- Sodium Chloride (Eastman Kodak Co., St. Louis, MO, USA) was used to prepare the 0.9% of saline solution for perfusing the organs before harvesting in the preclinical studies.

### 3.1.2 Supplies

- Alcohol wipes (Webcol<sup>®</sup> Alcohol Preps, Kendall Healthcare Products Co., Mansfield, MA, USA) were used to disinfect animal's skin prior to the administration of anesthesia.
- Centrifree<sup>®</sup> YM-30 devices (Millipore Ireland Ltd., Billerica, MA, USA) were used to evaluate the extent of free (unbound) Riluzole in human plasma
- Clear glass inserts, 1 mL (Waters Corp., Milford, MA, USA) were used for HPLC analysis of aqueous samples from *in vitro* experiments.
- Conical clear glass inserts, 150  $\mu$ l (Waters Corp., Milford, MA, USA) were used for HPLC analysis of plasma samples from *in vivo* experiments.
- Cotton swabs (Q-tips, 6 inch) (Sherwood Medical, St. Louis, MO, USA) were used during animal surgery procedures in pharmacokinetic studies.

- Gastric gavage blunt needle (20-gauge, 2.5 inch, curved, ball-end) (Harvard Apparatus Inc., Holliston, MA, USA), firmly attached to a 1 cc syringe, was used for the oral dosing of Riluzole to rats.
- Gloves (lightly powdered, Latex) used in handling Riluzole and animals.
- Insulin syringes (1/2 cc, sterile) (Becton Dickinson & Co., Rutherford, NJ, USA) were used to administer the anesthesia to the thigh muscle of the rats.
- Isothermal pad (model 39 DP, Braintree Scientific, Braintree, MA, USA) was pre-heated to 37°C to maintain body temperatures of rat during the preclinical pharmacokinetic studies.
- Masks (Alpha ProTech, Salt Lake City, UT, USA) were used for human protection in performing animal studies.
- Membrane filters (47 mm, 0.45 µm, hydrophilic polypropylene; Pall Corp., Ann Arbor, MI, USA) were used to filter the mobile phases.
- Octadecyl (C18) speedisk columns (J.T. Baker Co, Phillipsburg NJ, USA) were used for extraction of Riluzole from human CSF samples.
- Pipette tips (disposable, white: 1-10 µl, yellow: 10-100 µl and blue: 100-1000 µl; Dot Scientific Inc., MI, USA) were used along with Eppendorf® pipettes for measuring and delivering solutions for all experiments.
- Polyethylene microcentrifuge tubes (1.5 ml, Axygen Scientific Inc., Union City, CA, USA) were used (after heparinization) for collecting and storing samples from the different experiments including the pharmacokinetic studies.
- Surgical absorbent pads (Medline, Mundelein, IL, USA) were used during all animal procedures.

### 3.1.3 Equipment, Apparati and Softwares

- Balance (digital, 0.0001-g sensitivity, Mettler AE100, Mettler Instrument Corp., Hightstown, NJ, USA) was used for all weighting purposes.
- Centrifuge (Marathon 13K/M, B Hermle AG, Germany) was used in the preclinical and clinical pharmacokinetic studies to separate plasma from blood cells during sample collection.
- HPLC systems consisted of:
  - Symmetry® C18 guard column (2.1×10 mm, 3.5 µm) (Waters Corp., Milford, MA, USA) was placed right before the HPLC column as a filter for protection.
  - A Symmetry® C18 column (3.0×150 mm, 3.5 µm) (Waters Corp., Milford, MA, USA) was used in the HPLC assay method for the quantifications of Riluzole from both aqueous and biomatric samples.
  - Empower 2 chromatography software was applied for peak area integration with this system (Waters Corp., Milford, MA, USA)
  - Waters 515 pump was used as the solvent delivery system with a photodiode array detector (Waters 2996) and an auto-sampler (Waters 717)
- Microsoft Excel was used for Student's t test, pharmacokinetic data analysis and generation of pharmacokinetic parameters.

- NONMEM Software (v 7.2.0) was used for population pharmacokinetics analysis of repeated measures of Riluzole in acute SCI patients. The Population PK software is capable of analyzing clinical data with sparse samples, deviated sampling time and/or missing samples.
- pH-meter (Corning Scholar 425, Corning, NY, USA) was routinely used to measure the pH of the mobile phase and to confirm the pH of all the buffer solutions.
- Pipettes (VWR<sup>®</sup>, three sizes: 1-10  $\mu$ l, 10-100  $\mu$ l and 100-1000  $\mu$ l) were used along with appropriate pipette tips for measuring and delivering solutions for all experiments.
- Pipette-aid (Drummond Scientific, Broomall, PA, USA) was attached to glass pipettes (10 and 20 ml) and used to transfer liquids.
- Synergy 185 Water Purification System (Molsheim, France) was used for generating double distilled water (DDW).
- SYSTAT<sup>®</sup> 12 (Systat Software, Inc., Chicago, IL, USA) was applied for statistical data analysis including ANOVA, ANOVA post-hoc tests, as well as linear and logistic regressions for PK-PD correlations.
- Vortex mixer (Vortex-2 Genie, Scientific Industries, Bohemia, NY, USA) was used whenever sample mixing was required.
- WinNonlin Professional Version 3.3 (Pharsight Corp., Mountainview, CA, USA) was used for pharmacokinetic data analysis and generation of pharmacokinetic parameters.

## **3.2 Methods**

### **3.2.1 HPLC Assay**

#### **3.2.1.1 Rationale:**

Clinical reports on drug kinetics in SCI are often anecdotal, because it is extremely difficult to perform systematic pharmacokinetic studies in SCI patients. This difficulty is due to the important inter-individual variability in the extent and location of injury. Therefore, the use of experimental models appears to be a suitable strategy for understanding pharmacokinetic alterations due to acute SCI, as well as the pathophysiological mechanisms involved (Garcia-Lopez P et al., 1996; Garcia-Lopez P et al., 1997). By comparing Riluzole pharmacokinetic behaviors in plasma, brain and different segments of spinal cord in a spinal cord injured rat model with those in uninjured control group, we could begin to understand the impacts of acute SCI on Riluzole pharmacokinetics.

The NACTN, a consortium of six university affiliated hospitals carried out a Phase I clinical trial of Riluzole as a neuroprotective treatment for acute SCI. To develop a robust method for the quantification of Riluzole in human plasma and CSF is a prerequisite as a member of NACTN, the pharmacology center to support the clinical studies. Methods have been described for the determination of Riluzole in human plasma and urine based on high performance liquid chromatography with ultraviolet detection (HPLC-UV) (Le Liboux A et al., 1997; Van Kan HJ et al., 2004) or coupled with tandem mass spectrometry (LC/MS/MS) (Le Liboux A et al., 1999). There was no method described to

study the uptake of Riluzole in human CSF. Meanwhile, these methods do not appear to be capable of quantifying the drug in CNS tissues of animals. On the other hand, although some simple HPLC-UV methods (Maltese A et al., 2005; Colovic M et al., 2004) have been published for quantifying Riluzole in rat brain, mouse plasma and central nervous system tissues; however, if using two different methods (HPLC conditions and biological samples pre-treatment) for the quantification and preparation of Riluzole in different tissues and organs, it would cause inconveniences and more errors. Therefore, we established a single rapid and sensitive HPLC method for the quantification of Riluzole in both rodent and human biometric samples, capable of satisfying our preclinical and clinical studies and detection requirements.

### **3.2.1.2 Stock Solutions and Standards**

Stock solutions were prepared by dissolving Riluzole and 5-MOP (I.S.) (Figure 6), respectively, in methanol at the concentration of 1mg/ml. Working standard solutions of riluzole (10 µg/ml) and I.S. (50 µg/ml and 10 µg/ml) were prepared from the stock solutions by a dilution with methanol and double distilled water (1:1, v/v), respectively, and kept at +4°C in 15 ml plastic tubes.

Drug-free blank plasma, brain and spinal cord tissues were obtained from male Sprague-Dawley rats and stored at -80°C after collection and processing.

Drug-free blank human plasma and CSF used for the preparation of spiked samples were obtained from the Methodist Hospital (Houston, TX, U.S.A.) and frozen at -80°C

until use. Human plasma samples (50 ml) were collected in sodium heparin-treated tubes. Twenty-six of CSF samples (volume range of 1 to 14 ml) were received, with CSF protein concentrations ranging from 22 to 1,345 mg/dl, and grouped into low CSF protein (LP) and high CSF protein (HP) groups. Pooled LP sample of 47 ml has the final protein concentration of 53.9 mg/dl, and HP of 41.5ml with protein concentration of 348.2 mg/dl; Intermediate CSF protein (IP) group of 10 ml was prepared by mixing LP and HP samples at a ratio of 7:3 (v/v) to yield the protein concentration of 142.2 mg/dl.

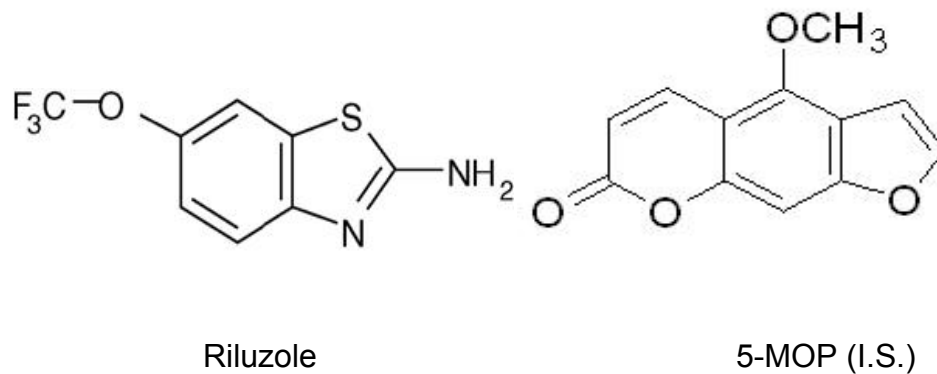


**Figure 6 Chemical Structures of Riluzole and 5-Methoxypsoralen (5-MOP, Internal Standard)**

### **3.2.1.3 Chromatographic Apparatus and Conditions**

The HPLC assay was developed using Waters system equipped with 717 plus auto sampler, 515 HPLC pump and 2996 UV detector set at 263 nm. Baseline resolution was achieved on Waters Symmetry® C18 column (3.0×150 mm, 3.5 µm) with Symmetry® C18 guard column (2.1×10 mm, 3.5 µm), eluted at the flow rate of 0.45 ml/min, with the mobile phase of acetonitrile: methanol: 0.1 M ammonium acetate (3:2:5, v/v/v), adjusted with acetic acid to pH 6.5.

### **3.2.1.4 Sample Preparations**

Plasma Samples: Two hundred µL of human plasma was mixed with 10 µl of 5-MOP (10 µg/ml, I.S.). After the addition of 1 ml of ethyl acetate, the mixture was vortexed for 30s and then centrifuged at 16,000 g for 20 minutes. Of the clear organic layer, about 1 ml was withdrawn and evaporated to dryness under the air stream. The residue was reconstituted in 200 µl of mobile phase, then mixed on a vortex for 30s and centrifuged at 16,000 g for 20 minutes. The clear supernatant samples were transferred into auto-sampler vials for HPLC assay analysis.

Similarly, 100 µl rat plasma was mixed with 10 µl of 5-MOP (50 µg/ml, I.S.), and centrifuged after the addition of 500 µl of ethyl acetate to withdraw about 500 µl of supernatant. The air stream dried residue was reconstituted in 1 ml of mobile phase.

Brain and spinal cord samples: The brain and spinal cord (cervical and thoracic segments) samples from rats were thawed, accurately weighed, and added to appropriate volumes of normal saline with the weight/volume ratio of 0.2. The samples were vortex-mixed and homogenized with tissue tearor homogenizer until thoroughly homogenized. 100  $\mu$ l brain and spinal cord (cervical and thoracic segments) homogenate samples were mixed with 10  $\mu$ l of 5-MOP (50  $\mu$ g/ml, I.S.), respectively. After the addition of 500  $\mu$ l ethyl acetate, the mixture was vortexed for 30s and then centrifuged at 16,000 g for 20 minutes. Of the clear organic layer, about 500  $\mu$ l was withdrawn and evaporated to dryness under the air stream. The residue was reconstituted in 1 ml of mobile phase, then mixed on a vortex mixer for 30s and centrifuged at 16,000 g for 20 minutes. The clear supernatant samples were transferred into auto-sampler vials for HPLC assay analysis.

CSF Samples: Two hundred  $\mu$ L CSF was mixed with 10  $\mu$ l 5-MOP (10  $\mu$ g/ml, I.S). The mixed aliquot was applied for solid phase extraction onto 3 ml Octadecyl (C18) speedisk columns, previously activated with 2 ml methanol and 2 ml water. After washed by 1 ml water and then eluted with 1 ml methanol, the methanol eluent was evaporated to dryness under a stream of air. The residual was reconstituted in 200  $\mu$ l mobile phase, then vortexed for 30s and centrifuged at 16,000 g for 20 minutes. The clear supernatant was transferred into auto-sampler vials for HPLC assay analysis.

### **3.2.1.5 Effects of Different CSF Protein Concentrations on Recovery and Accuracy of Quantification of CSF Samples**

The blank CSF samples received contained various CSF protein concentrations ranging from 22 to 1,345 mg/dl. Riluzole is highly protein binding drug, 96% in plasma. Therefore, we investigated if such different CSF protein concentrations would have impacts on the quantification of CSF samples. As previously mentioned, we randomly chose twenty-six CSF samples and classified into three groups [LP (53.9 mg/dl), IP (142.2 mg/dl) and HP (348.2 mg/dl)]. Spiked human CSF samples of these three groups were prepared at Riluzole levels of 7.8, 15.6, 31.25, 62.5, 125, 250, 500 and 1,000 ng/ml as daily calibrators. Calibration curves for LP, IP and HP samples were run repeatedly five, two and five times, respectively. Three spiked CSF samples at each Riluzole concentrations of 62.5 and 1,000 ng/ml were prepared at each CSF protein level and analyzed on the same day to calculate the accuracies. The procedure was repeated on a second day.

### **3.2.1.6 Validation Process**

#### ***Recovery***

For the rat and human plasma samples, the recovery and reproducibility of the extractions of Riluzole and 5-MOP were determined, respectively, by the analysis of nine independent spiked samples at each of three quantification levels (15.6, 125 and 1,000 ng/ml). Results were calculated by comparing the peak areas obtained from the direct

injections of standard solutions of compounds with those by extractions from spiked human plasma samples through the assay procedure previously described.

For the rat brain and spinal cord samples, the recovery and reproducibility of the extractions of both Riluzole and 5-MOP were determined by the analysis of nine independent fortified samples at three quantification levels (31.25, 500 and 4,000 ng/g). Results were calculated by comparing the peak areas obtained from the direct injections of standard solutions of compounds with those by extractions from spiked rat brain and spinal cord samples through the assay procedure described.

For the human CSF samples, the recovery and reproducibility of the extractions of both Riluzole and 5-MOP were determined by the analysis of eighteen independent fortified samples at two quantification levels (62.5 and 1,000 ng/ml). Results were calculated by comparing the peak areas obtained from the direct injections of standard solutions of compounds with those by extractions from spiked human CSF samples through the assay procedure described.

### ***Linearity, accuracy and precision***

The lower limit of quantification (LLOQ) was defined as the mean Riluzole concentration resulting in a peak response with a signal to noise ratio of 10. A least-squares linear regression method ( $1/x^2$  weighting) was used to determine the slope, intercept and correlation coefficient of linear regression equation.

For the rat and human plasma samples, the linearity of response was evaluated in the concentration range of 7.8 to 1,000ng/ml. Spiked plasma samples at levels of 7.8, 15.6, 31.25, 62.5, 125, 250, 500 and 1,000 ng/ml were used as daily calibrators. Nine spiked plasma samples at each level of 15.6, 125 and 1,000 ng/ml were analyzed on the same day to calculate the accuracy and intra-day precision of the assay, using the established calibration curve. The inter-day precisions at the three levels were examined three times on five separate days.

For the rat brain and spinal cord samples, the linearity of response was similarly evaluated between 31.25 and 4,000 ng/g. Spiked brain and spinal cord samples at levels of 31.25, 62.5, 125, 250, 500, 1,000, 2,000 and 4,000 ng/g were used as daily calibrators. Nine spiked biometric samples at concentrations of 31.25, 500 and 4,000 ng/g were prepared and analyzed on the same day to calculate the accuracy and intra-day precision of the assay, using the established calibration curve. The inter-day precisions at the three levels were examined three times on five separate days.

For the human CSF samples, the linearity of response was also evaluated between 7.8 and 1,000 ng/ml. Triplicate spiked CSF samples at concentrations of 62.5 and 1,000 ng/ml were prepared at individual CSF protein levels (LP, IP and HP) and analyzed on the same day to calculate the accuracy and intra-day precision of the assay, using the individual calibration curves and the pooled calibration curve, respectively. Inter-day precisions at 62.5 and 1,000 ng/ml were determined on two separate days.

### ***Stability test***

We investigated three kinds of stabilities for rodent and human samples, bench-top stability, three-cycle freezing and thawing stability and long-term stability.

The bench-top stabilities of rat and human plasma samples at 15.6, 250 and 1,000 ng/ml levels were investigated by repeated injection immediately after work-up, as well as 8 and 24 h post the preparation. The bench-top stabilities of rat brain and spinal cord samples was investigated at 62.5, 500, 4,000 ng/g levels. The bench-top stability of human CSF samples was investigated at 15.6, 125 and 1,000 ng/ml levels. The influence of temperature changes on the stored rodent and human biometric samples was evaluated by analyzing samples (n=3) of three Riluzole levels after three cycles of freezing (-80°C) and thawing cycles, to +4°C for 48 hr storage. The long-term stabilities of the Riluzole in spiked samples were evaluated after storage at -80°C for one month at respective three levels for these biometric samples.

## **3.2.2 Pharmacokinetics of Different Formulations in Rats**

### **3.2.2.1 Rationale**

Whether a change in Riluzole formulations would alter the pharmacokinetics of Riluzole was investigated in a normal rat model. The formulated oral suspension and solution would be expected to have more consistent Riluzole exposures and higher bioavailabilities than other formulations (oral tablet and paste). Because the acute SCI patients enrolled in clinical phase I trial would receive the Riluzole treatment as oral tablet or nasogastric paste (crushed from the tablets), it was unclear whether the alteration of Riluzole formulation/administration would affect the bioavailability of Riluzole, which in turn might result in different levels of side effects or efficacy of Riluzole in the acute SCI patients. Therefore, we conducted a preclinical study to test our hypothesis.

### **3.2.2.2 Dosing of Riluzole of Different Formulations**

Crushed tablet and paste were grinded from the marketed oral Riluzole film-coated tablet (Riluzek<sup>®</sup>), of which paste was further grinded from tablet to fine particle. Oral suspension was prepared by dissolving Riluzole powder (from Sigma) into the suspension vehicle (purchased from PCCA). The solutions for oral and intravenous administration were prepared by dissolving Riluzole powder into the mixture of propylene glycol and double distilled water (40:60, v/v).

Sprague-Dawley rats, with a body weight between 250 and 300 g, were used in this study. Animals were kept in standard animal facilities with free access to food and water, in a temperature and humidity-controlled room with 12 h on-off light cycle. All experiments would be conducted in accordance with NIH Guidelines for the Care and Use of Animals and with an approved animal protocol from the University of Houston Institutional Animal Care and Use Committee (IACUC). Based on the clinical dose 100 mg/70 kg per day for patients and LD<sub>50</sub> reported in product monograph (oral: 45 mg/kg and intravenous: 21 mg/kg in rats) (FDA website), the oral dosage of 10 mg/kg and intravenous (i.v.) dose of 5 mg/kg were selected for this animal study, taking into consideration of the body surface area and toxicity. The animals were divided into six groups (n=5 each; except crushed paste alone, n=3), five groups of animals received Riluzole crushed tablet, crushed paste alone, crushed paste with glycerin, suspension and solution orally at the dose of 10 mg/kg, respectively, and the sixth group received Riluzole solution intravenously at the dosage of 5 mg/kg as a reference to calculate the absolute bioavailability. Two hundred µl of the blood samples were withdrawn via tail vein at 15 min, 30 min, 1 hr, 2 hr, 4 hr, 6 hr, 8 hr, 10 hr, 12 hr and 24 hr for the oral groups, and at the same time points up to 12 hr for the i.v. group. The blood samples were centrifuged at 16,000 g for 15 minutes immediately to collect the plasma samples to be stored at -80°C until analysis.

### **3.2.2.3 Pharmacokinetic Data Analysis**

Data from the pharmacokinetic studies were analyzed using WinNonLin Professional version 3.3 to ensure which compartment model is the best fitted model to

pharmacokinetic data. One-compartmental and two-compartmental model with or without different weighting factors (uniform weighting,  $1/Y$  and  $1/Y^2$ ) were fitted for each plasma-time profile with the non-linear least-squares regression analysis. Appropriate model selection was based on: (a) Minimum value for the diagnostic statistics of Akaike's information criterion (AIC) as calculated by Equation 1; (b) Coefficient of determination ( $R^2$ ) between the observed data points and the corresponding calculated ones based on the selected model; and (c) Visual inspection of the observed data points and the corresponding model-generated plasma concentration-time profiles:

$$AIC = N \times \ln WSS + 2p \quad \text{Equation 1}$$

Where  $N$  is the number of data points,  $p$  is the number of parameters to be estimated and  $WSS$  is the weighted sum of squares calculated according to Equation 2.

$$WSS = \sum (Y_{obs,i} - Y_{cal,i})^2 \times W_i \quad \text{Equation 2}$$

Where  $W_i$  is a weighting factor for fitting the model to the experimental data (drug concentrations) and can be 1,  $1/Y$  or  $1/Y^2$ ,  $Y_{obs,i}$  is the measured drug concentration and  $Y_{cal,i}$  is the estimated value for the drug concentration. Uniform weighting was usually applied and any weighting factors ( $1/Y$  or  $1/Y^2$ ) were applied only when necessary since the best model is the one with the least number of variables/assumptions.

Compartmental analysis is employed for a more extensive characterization of the generated plasma concentration-time profiles.

Plasma concentration-time profile was constructed on a semi-log plot by using Microsoft Excel. Key pharmacokinetic parameters such as peak concentration ( $C_{max}$ ), time to reach peak ( $t_{max}$ ), area under the curve (AUC), absorption rate constant ( $k_a$ ), elimination rate constant ( $k$ ), clearance (CL) and volume of distribution ( $V$ ) were generated by fitting the plasma concentration-time profiles for each group. Elimination rate constant ( $k$ ) was determined from the terminal phase by linear regression. Area under the plasma concentration-time curve (AUC) was calculated by trapezoidal rule. The absolute bioavailability ( $F$ ) was the ratio of AUC for oral dosing of Riluzole to AUC for i.v. dosing of Riluzole solution. The total body clearance (CL) was calculated by dividing dose by AUC (Dose/AUC). Volume of distribution ( $V$ ) was calculated by dividing CL by  $k$  (CL/ $k$ ). The time for maximum concentration ( $t_{max}$ ) and the maximum concentration ( $C_{max}$ ) were calculated by Equation 3 and Equation 4, respectively.

$$t_{max} = \frac{\ln(k_a/k)}{k_a - k} \quad \text{Equation 3}$$

$$C_{max} = [F \cdot D \cdot k_a / V(k_a - k)] [e^{-k \cdot t_{max}} - e^{-k_a \cdot t_{max}}] \quad \text{Equation 4}$$

### **3.2.2.4 Statistical Data Analysis**

The statistical significance of differences among groups in the parameters of pharmacokinetic studies was evaluated by ANOVA and Tukey's post-hoc at  $p < 0.05$ , using the statistical software "SYSTAT 12".

## **3.2.3 Impacts of Acute Spinal Cord Injury on Riluzole**

### **Pharmacokinetics in Rats**

#### **3.2.3.1 Rationale**

Acute spinal cord injury (SCI) results in a devastating loss of neurological function below the level of injury and adversely affects multiple physiological systems within the body. However, it is unclear how these alterations will affect the pharmacokinetics of absorption, distribution, metabolism and excretion of therapeutic agents. Spinal cord injured rats and uninjured controls would be used to establish the impacts of SCI on Riluzole pharmacokinetics in absorption, distribution, metabolism and excretion by (a) monitoring pharmacokinetic profiles of Riluzole in plasma, brain and spinal cord after a single dose of 8 mg/kg, and (b) evaluating the steady-state concentrations of Riluzole in each of the bio-matrices after multiple-dosing regimen for 3-day treatment (8 mg for the first dose, followed by 6 mg/kg dose every 12 hr for five doses) in cervical spinal cord injured (SCI) rats (female Wistar rats), respectively. The uninjured rats receiving the same regimens served as the control group.

### **3.2.3.2 Pharmacokinetic Studies**

Exploring the effects of acute SCI on the pharmacokinetics of Riluzole is a collaborative effort with Dr. Michael Fehlings (Professor of Neurosurgery), in Division of Genetics & Development, Toronto Western Research Institute (TWRI) of Canada. They are experienced in animal spinal cord injured model. Therefore, the treatment and sample harvesting of animals were performed by Dr. Fehling's group.

Two models of female Wistar rats (250-300 g) with cervical spinal cord injury (SCI) and of the matched uninjured control, respectively, were used. A laminectomy was performed from C7 to T1. Each rat received a 1-minute extradural clip compression injury of the cervical cord between C7 and T1 with a modified aneurysm clip precalibrated to deliver a closing force of 35 g for 1 minute. The control group of rats was randomly assigned to receive sham operations; each of these control rats had only a C7-T1 laminectomy.

Riluzole powder was solubilized in 22.5% 2-hydroxypropyl- $\beta$ -cyclodextrin (HB- $\beta$ -CD, Sigma) to a concentration of 8 mg/ml, and then diluted with normal saline to a concentration of 2.4 mg/ml for injections.

Two regimens of Riluzole treatment were given by intraperitoneal (I.P.) administration at 1 hour post SCI. One regimen group (n=28) was of a single dose of 8 mg/kg, with plasma, brain and spinal cord of cervical and thoracic segments collected at 15 min, 30 min, 1 hr, 3 hr, 6 hr, 9 hr and 12 hr (plasma only), respectively (brain: only 6 hr and 9 hr

for acute SCI rats) (n=4 for each time point). Another regimen group (n=28) was of multiple-dosing with the first dose of 8 mg/kg and the following five doses of 6 mg/kg every 12 hours for 3 days (n=4 for each time point). The samples of plasma, brain and spinal cord of cervical and thoracic segments were collected at 12 hrs after the 2nd injection (2nd dose, Day 1) and 2 hrs after the last injection (the 6th dose, Day 3). The plasma samples of 500  $\mu$ l were collected by adding 100  $\mu$ l of 50 mM EDTA to 1 ml of whole blood and centrifuging at 3,000 g for 10 min at 4°C.

All the brain, plasma and spinal cord samples were shipped in packages with dry ice, from University of Toronto to College of Pharmacy, University of Houston, and were stored at -80° C upon receipt until HPLC assay analysis.

### **3.2.3.3 Pharmacokinetic Data Analysis**

The basic pharmacokinetic parameters, such as k,  $t_{1/2}$ ,  $C_{max}$ ,  $t_{max}$  and AUC were derived using WinNonLin Professional version 3.3. The one-compartment first order assumption with no lag time and first order elimination model was used.

The accumulation or multiple dose factors at steady state ( $MDF_{ss}$ ) were calculated by the equation:

$$MDF_{ss} = [1 / (1 - e^{-kT})]$$

**Equation 5**

Where  $\tau$  is dosing interval in hr,  $k$  is the repeating elimination rate constants in individual compartments.

The tissue/plasma partition coefficient ( $K_p$ ) of Riluzole for brain and spinal cords were derived experimentally from the tissue/plasma ratios, respectively, toward the end of the study by the following equation:

$$\frac{AUC(t)_{tissue}}{AUC(t)_{plasma}} = \frac{\int_0^t C_{tissue}(t)dt}{\int_0^t C_{plasma}(t)dt} = K_p \quad \text{Equation 6}$$

In order to explain the PK behaviors of Riluzole among plasma, brain and spinal cord, a three-compartment model was built by the ADAPT II pharmacokinetic software package (Biomedical Simulations Resource, Los Angeles, CA, USA) based on the data from the single-dose study. The kinetics of Riluzole among the these compartments were to be described by the following model structure (Figure 7). If we let  $x_0(t)$ ,  $x_1(t)$ ,  $x_2(t)$  and  $x_3(t)$  represent the amounts of drug input after I.P. administration and in compartments 1, 2 and 3 , respectively, according to mass balance rule, the following differential and output equations (7-10) described the model depicted above.

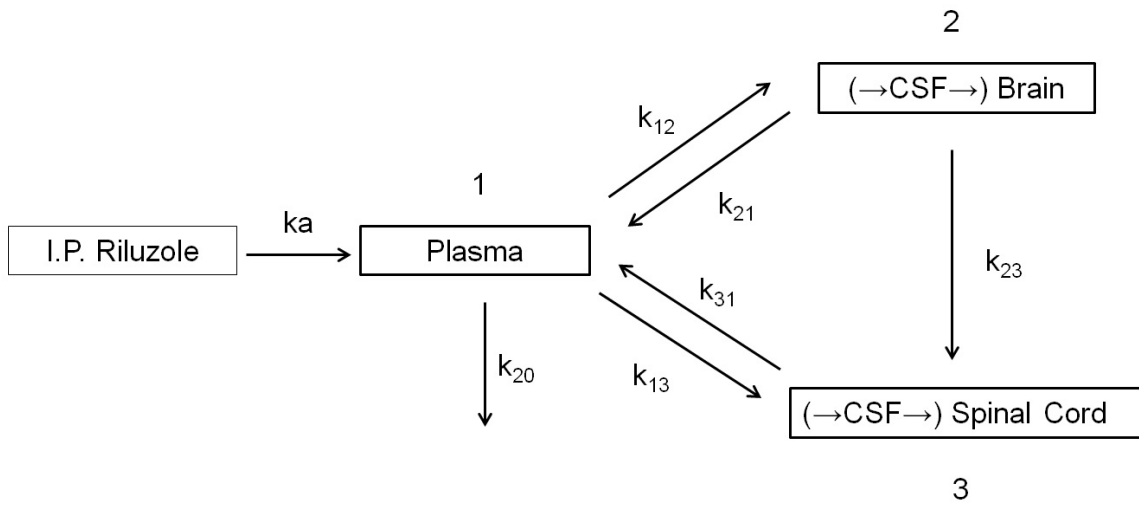


**Figure 7 Final Model Structure of Riluzole in Plasma, Brain and Spinal Cord Built by ADAPT II**

**Compartment 1 is Riluzole in Plasma, Compartment 2 is Riluzole in Brain, and Compartment 3 is Riluzole in Spinal Cord**

**ka: Absorption rate constant,**

**k<sub>20</sub>: Elimination rate constant from plasma,**

**k<sub>12</sub> and k<sub>21</sub>: Transferring rate constants of Riluzole between plasma and brain compartments,**

**k<sub>23</sub>: Transferring rate constant of Riluzole from brain to spinal cord compartments,**

**k<sub>13</sub> and k<sub>31</sub>: Transferring rate constants of Riluzole between plasma and spinal cord compartments.**

The three-compartment model was constructed based on the data from SCI and control uninjured groups, respectively, after the single I.P. dose. The parameter of absorption rate constant ( $k_a$ ) and micro-constants of  $k_{12}$ ,  $k_{21}$ ,  $k_{13}$ ,  $k_{31}$ , and  $k_{23}$  would be derived (Figure 7). With the model, the impacts of SCI on individual micro-constants and the extent of the effects could be determined quantitatively between SCI and uninjured rats.

The model selection with different initial estimations of parameters was based on: (a) Minimum value for the diagnostic statistics of Akaike's information criterion (AIC); (b) Coefficient of determination ( $R^2$ ) between the observed data points and the calculated ones based on the selected model; and (c) Rationality of the predicted pharmacokinetic parameters.

$$dX_0/dt = -X_0 \times k_a \quad \text{Equation 7}$$

$$dX_1/dt = -X_0 \times k_a + X_2 \times k_{21} + X_3 \times k_{31} - X_1 \times k_{12} - X_1 \times k_{20} - X_1 \times k_{13} \quad \text{Equation 8}$$

$$dX_2/dt = X_1 \times k_{12} - X_2 \times k_{21} - X_2 \times k_{23} \quad \text{Equation 9}$$

$$dX_3/dt = X_1 \times k_{13} + X_2 \times k_{23} - X_3 \times k_{31} \quad \text{Equation 10}$$

The established model was validated by the comparisons of simulated and observed Riluzole concentrations after multiple-dosing study. The simulation was performed using the parameters derived from the single dose experiment.

#### **3.2.3.4 Statistical Data Analysis**

The statistical significance of differences between SCI injured and uninjured groups in the Riluzole concentrations of pharmacokinetic studies was evaluated by Student's t-test, at significant level  $p < 0.05$ , using the Microsoft excel.

## **3.2.4 Phase I Clinical Trial of Riluzole in Acute Spinal Cord**

### **Injured Patients**

#### **3.2.4.1 Rationale**

Several studies have demonstrated that Riluzole is neuroprotective and promotes functional neurological recovery in various species of animal models of brain and spinal cord ischemic and traumatic injury (Heurteaux C et al., 2006; Ates O et al., 2007; Lang-Lazdunski L et al., 1999; chwartz G and Fehlings MG, 2001). Other authors have reported that the effects of Riluzole are synergistic with those of methylprednisolone, which is the only drug used in routine clinical practices to attempt to attenuate secondary injury effects after SCI (Mu X et al., 2000). Therefore, NACTN set up a phase I trial of Riluzole which was conducted as a multi-site, single arm active treatment pilot study with an enrollment goal of 36 patients.

#### **3.2.4.2 Criteria of Patient Selection**

Total thirty-six (36) SCI patients were enrolled at six sites; 35 patients completed the full dosing regimen.

##### *Inclusion Criteria:*

Age:  $\geq 18$  years and  $\leq 70$  years

- Written informed consent to participate in the study
- No other life-threatening injury
- Spinal cord injury at neurologic level from C4 to T12

- ASIA impairment scale (AIS) level A, B or C
- No cognitive impairment which would preclude an informed consent (including moderate or severe traumatic brain injury)
- Dosing time: within 12 hours since injury

*Exclusion Criteria:*

- Hypersensitivity to riluzole or any of its components
- Unable to receive riluzole orally or via NG tube
- History of liver or kidney disease (e.g. Hepatitis A, B or C, Cirrhosis, etc.)
- A recent history of regular substance abuse (illicit drugs or alcohol)
- Unconscious
- Penetrating spinal cord injury
- Pregnancy as established by urine pregnancy test
- Is currently involved in another SCI research study
- Has a mental disorder or other illness, which in the view of the site investigator, would preclude accurate evaluation
- Unable to commit to the follow-up schedule
- Is a prisoner
- Unable to converse, read or write English at the elementary school level

### **3.2.4.3 Treatment with Riluzole (Rilutek®)**

Patients received Riluzole (Rilutek®, Sanofi-Aventis, USA, supplied by the hospital pharmacy at each center) of 50 mg by oral or nasogastric (NG) administration every 12 hours, starting within 12 hours of injury for 28 doses. On the 3rd and 14th days, plasma samples were collected one hour pre-dose and one or two hours post-dose for trough and peak concentrations, respectively. All other treatments were per standard of care. Five patients received concomitant methylprednisolone.

### **3.2.4.4 Plasma Protein Binding**

In order to evaluate the extent of free (unbound) Riluzole in human plasma, ultrafiltration was employed. Centrifree® YM-30 devices (Millipore Ireland Ltd.) were used. One ml human plasma samples were added into the ultrafiltration device and centrifuged at 1,000 g with fixed angle rotor. Ultrafiltrate (100 µl) from each subject was collected, and mixed with 5 µl 5-MOP (internal standard). The same extraction and reconstitute procedures previously described in [section 3.2.1.4](#) were followed. The clear supernatant samples were analyzed by the validated HPLC assay.

### **3.2.4.5 Pharmacokinetic Evaluation**

#### **3.2.4.5.1. Plasma Sampling**

Plasma blank control (5 ml) and two plasma samples for peak and trough concentrations on Day 3 and Day 14, respectively, were collected by centrifugation of blood samples immediately at 2,700 g for 10 min, then stored at -80°C (or at least as low as -20°C) prior

to the shipment with dry ice to the Pharmacology Center of NACTN at University of Houston, College of Pharmacy at Texas Medical Center. The blood samples were labeled to conceal patient identity.

Plasma, instead of serum, samples were collected, because it has been established that Riluzole concentrations in plasma and serum are comparable at concentration < 500 ng/ml (Van Kan HJ et al., 2004). With a standard drug regimen of 50 mg twice daily, Riluzole serum concentrations are anticipated in the range of 20-250 ng/ml (Groeneveld GJ et al., 2003). The plasma samples retaining clotting factors will have less variability than serum samples removing the factors.

### 3.2.4.5.2. Individual Pharmacokinetic Analysis

Individual pharmacokinetics were evaluated using two concentration-time data on each day (Day 3 and Day 14) to obtain the elimination rate constants (k), then using the standard pharmacokinetic equations (11-14) to estimate other parameters of clearance (CL/F) and volume of distribution (V/F) normalized by the bioavailability (F).  $AUC_{0-12}$  and  $AUC_{0-\infty}$  were calculated using the trapezoidal rule.

$$t_{1/2} = 0.693/k$$

**Equation 11**

$$AUC_{0-\infty} = AUC_{0-t} + C_t/k,$$

when  $C_t$  was the trough concentration calculated from the pre-dosing sampling time

**Equation 12**

$$CL/F = \text{Dose} / AUC_{0-\infty}$$

**Equation 13**

$$V/F = CL/k$$

**Equation 14**

### **3.2.4.5.3. Population Pharmacokinetic Analysis**

#### ***Non-linear Mixed Effect Modeling (NONMEM)***

The Population PK analysis for repeated measures was conducted via nonlinear mixed-effects modeling using software of NONMEM v 7.2.0. NONMEM is a computer program, written in using Abbreviated Fortran, designed to fit general statistical (nonlinear) regression models to data. Proper modeling of such data involves accounting for both unexplainable inter- and intra-subject effects (random effects), as well as measured concomitant effects (fixed effects).

NONMEM allows for this ‘mixed effects modeling’. R-program is a statistical software package used for data visualization and exploration, as well as statistical programming and simulation. In the current dissertation, R-program has been used mostly for creating graphics, bootstrapping, and simulation based on the bootstrap estimates.

#### ***Basic Model Structure***

The Population PK software is capable of analyzing clinical data with sparse samples, deviated sampling time and/or missing samples. Riluzole plasma concentration-time data were fitted by one compartment structural pharmacokinetic models with first-order absorption and elimination. The first-order conditional estimation method with  $\eta$ - $\epsilon$

interaction (FOCEI) was used for all model runs. Riluzole concentration observations that were below the analytical assay quantification limit or any values that were otherwise missing were excluded from the analysis. Observed values of any time-dependent covariates were inserted chronologically in the population PK data set with linear interpolation for data records between observed time points.

Model selection was guided by various goodness-of-fit criteria, including diagnostic scatter plots, plausibility of parameter estimates and precision of parameter estimates.

The basic pharmacokinetic parameters are clearance (CL/F), volume of distribution (V/F), and absorption constant (ka). The first-order elimination rate constant (k) was calculated as follows:

$$k = (CL/F)/(V/F) \quad \text{Equation 15}$$

Inter-individual variabilities in clearance and volume of distribution were modeled by the use of a proportional error model as follows:

$$CL_j = \widetilde{CL}_j \exp(\eta_{jCL}) \quad \text{Equation 16}$$

$$V_j = \widetilde{V}_j \exp(\eta_{jV}) \quad \text{Equation 17}$$

Where  $\eta_{jCL}$  represents the (proportional) difference between the true clearance of individual  $j$  ( $CL_j$ ) and the typical value ( $\widetilde{CL}_j$ ) predicted for the patient by the regression model, and  $\eta_{jV}$  represents the (proportional) difference between the true volume of distribution in individual  $j$  ( $V_j$ ) and the typical value predicted for the patient by the regression model ( $\widetilde{V}_j$ ). The random variables of  $\eta_{jCL}$  and  $\eta_{jV}$  are distributed with means of zero and variances of  $\omega^2_{CL}$  and  $\omega^2_V$ , respectively. The variances  $\omega^2_{CL}$  and  $\omega^2_V$  represent the magnitude of inter-individual variability in clearance and volume of distribution, respectively, which are not explained by the regression models in this population.

Residual variability was modeled using an additive and proportional combined error model as follows:

$$C_{obsij} = C_{predij} \times (1 + \varepsilon_{propij}) + \varepsilon_{addij} \quad \text{Equation 18}$$

In which  $C_{obsij}$  and  $C_{predij}$  are the measured and predicted plasma riluzole concentrations, respectively, for individual  $j$  on occasion  $i$ . Random variable  $\varepsilon_{ij}$  denotes the residual intra-individual error, which is distributed with a mean of zero and a variance of  $\sigma^2$ .

### **Covariate Model**

Covariates considered for inclusion in the regression analysis included demographic factors (age, gender, race, and body weight), laboratory parameters (hepatic function, serum creatinine, creatinine clearance, albumin, and proteins), smoking status, and concomitant medications. Covariate effects on volume of distribution were only considered after the final regression model was obtained for clearance.

The influence of each patient covariate on the clearance was individually assessed by univariate analysis. A full covariate regression model for clearance was subsequently derived by incorporating all significant covariates, and this was tested against restricted models by removing each covariate in turn to arrive at a final regression model. The regression relationship was modeled for continuous covariates, such as body weight (WT), as follows:

#### Linear

$$CL_i = CL_{pop} + slope * WT_i \quad \text{Equation 19}$$

$$CL_i = CL_{pop} + slope * (WT_i - WT_{pop}) \quad \text{Equation 20}$$

(Centered around population mean)

#### Power

$$CL_i = CL_{pop} * WT_i^{exponent} \quad \text{Equation 21}$$

(Allometric model: exponent=0.75)

$$CL_i = CL_{pop} * (WT_i / WT_{pop})^{exponent} \quad \text{Equation 22}$$

(Normalized by population mean)

Exponential

$$CL_i = CL_{pop} * \exp(\text{slope} * WT_i) \quad \text{Equation 23}$$

Where  $CL_i$  and  $CL_{pop}$  are individual and population clearance, and  $WT_i$  and  $WT_{pop}$  are individual and population body weight.

For dichotomous covariates, such as sex (as signed a value of 0 for female or 1 for male), the relationship was modeled as follows:

Power

$$CL_i = CL_{pop} * \text{slope}^{\text{Sex}} \quad \text{Equation 24}$$

Exponential

$$CL_i = CL_{pop} * \exp(\text{slope} * \text{Sex}) \quad \text{Equation 25}$$

The change in the NONMEM objective function produced by the inclusion of a covariate term (asymptotically distributed as  $\chi^2$  with degrees of freedom equal to the number of parameters added to the model) was used to compare alternative models (likelihood ratio test). A change in objective function of at least 3.8, associated with a p value of <0.05 with one degree of freedom, was required for statistical significance at the initial

covariate screening stage; this was increased to 7.8, associated with a p value of <0.005 with one degree of freedom, at subsequent stages (multivariate analysis).

### ***Model Evaluation***

The final population PK model was evaluated using a stratified nonparametric bootstrap and a predictive check. For the nonparametric bootstrap procedure, 1000 replicate data sets were generated by random re-sampling from the original data set with replacement, using the individual as the sampling unit. Population parameters for each data set were subsequently estimated using NONMEM, and empirical 95% confidence intervals (CIs) were constructed by observing the 2.5<sup>th</sup> and 97.5<sup>th</sup> quantiles of the resulting parameter distributions for all bootstrap runs.

For the predictive check, 100 Monte Carlo simulation replicates of the original data set were generated using the final population PK model, and the distribution of the median concentration ( $C_{med}$ ) in the simulated data was compared with the distribution of the same characteristics in the observed data using exploratory graphics.

#### **3.2.4.6 Monitoring of Potential Hepatotoxicity and Metabolic Status**

Blood for monitoring the levels of liver enzymes was drawn on admission and on days 3, 7, 10 and 14, as well as at 3-month and 6-month follow-ups. The enzymes monitored at individual sites were Alanine Transferase (ALT), Aspartate Transaminase (AST), Gamma-glutamyl Transpeptidase (GGT) and Alkaline Phosphatase (ALP). Albumen and

Bilirubin were also monitored, as well as the hemogram, platelets, electrolytes, glucose, blood urea nitrogen, creatinine, prothrombin time and International Normalized Ratio. We used the following equation to calculate the upper limit of normal range (ULN) ratios (Equation 26) of ALT and AST for later PK-PD correlations. Liver enzyme levels had mild, moderate and severe elevations when ULN ratios fell in 1-2.5 times, 2.5-5.0 times and 5.0-25.0 times of ULN, respectively.

Upper limit of normal range (ULN) Ratio = ALT or AST Value/ULN of ALT or AST at each corresponding site

**Equation 26**

Where Day 3, Day 14 and Maximal ULN ratios would be calculated.

#### **3.2.4.7 Monitoring of Efficacy**

The ASIA motor, sensory, impairment scores would be examined and recorded at individual sites on day 1 as baseline, day 3 and day 14, upon discharge, as well as at 6-week, 3-month and 6-month follow-ups. The efficacy outcomes were calculated using the following equation:

Maximal Score Change = Maximal score – baseline score

**Equation 27**

Maximal score was obtained at any time within 6-month follow-up, maximal motor and sensory score changes would be calculated.

Score Change = Score during the follow-up examinations – Baseline score

**Equation 28**

Two-week, 3-month and 6-month motor and sensory score changes would be obtained.

#### **3.2.4.8 Pharmacokinetic/Pharmacodynamic (PK/PD) Correlations**

Linear and logistic regressions were used to establish the correlations of PK parameters ( $C_{max}$  or AUC) on Day 3 and/or Day 14 with PD outcomes (ULN ratios of ALT, AST; The 3-month, 6-month or maximal changes of ASIA motor and sensory scores). The correlations were selected based on the p values for both linear and logistic regressions at  $p < 0.05$ . Meanwhile, the odds ratio is the primary measure of effect size for logistic regression, an odds ratio of one indicates that the odds of a case outcome are likely to be equal for both groups under comparison. The further deviation of the odds deviate from one, the stronger the relationship is.

## **CHAPTER 4. RESULTS**

### **4.1 HPLC Assay**

#### **4.1.1 UV Spectrum**

The 3-dimension UV absorbance for Riluzole was scanned from 200 to 400 nm (Figure 8). The maximum absorption wavelengths were 224 and 263 nm for Riluzole, which could be precisely measured (Figure 9). The wavelength of 263 nm was selected to monitor Riluzole, because the wavelength of 224 nm might pose a problem of interference from the absorbance of acetonitrile, the organic solvent used in the mobile phase, meanwhile the I.S. also had strong absorbance at 263 nm.

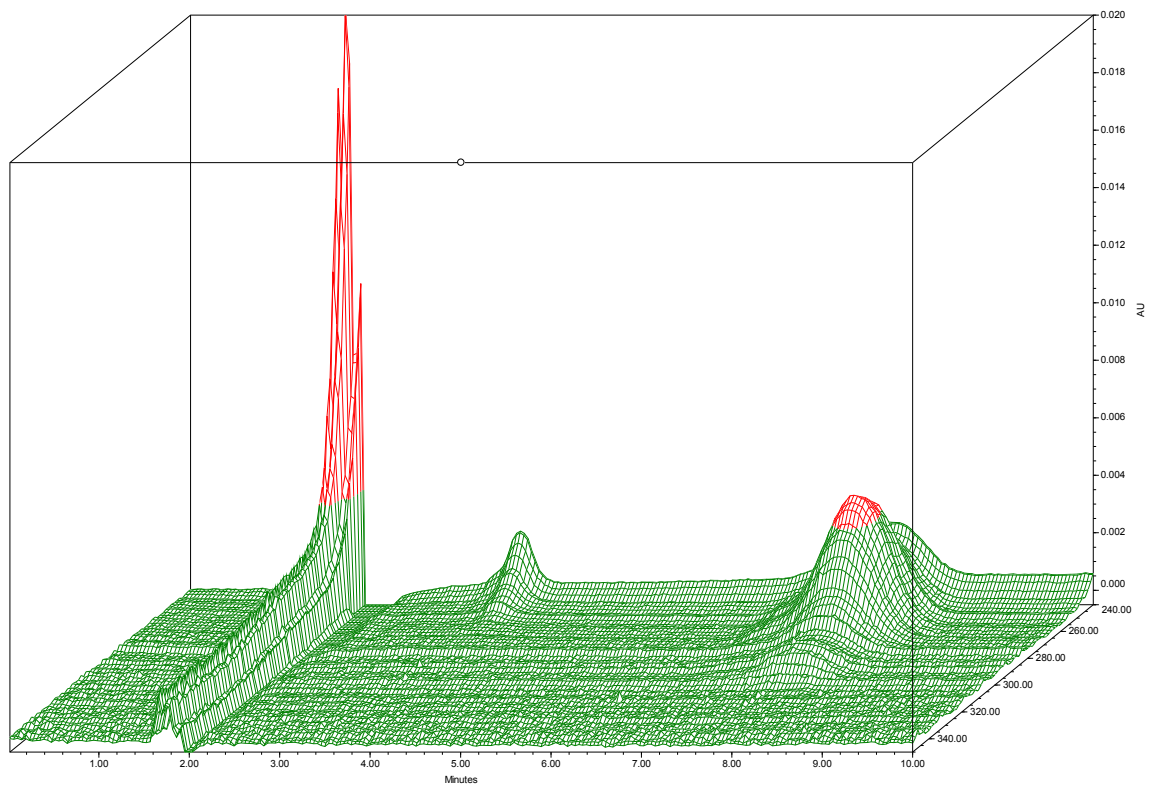


**Figure 8 3D Diagram of UV Absorbance of Riluzole from 200 to 400 nm**

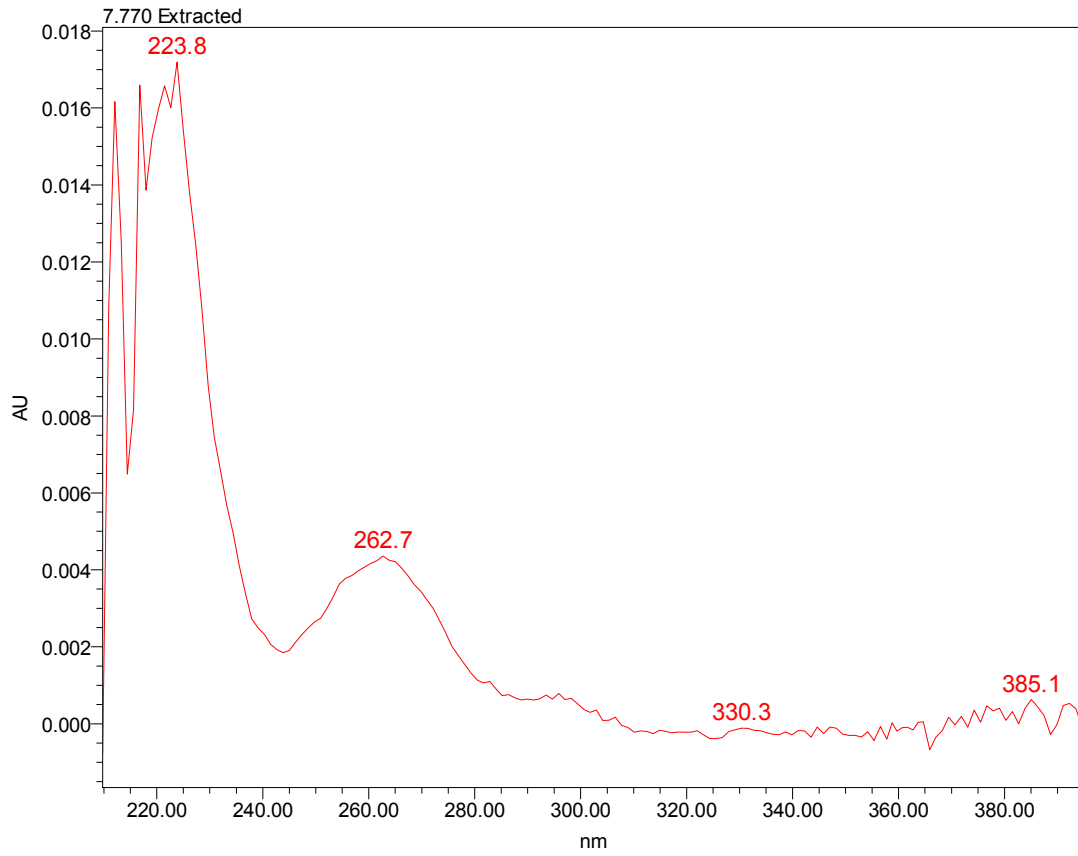


**Figure 9 2D Diagram of UV Absorbance of Riluzole from 200 to 400 nm**

### **4.1.2 HPLC Assay Validation**

A specific, accurate and precise HPLC method with UV detection was developed and validated for the quantification of Riluzole in rodent and human biomatrix samples. The method requires only a small volume (100 µl for rodent samples or 200 µl for human samples) of various biomatrix samples, and the assay sensitivities at the concentration of 7.8 ng/ml for rat and human plasma, and human CSF samples, as well as 31.25 ng/g for rat brain and spinal cord samples are sufficient for the preclinical and clinical studies.

#### **4.1.2.1 HPLC Chromatogram**

Riluzole was recovered efficiently from the rodent and human biomatrix samples using ethyl acetate extraction and human CSF samples with solid phase extraction, respectively. Retention times of Riluzole and I.S. were 7.1 and 9.0 minutes, respectively. No interfering peaks were observed in the chromatograms of all the blank biomatrix samples and samples with concomitant medications (Figures 10-14).

#### **4.1.2.2 Linearity**

For the rodent samples, the lower limit of quantification (LLOQ) were 31.25 ng/g for brain and spinal cord, and 7.8 ng/ml for plasma (density of plasma = 1.005 g/ml). The assay was linear from 31.25 to 4,000 ng/g for brain and spinal cord samples, and 7.8ng/ml to 1,000 ng/ml for plasma samples with correlation coefficients of 0.9999 (Figures 15A-15C). The recoveries of Riluzole from spinal cord, brain and plasma from liquid-liquid extraction with ethyl acetate were quantitative, 104%, 100% and 97%, respectively.

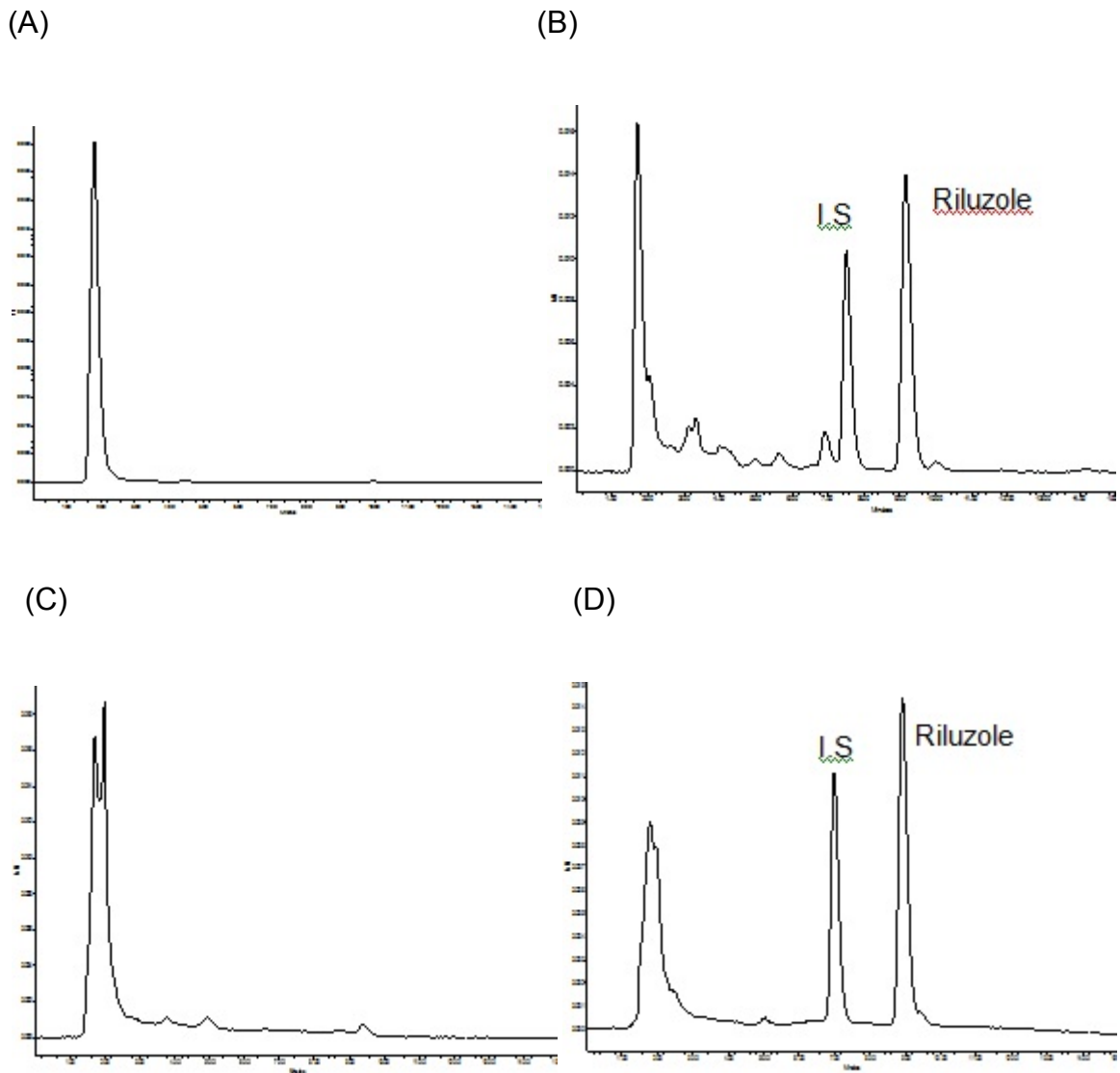


**Figure 10 Authentic HPLC Chromatograms of Extracts from (A) Blank Human Plasma, (B) Spiked Plasma Sample, (C) Blank Human CSF, and (D) Spiked CSF Sample (Riluzole:1,000 ng/ml, retention time of 9.0 min; I.S. : 500 ng/ml, retention time of 7.1 min)**

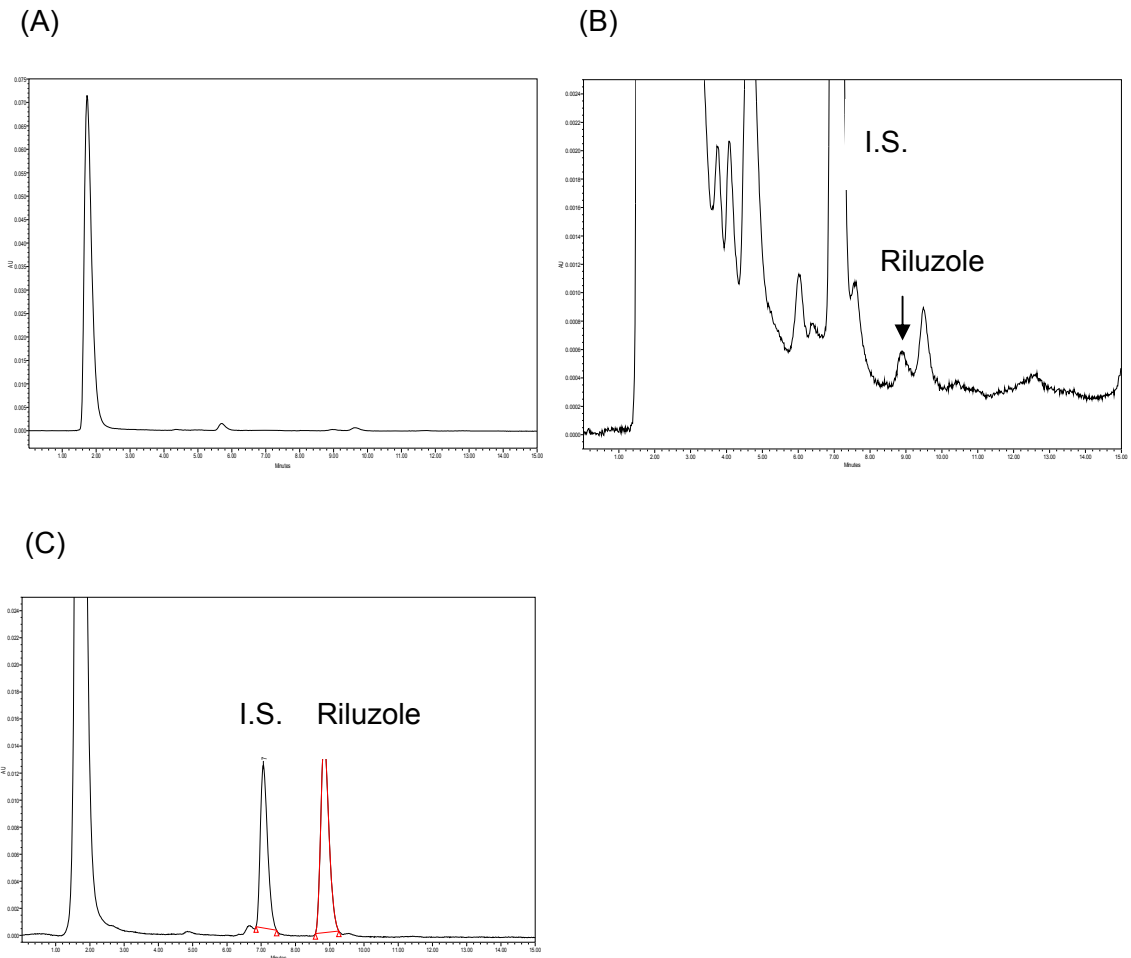


**Figure 11 Authentic HPLC Chromatograms of Extracts of (A) Blank Spinal Cord, (B) Spiked Spinal Cord Sample at LLOQ (31.25 ng/g) and (C) Spiked Spinal Cord Sample at 4,000 ng/g (Retention time: 9.0 min for Riluzole and 7.1 min for I.S., respectively)**

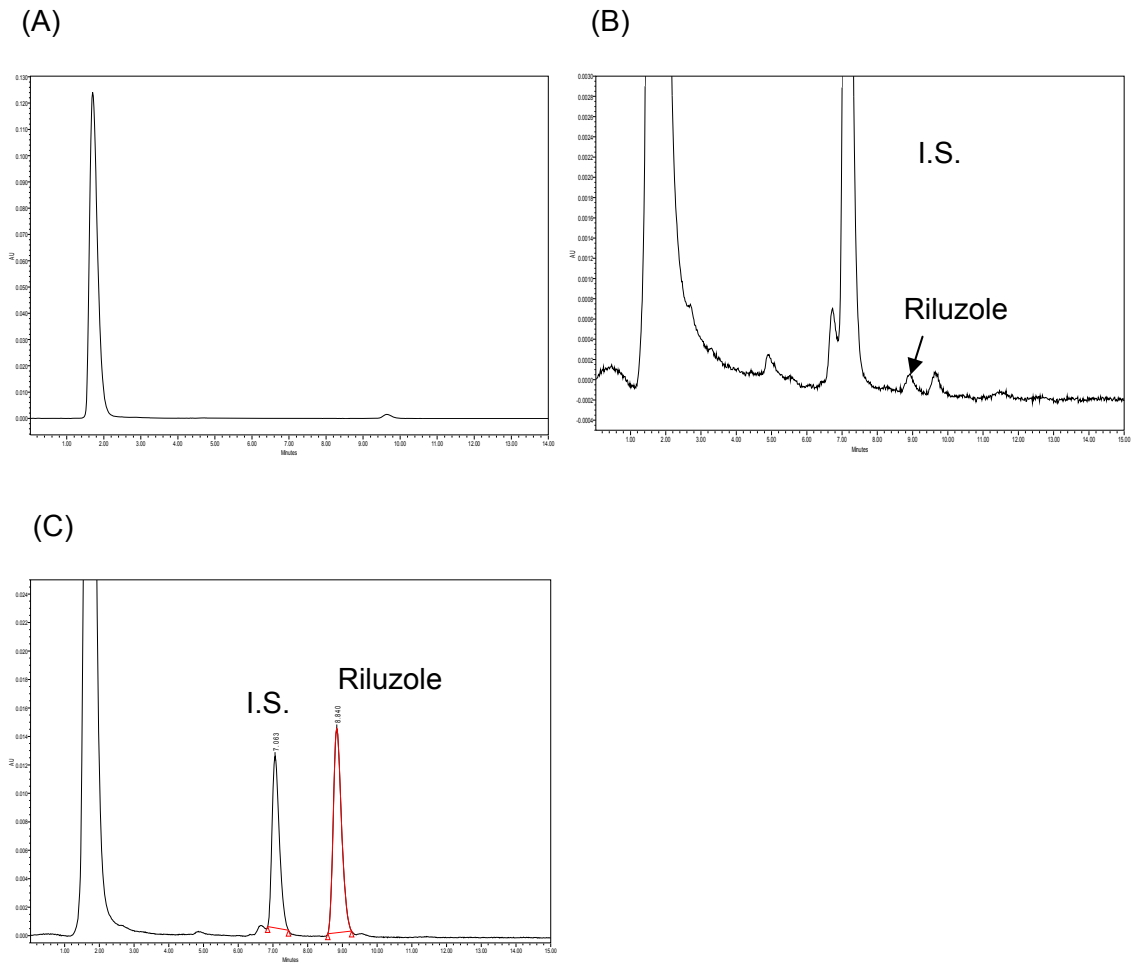


**Figure 12 Authentic HPLC Chromatograms of Extracts of (A) Blank Brain, (B) Spiked Brain Sample at LLOQ (31.25 ng/g) and (C) Spiked Brain Sample at 4,000 ng/g (Retention time: 9.0 min for Riluzole and 7.1 min for I.S., respectively)**

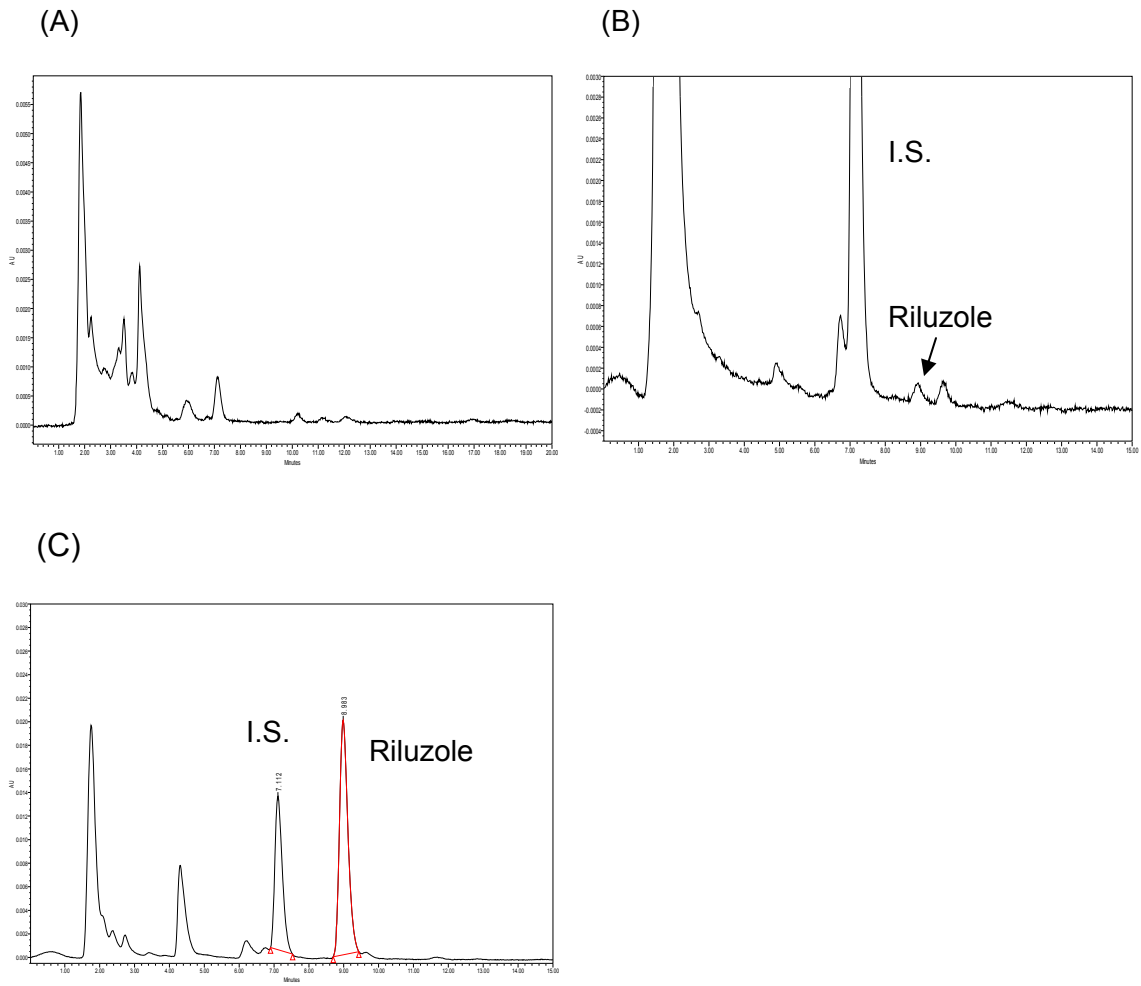


**Figure 13 Authentic HPLC Chromatograms of Extracts of (A) Blank Plasma, (B) Spiked Plasma Sample at LLOQ (7.8 ng/ml) and (C) Spiked Plasma Sample at 1,000 ng/ml (Retention time: 9.0 min for Riluzole and 7.1 min for I.S., respectively)**

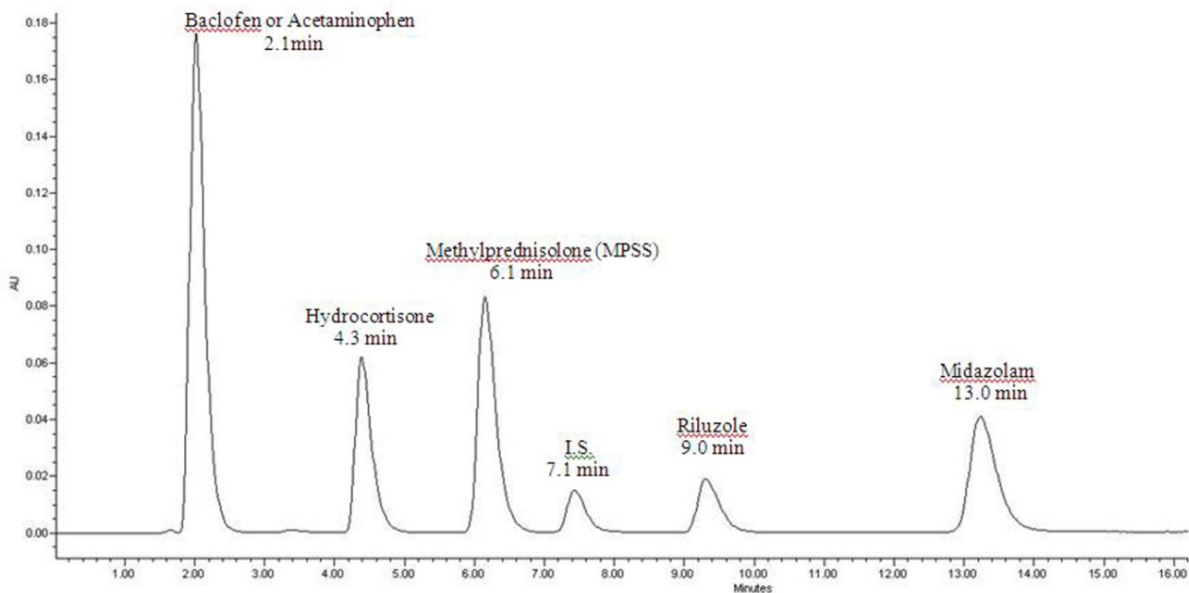
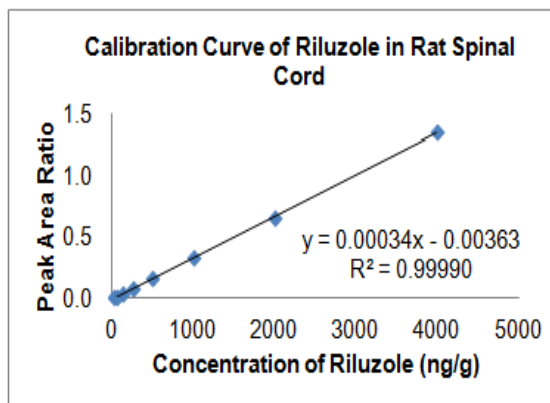
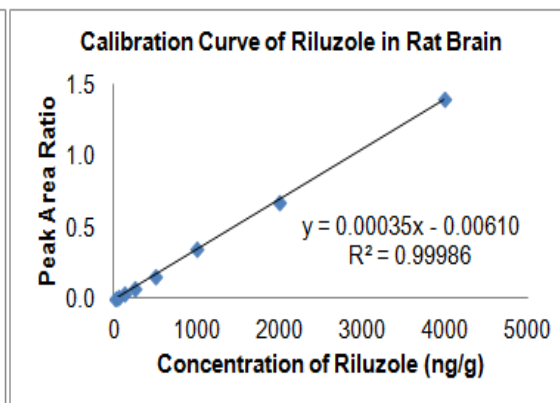


**Figure 14 HPLC Chromatogram of Riluzole and Internal Standard (I.S.) for Samples with Concomitant Medications of Acetaminophen, Baclofen, Hydrocortisone, Methylprednisolone (MPSS) and Midazolam (Retention times: Baclofen+Acetaminophen, 2.1 min; Hydrocortisone, 4.3 min; MPSS, 6.1 min; I.S., 7.1 min; Riluzole, 9.0 min; Midazolam, 13.0 min)**

(A)



(B)



(C)

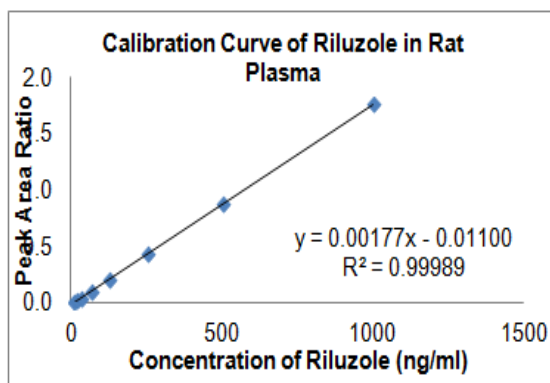


**Figure 15 Calibration Curves of Riluzole for Rat (A) Spinal Cord, (B) Brain and (C) Plasma Sample**  
**(Linear Range was 31.25 - 4000 ng/g for Rat Brain and Spinal Cord; 7.8 - 1000 ng/ml for Rat Plasma)**

Since Riluzole serum concentrations are in the range of 10-500 ng/ml in patients with ALS given a standard drug regimen of 50 mg twice daily (Le Liboux A et al., 1997; Van Kan HJ et al., 2004), the linear range we chose would be sufficient for the quantification of Riluzole in blood plasma in 36 acute SCI patients who have been treated with the same dosing regimen of 50 mg orally twice daily.

A representative standard curve with a linear range of 7.8-1000 ng/ml for human plasma samples was constructed for Phase I clinical study (**Error! Reference source not found.** 16).

#### **4.1.2.3 Recovery, Accuracy and Precision**

Rat and human plasma samples: The LLOQ was 7.8 ng/ml and the assay was linear from 7.8 to 1,000 ng/ml, for both rat and human plasma with correlation coefficients of 0.9995 and 0.9996, respectively. In plasma samples, intra-day and inter-day precision coefficients of variation at each Riluzole level of 15.6, 125 and 1,000 ng/ml were within 9% and 3% for human and rat samples, respectively. The accuracies were 103.38%, 95.99% and 94.56% (n=15 each), respectively, for rat plasma samples, and 106.8%, 94.6% and 102.8% (n=15 each), respectively, for human plasma samples for the three levels. The recoveries were 92.69-98.94% for the three levels with a mean of  $96.84 \pm 3.73\%$  (n=45) for rat plasma samples (Table 4), and 76.0-82.7% with a mean of  $78.9 \pm 6.5\%$  (n=45) for human plasma samples (Table 5).

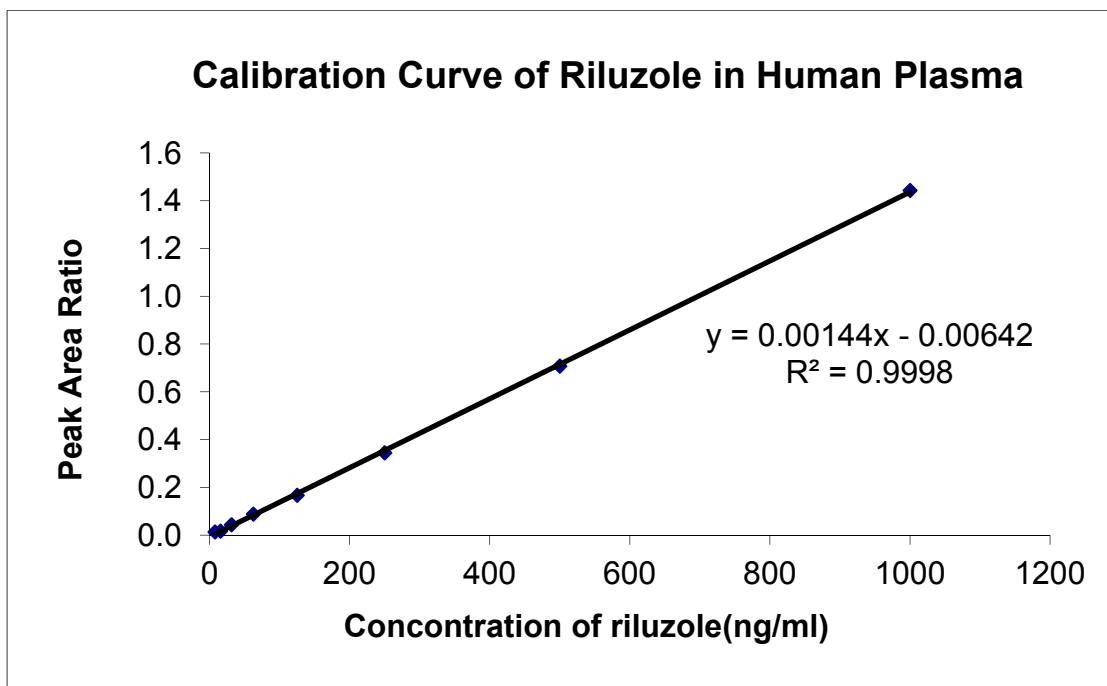


**Figure 16 Representative HPLC Calibration Curve of Riluzole in Human Plasma  
(Linear Range was 7.8-1000 ng/ml)**

**Table 4 Accuracy, Precision and Recovery of Riluzole at Levels of 15.6, 125 and 1,000 ng/ml for Rat Plasma Samples and at Levels of 62.5, 500 and 4,000 ng/g for Rat Brain and Spinal Cord Samples (N = 15)**

Added Concentration (ng/ml for plasma and ng/g for tissues) n=15 each	Measured Concentrations (ng/ml or ng/g)  mean ± SD	Accuracy (%)	Precision (%)		Recovery (%)  mean ± SD
			Intra-day	Inter-day	
<b>Plasma</b>					
15.6	16.13 ± 0.26	103.38	1.3	1.6	92.69 ± 2.42
125	119.98 ± 1.81	95.99	0.8	1.5	98.91 ± 1.57
1,000	945.63 ± 26.24	94.56	1.1	2.8	98.94 ± 2.76
<b>Brain</b>					
62.5	62.33 ± 0.85	99.88	1.4	1.4	107.62 ± 2.03
500	490.05 ± 8.32	98.01	0.3	1.7	96.17 ± 1.69
4,000	3947.38 ± 46.61	98.68	0.2	1.2	96.10 ± 1.14
<b>Spinal cord</b>					
62.5	57.94 ± 1.50	92.70	0.4	2.6	112.50 ± 3.58
500	506.68 ± 6.17	101.34	2.0	1.2	100.23 ± 1.25
4,000	4048.62 ± 66.72	101.22	0.2	1.6	98.06 ± 1.62

**Table 5 Accuracy, Precision and Recovery of Riluzole at Levels of 15.6, 125 and 1,000 ng/ml for Human Plasma Samples and at Two Concentration Levels (62.5 and 1,000 ng/ml) Levels for Human CSF Samples (N = 15 for Plasma Samples; N = 18 for CSF Samples)**

Added Concentration (ng/ml)	Measured Concentrations (ng/ml) mean ± SD	Accuracy (%)	Precision (%)		Recovery (%) mean ± SD
			Intra-day	Inter-day	
Plasma (n=15 each)					
15.6	16.7 ± 0.6	106.8	3.2	3.5	76.0 ± 9.3
125	118.2 ± 3.8	94.6	8.3	3.2	78.0 ± 3.8
1000	1025.8 ± 21.1	102.8	3.9	2.0	82.7 ± 3.1
CSF (n=18 each)					
62.5	61.0 ± 3.7	97.6	4.4	6.8	68.7 ± 4.6
1000	1005.9 ± 123.0	100.6	3.8	12.3	73.6 ± 9.1

Brain and spinal cord samples: The LLOQ was 31.25 ng/g and the assay was linear from 31.25 to 4,000 ng/g, with correlation coefficients of 0.9991 and 0.9999 for rat brain and spinal cord samples. The intra-day and inter-day precision coefficients of variation at each Riluzole level of 62.5, 500 and 4,000 ng/g were within 3% for these biological matrixes. The accuracies were all within 90-110% which satisfied the requirements of FDA (n=15 at each concentration). The recoveries were 96.10-107.62%, 98.06-112.50% and 87.55-108.31% with a mean of  $99.96 \pm 5.75\%$ ,  $103.60 \pm 6.87\%$  and  $95.95 \pm 9.42\%$  (n=45) for brain and spinal cord samples (Table 4).

Human CSF samples: The intra-day and inter-day precision coefficients of variation of two concentrations (62.5 ng/ml and 1,000 ng/ml) were within 13%. The accuracies were 97.6% and 100.6% (n=18) for each concentration and the recoveries were 68.7-73.6% with a mean of  $71.1 \pm 7.5\%$  (n=36) (Table 5).

#### **4.1.2.4 Stability**

Both rodent and human biometric samples of Riluzole were stable for at least 24 h at room temperature, and longer than 48 h at +4°C. Furthermore, Riluzole was stable up to one month when stored at -80°C. Therefore, all the biometric samples can be stored at -80°C until HPLC assay within a month. The bench-top stability of pretreated samples, the temperature influence on the stored samples and the long-term stability of human samples, expressed as percentage remaining of the original concentration, were summarized with no appreciable degradation in Tables 6.

**Table 6 Stability (% Remaining) of Riluzole in Human Plasma and CSF Samples, at Room Temperature, after Repeated Freeze-thaw and Long-term Storage (N = 3 at Each Condition)**

Added Riluzole Concentration (ng/ml)	Room Temperature		Stored	Freeze and	Stored at
	8h	24h	at +4°C for 48h	Thaw three times	-80°C for one month
Plasma					
15.6	94.5	99.7	99.1	91.4	98.5
250	102.6	101.4	103.9	103.5	102.4
1000	101.1	101.7	102.0	102.1	100.5
CSF					
15.6	96.1	113.0	107.1	112.2	99.2
125	95.6	95.8	97.0	106.0	98.1
1000	102.5	102.3	88.8	104.3	98.4

### **4.1.3 Effects of CSF Protein on Recovery and Accuracy of the Quantification of CSF Samples**

The different CSF protein concentrations had no significant effects on the recovery and accuracy of the quantification of CSF samples (Tables 7 & 8). Therefore, the pooled calibration curve could be used as daily calibrators for the future experiments.

**Table 7 Calibration Curves of Riluzole of CSF with Different Protein Concentrations  
 [LP Samples (53.9 mg/dl), IP Samples (142.2 mg/dl) and HP Samples (348.2  
 mg/dl)] (N = 2 for IP Group; N = 5 for LP and HP Groups)**

Groups	N	Slope of Standard Curve	Mean ± SD	CV (%)
LP	5	0.00137 0.00163 0.00158 0.00116 0.00114	0.00138 ± 0.00023	16.6
IP	2	0.00133 0.00123	0.00128 ± 0.00007	5.7
HP	5	0.00133 0.00137 0.00149 0.00142 0.00126	0.00137 ± 0.00009	6.4
Pooled Standard Curves	12		0.00137 ± 0.00015	11.2

The calibration curves of Riluzole with different protein levels were constructed on 5 separate days

**Table 8 Comparisons of Accuracies and Precisions Using Individual and Pooled Calibration Curves (N = 6 for Individual Curve; N = 18 for Pooled Curve)**

Added Riluzole Concentration (ng/ml)	CSF Protein Groups	Calculation using Respective Curves (n=6)		Calculation using Pooled Curves (n=18)	
		Accuracy (%)	Precision (%)	Accuracy (%)	Precision (%)
62.5	LP	89.4	9.7	97.6	6.0
	IP	103.7	2.9		
	HP	99.8	5.6		
1000	LP	90.6	20.6	100.6	12.2
	IP	110.2	3.5		
	HP	103.7	5.5		

## 4.2 Pharmacokinetics of Different Formulations

The Sprague-Dawley rats received Riluzole at the dose of 10 mg/kg orally (p.o.) and at the dose of 5 mg/kg intravenously (i.v.), which were selected with the allometric considerations of the different body surface area and known toxicity from the human regimen in ALS and LD<sub>50</sub> in rats (45 mg/kg p.o. and 21 mg/kg i.v.).

The PK profiles of mean plasma concentrations of Riluzole normalized by the dose versus time in semi-log scale were constructed (Figure 17) and parameters were derived (Table 9). The maximum plasma concentrations (C<sub>max</sub>) of Riluzole were observed at around 2 h after the oral administration. The crushed paste and tablet groups had the lowest Riluzole concentrations and exposures; Oral solution and suspension groups had the highest Riluzole concentrations and exposures.

The PK parameters were derived by using WinNonLin software. For the oral groups, a one compartment model was the best fit; for the i.v. group, a two compartment IV-bolus model was the best fit. The AUC/dose of Riluzole in crushed tablet and paste alone groups were comparable (2346.09 ± 886.98 vs. 1510.23 ± 622.56 ng\*hr/ml/mg) with no significant difference; The AUC/dose of Riluzole in crushed paste with glycerin, oral suspension and solution groups were comparable (5222.29 ± 1302.12, 9199.22 ± 2254.43 and 7886.63 ± 1781.34 ng\*hr/ml/mg), but significantly higher than those in crushed tablet and paste alone groups.

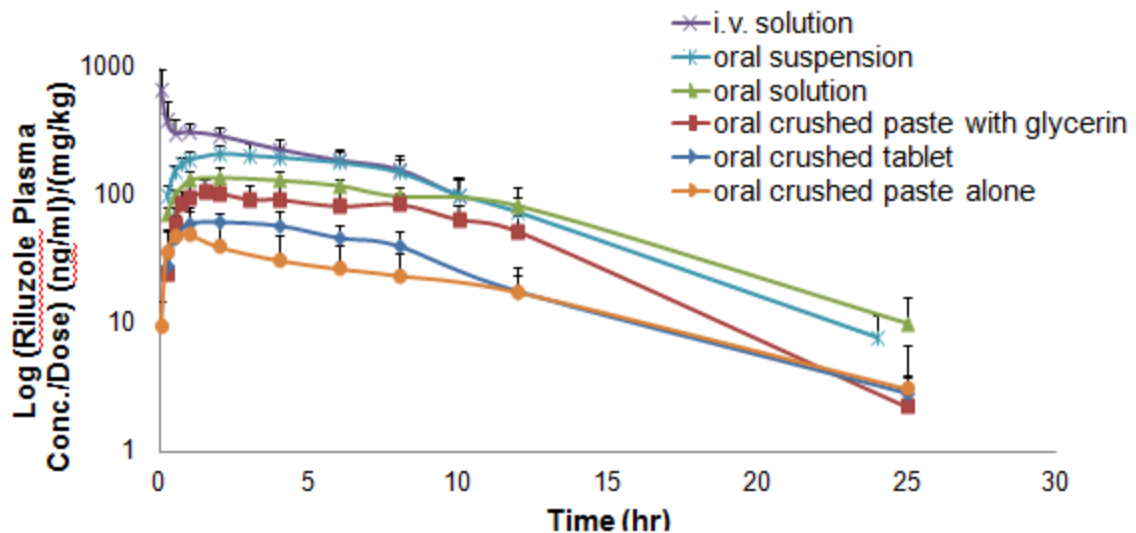


**Figure 17 Mean Plasma Concentrations/Dose-time Profiles of Riluzole after Oral and I.V. Administration (N = 3-5 for Each Group)**

[Oral groups: crushed tablet (◆), crushed paste alone (●), crushed paste with glycerin (■), suspension (x) and solutions (▲); I.V. group: solutions (x)]

**Table 9 Pharmacokinetic Parameters of Riluzole After Oral Administrations (10 mg/kg) of Crushed Tablet, Crushed Paste, Suspension and Solution, and I.V. Administration (5 mg/kg) of Riluzole Solution in Sprague-Dawley Rat (N = 3-5 for Each Group; \* indicates p < 0.05)**

Pharmacokinetic Parameters	Oral Mean ± SD (CV%)					I.V. Mean ± SD (CV%)
	Crushed tablet	Paste alone	Paste with glycerin	Suspension	Solution	Solution
No. of SD rats	5	3	5	5	4	4
Dosage (mg/kg)	8.67 ± 0.76 (8.78)	2.71 ± 0.18 (6.77)	9.76 ± 0.18 (1.89)	10.00	10.00	5.00
C <sub>max</sub> /Dose (ng/ml/mg)	209.51 ± 36.18 (17.28)	141.41 ± 69.58 (49.21)	363.01 ± 98.87* (27.24)	758.25 ± 154.12* (20.33)	492.54 ± 77.62* (16.76)	4696.32 ± 1955.84** (41.65)
AUC/Dose (hr*ng/ml/mg)	2346.09 ± 886.98 (37.81)	1510.23 ± 622.56 (41.22)	5222.29 ± 1305.12* (24.99)	9199.22 ± 2254.43* (24.51)	7886.63 ± 1781.34* (22.59)	12356.89 ± 3531.58** (28.58)
Bioavailability (F)	18.99	12.22	42.26	74.45	63.82	100.00
k (hr <sup>-1</sup> )	0.12 ± 0.04 (33.99)	0.11 ± 0.06 (60.27)	0.09 ± 0.02 (24.64)	0.08 ± 0.04 (44.49)	0.10 ± 0.03 (28.92)	0.10 ± 0.04 (39.33)
t <sub>1/2,distribution</sub> (hr)						0.07 ± 0.05 (68.01)
t <sub>1/2,absorption</sub> (hr)	0.53 ± 0.34 (65.06)	0.15 ± 0.06 (35.92)	0.55 ± 0.16 (28.95)	0.46 ± 0.13 (28.11)	0.40 ± 0.13 (31.06)	
t <sub>1/2,elimination</sub> (hr)	6.07 ± 0.85 (30.51)	7.88 ± 3.87 (49.08)	8.34 ± 1.96 (23.43)	7.01 ± 1.71 (24.27)	10.07 ± 4.00 (39.73)	8.01 ± 3.49 (43.61)
Clearance (CL/F, ml/hr)	89 ± 34 (38)	89 ± 37 (41)	84 ± 21 (25)	85 ± 21 (25)	85 ± 19 (23)	85 ± 23 (27)
Volume of Distribution (V/F, ml)	704 ± 266. (38)	1034 ± 426 (41)	974 ± 243 (25)	841 ± 206 (25)	1147 ± 259 (23)	896 ± 220 (25)

Differences were evaluated using one-way ANOVA, Tukey's post hoc, at significance level of P<0.05.

\*indicates statistically different from the crushed tablet group and crushed paste alone;

\*\*indicates statistically different from all the other groups, except oral suspension and solution groups.

The bioavailabilities of Riluzole from oral paste with glycerin, suspension and solution were enhanced from 12-18% to 42.26-74.45% compared to those in oral crushed paste and tablet. Elimination half life ( $t_{1/2}$ ) and elimination rate constant of Riluzole in six groups were not statistically different, within the range of 6.07-10.07 hr and 0.08-0.12 hr<sup>-1</sup>. Clearance (CL/F) and volume of distribution (V/F) of Riluzole after normalized by bioavailability (F) among these six groups were not significantly different, within the range of 84-89 ml/hr and 704-1147 ml (Table 9).

## **4.3 Impacts of Acute Spinal Cord Injury on Riluzole**

### **Pharmacokinetics**

The Riluzole concentrations in rat plasma, brain and (cervical and thoracic) spinal cord samples from the I.P. single-dose (8 mg/kg) and multiple-dose (loading dose of 8mg/kg followed by five doses of 6 mg/kg) groups were quantified in cervical spinal cord injured (SCI) and uninjured control rats, respectively. The pharmacokinetic profiles up to 12 hr were constructed (Figures 18A-B) and parameters were derived (Table 10).

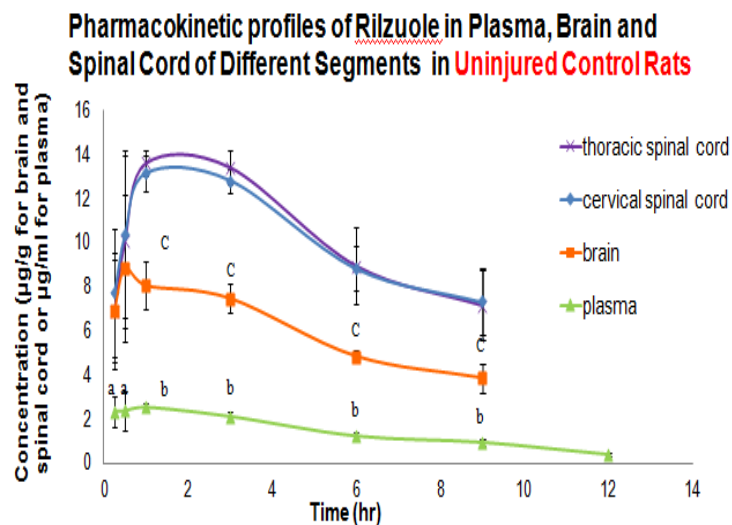
The pharmacokinetic profiles and parameters of Riluzole in plasma, brain, as well as cervical and thoracic spinal cords after single dose were compared between the SCI and uninjured rats (Figures 19A-19D & Table 10). The comparisons of Riluzole concentrations in these samples were also performed for Day 1 and Day 3 (Figures 20-21) after the multiple-dose regimen.

#### **4.3.1 Single Dose Treatment of Riluzole**

##### **4.3.1.1. Uninjured Control Group**

In uninjured rats, Riluzole concentration profiles in cervical and thoracic spinal cords were comparable and could be considered as within the same compartment pharmacokinetically, after I.P. administration of a single dose of the cyclodextrin-enclosed Riluzole liquid formulation. The profiles were characterized by a rapid distribution from the plasma to reach a maximal concentration ( $C_{max}$ ) of 13.71-14.50  $\mu\text{g/g}$

(A)



(B)

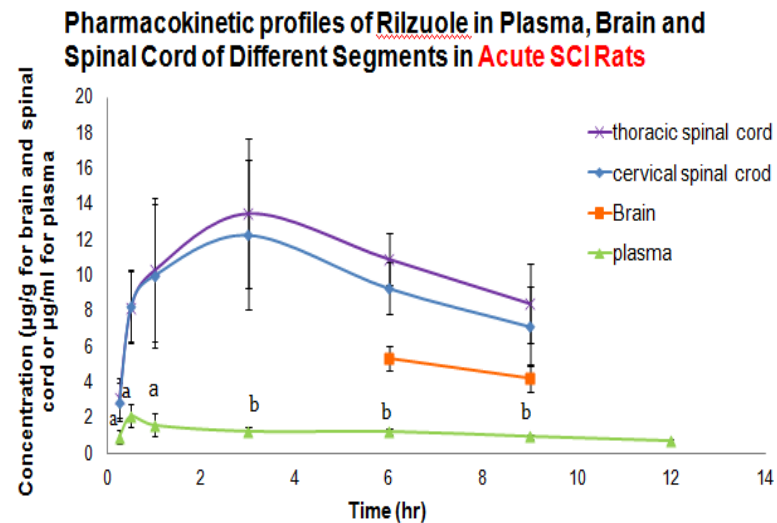


**Figure 18 Pharmacokinetic Profiles of Riluzole in Plasma, Brain and Spinal Cords (Cervical and Thoracic Segments) after Single I.P. Administration (8 mg/kg) (A) Uninjured Control and (B) Cervical Spinal Cord Injured (SCI) Rats (n=4 for Each Time Point, Mean  $\pm$  SD)**

**a: Significantly lower than those in cervical and thoracic spinal cord,**

**b: Significantly lower than those in cervical, thoracic spinal cord and brain,**

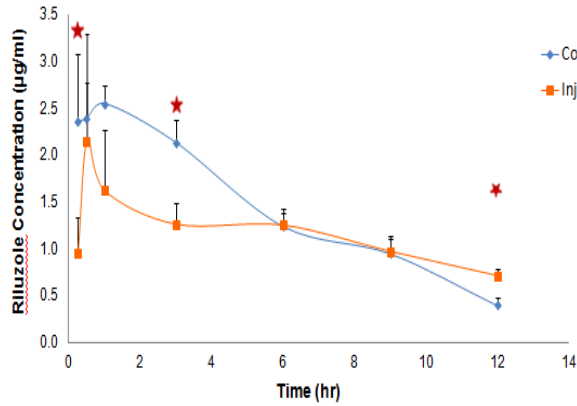
**c: Significantly lower than those in cervical and thoracic spinal cord, but higher than that in plasma**

**Table 10 Pharmacokinetic Parameters of Riluzole in Plasma, Brain and Spinal Cord Samples between Uninjured Control Group and Cervical Spinal Cord Injured (SCI) Group after Single I.P. Administration of 8 mg/kg**

Pharmacokinetic Parameters	Uninjured Control Group				SCI Group		
	Spinal Cord		Brain	Plasma	Spinal Cord		Plasma
	Cervical	Thoracic			Cervical	Thoracic	
$C_{max}$ ( $\mu\text{g/ml}$ for plasma, $\mu\text{g/g}$ for spinal cord and brain)	13.71	14.50	8.69	2.61	12.51	13.60	1.75
$t_{max}$ (hr)	1.37	1.58	0.57	0.71	2.21	2.48	0.90
$AUC_{0-9hr}$ ( $\mu\text{g}\cdot\text{hr/g}$ for spinal cord and $\mu\text{g}\cdot\text{hr/ml}$ for plasma)	91.98	93.78	54.19	15.15	85.72	96.09	13.94
$AUC_{0-\infty}$ ( $\mu\text{g}\cdot\text{hr/g}$ for spinal cord and $\mu\text{g}\cdot\text{hr/ml}$ for plasma)	172.22	158.35	91.66	21.19	162.22	198.98	22.92
$t_{1/2}$ (hr)	7.70	6.40	6.80	5.21	7.28	8.22	8.43
$k$ ( $\text{hr}^{-1}$ )	0.09	0.11	0.10	0.13	0.10	0.08	0.08

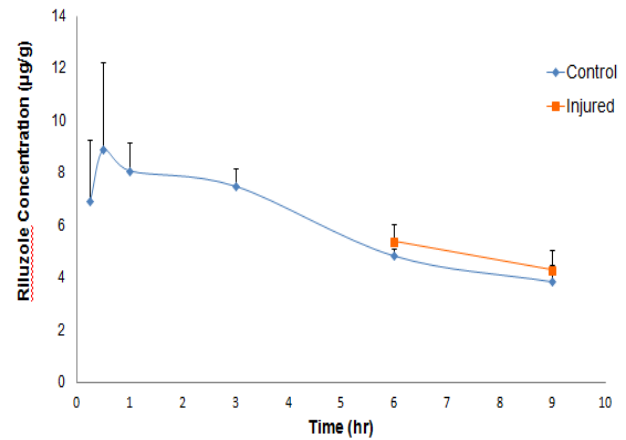
(A)

The Comparison of **Plasma** Pharmacokinetic Profiles between **Injured Group** and **Control Group**



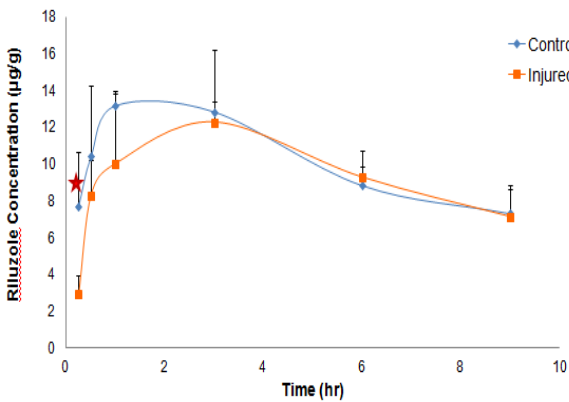
(B)

The Comparison of **Brain** Pharmacokinetic Profiles between **Injured Group** and **Control Group**



(C)

The Comparison of **Cervical Spinal cord** Pharmacokinetic Profiles between **Injured Group** and **Control Group**



(D)

The Comparison of **Thoracic Spinal cord** Pharmacokinetic Profiles between **Injured Group** and **Control Group**

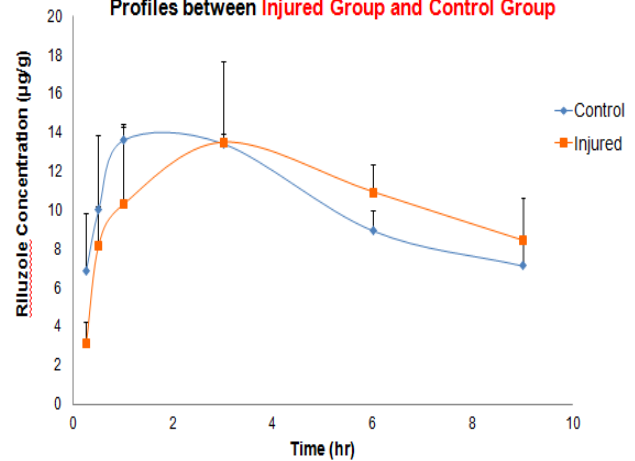


**Figure 19 Comparisons between SCI and Uninjured Rats of Riluzole**

**Pharmacokinetic Profiles after Single I.P. Dose of 8 mg/kg**

**(A) Plasma, (B) Brain, (C) Cervical Spinal Cord and (D) Thoracic Spinal**

**Cord (N = 4 at Each Time Point, Mean ± SD; \* indicates p < 0.05)**

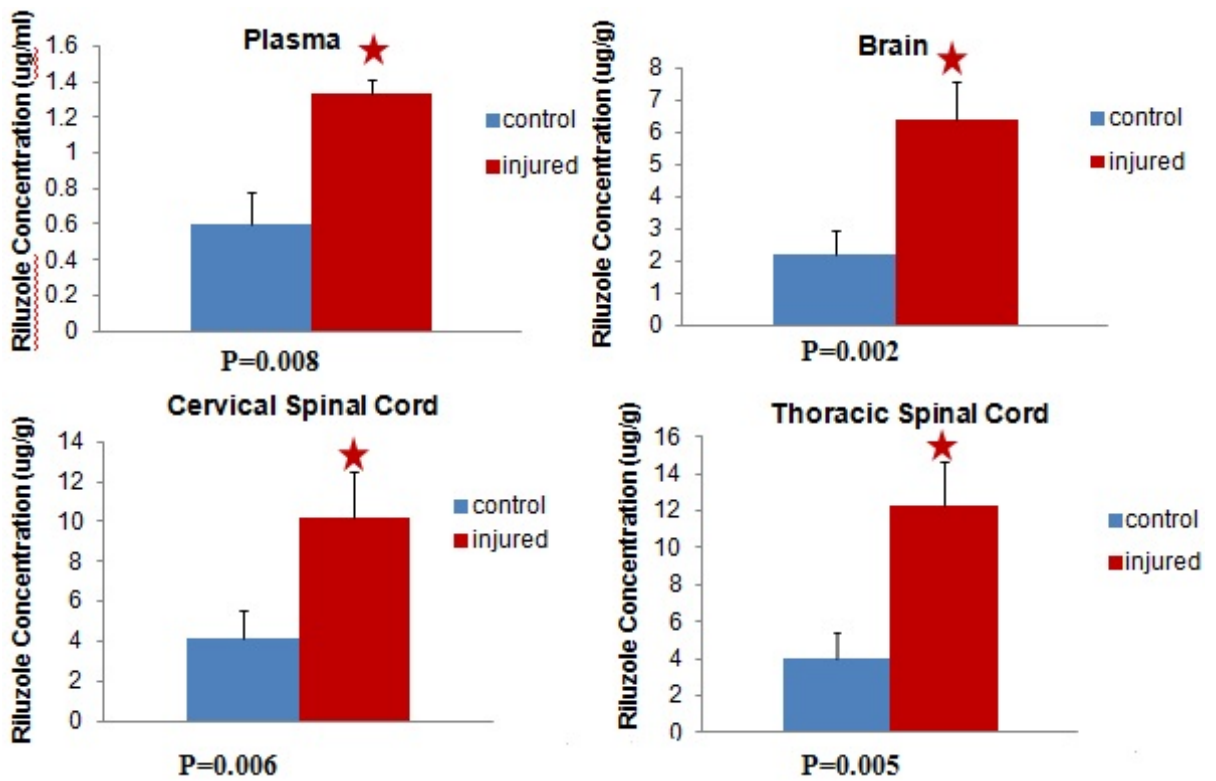


**Figure 20 Comparisons of Riluzole Concentrations between Uninjured Control and Cervical SCI Groups in Plasma, Brain, Cervical and Thoracic Spinal Cords after Two I.P. Doses Every 12 Hours (n=4 for Each Group, Mean ± SD; \* indicates p < 0.05) (8 mg/kg as loading dose + 6 mg/kg, 2 Doses; Samples Collected at 12 hrs after the Second Dose)**

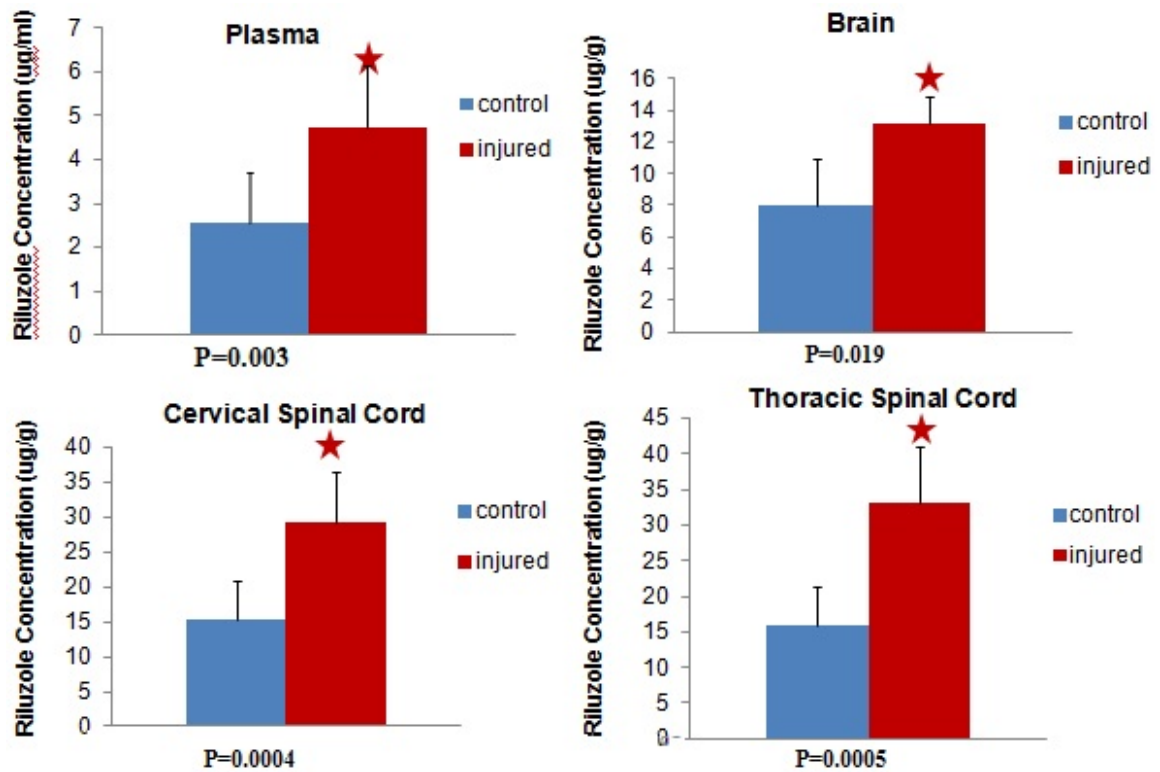


**Figure 21 Comparisons of Riluzole Concentrations between Uninjured Control and Cervical SCI Groups in Plasma, Brain, Cervical and Thoracic Spinal Cords after Six I.P. Doses Every 12 Hours for 3-day Treatment (n=4 for Each Group Mean ± SD; \* indicates p < 0.05)**  
**(First Dose of 8 mg/kg as loading dose and the Following 5 Doses of 6mg/kg, 6 Doses; Samples Collected at 2 hrs after the Last Dose)**

at  $t_{\max}$  of 1.5 hr, followed by a decline with the elimination half-lives ( $t_{1/2}$ ) of 7.7 hr and 6.4 hr, for cervical and thoracic spinal cords, respectively (Figure 18A & Table 10).

The Riluzole concentration profile in the brain yielded significantly lower level than those in the spinal cords after one hour post dose (Figure 18A). The brain may be considered as a distinct compartment from that of spinal cords. The  $C_{\max}$  was reached at 8.69  $\mu\text{g/g}$  at  $t_{\max}$  of 0.57 hr. The plasma profile was significantly lower than those in brain and spinal cords, with  $C_{\max}$  of 2.61  $\mu\text{g/ml}$  at  $t_{\max}$  of 0.71 hr. The half-lives ( $t_{1/2}$ ) of Riluzole in brain and plasma were 6.8 hr and 5.2 hr, respectively, comparable to those in the spinal cords.

The Riluzole distributions from IP injection site to plasma, brain and spinal cords were rapid, reaching equilibrium in about 1 hr. The Riluzole exposures in cervical and thoracic spinal cords and brain were substantial with the  $\text{AUC}_{0-9}$  ratios of cervical and thoracic spinal cords/plasma of 6.07 (91.98/15.15) and 6.19 (93.78/15.15), respectively, and that of brain/plasma 3.58 (54.19/15.15) (Table 10). The Riluzole exposures in spinal cords were higher than that in the brain, with the  $\text{AUC}_{0-9}$  ratios of cervical and thoracic spinal cords/brain of 1.70 (91.98/54.19) and 1.73 (93.78/54.19), respectively.

#### **4.3.1.2. Cervical Spinal Cord Injured Group**

The similar trends of Riluzole concentrations in plasma and spinal cords were also observed in cervical spinal cord injured rats. The concentration levels of Riluzole in cervical and thoracic spinal cords of SCI rats after the single-dose treatment were

similar, again confirming that cervical and thoracic spinal cords were within the same pharmacokinetic compartment. Riluzole was readily absorbed and distributed to spinal cords, reaching  $C_{max}$  of 12.51-13.60  $\mu\text{g/g}$  more slowly, with the  $t_{max}$  of 2.2-2.5 hr in SCI rats vs 1.4-1.6 hr in uninjured control group (Figure 18B & Table 10).

The Riluzole concentration levels up to 9 hr in spinal cords were comparable after the single-dose treatment between uninjured control and acute SCI rats (Figures 19C-19D). The elimination  $t_{1/2}$  of Riluzole from spinal cords in SCI rats was 7.3-8.2 hr (Table 10 and Figures 19C-19D), comparable with those in uninjured counterpart, 7.7-6.4 hr. However, we recognized that the Riluzole concentrations in plasma, brain, cervical and thoracic spinal cord of SCI rats were slightly higher than those in the uninjured control group after 6 hr post-dose.

The plasma profile was significantly lower than those in spinal cords, with  $C_{max}$  of 1.75  $\mu\text{g/ml}$  at  $t_{max}$  of 0.9 hr versus 12.51-13.60  $\mu\text{g/g}$  at 2.21-2.48 hr (Figure 18A & Table 10). The half-lives ( $t_{1/2}$ ) of Riluzole in plasma in SCI rats were 8.4 hr, which was slightly longer than that in the control group 5.2 hr (Figure 19A & Table 10).

The  $AUC_{0-9}$  ratios of cervical and thoracic spinal cords/plasma of Riluzole in SCI rats were 6.15 (85.72/13.94) and 6.89 (96.09/13.94), respectively, with those in uninjured rats, 6.07 and 6.19 (Table 10).

#### **4.3.1.3. Comparative Tissue/Plasma Partition Coefficients of Riluzole**

For the control group, Riluzole partition to brain reached steady state at the level of 3.5 rapidly within half an hour. The partition to spinal cords were at a much higher level and reached the plateau of 6.8 and 6.9 at 9 hr (Figure 22).

For the injured group, Riluzole partition to spinal cords reached the steady state at a higher level of 8.1 and 9.1 at 6 hr than in the control group (Figure 22).

### **4.3.2 Multiple Doses Treatment of Riluzole**

#### **4.3.2.1. Uninjured Control Group**

After the multiple dosing with the first Riluzole loading dose of 8 mg/kg and the following doses of 6 mg/kg every 12 hours for 3 days by I.P. administration, the plasma, brain, as well as cervical and thoracic spinal cords were collected at 12 hr post the 2nd dose on Day 1 and 2 hr post the 6th dose on Day 3 after the last injection. For 1-day treatment, Riluzole concentrations were  $0.60 \pm 0.18$  µg/ml,  $2.17 \pm 0.76$  µg/g,  $4.14 \pm 1.43$  µg/g and  $3.97 \pm 1.81$  µg/g in plasma, brain, cervical spinal cord and thoracic spinal cord (n=4 each), respectively, with respective C.V. of 30.0%, 35.0% , 34.5% and 45.6% (Figure 20). For 3-day treatment, Riluzole concentrations in plasma, brain, cervical spinal cord

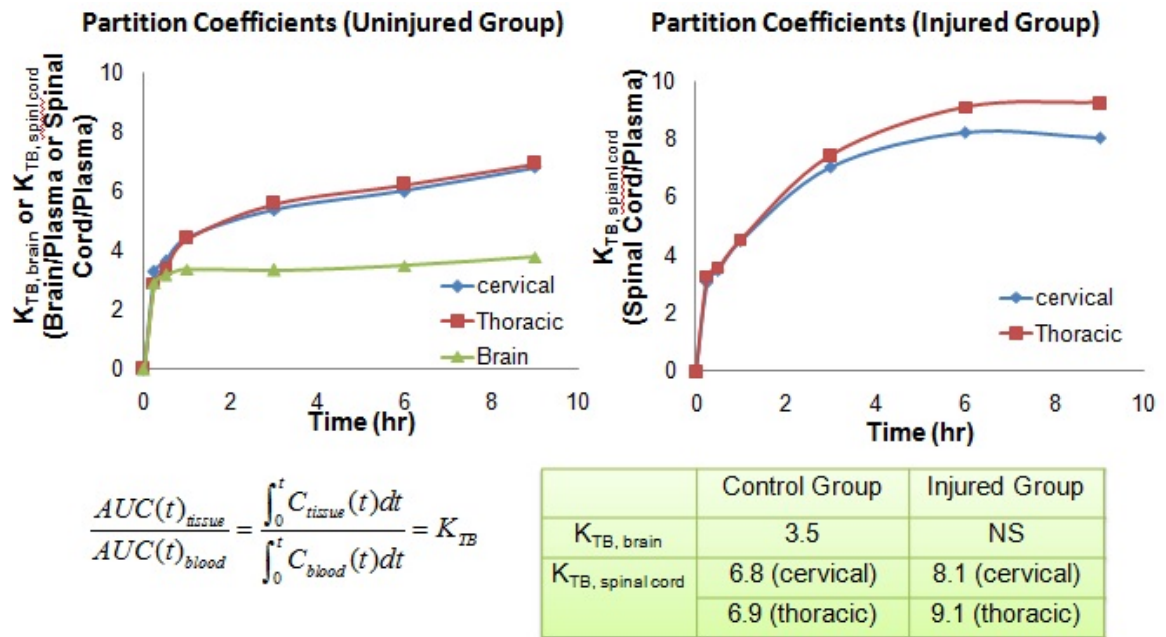


**Figure 22 Profiles of Partition Coefficients (Kp) of Riluzole in Brain and Spinal Cords for both Uninjured Control and Cervical SCI Groups**

and thoracic spinal cord (n=4 each) were  $1.88 \pm 0.73 \mu\text{g/ml}$ ,  $8.05 \pm 2.87 \mu\text{g/g}$ ,  $14.53 \pm 5.48 \mu\text{g/g}$  and  $15.18 \pm 5.59 \mu\text{g/g}$ , respectively (Figure 21). The  $t_{1/2}$  of Riluzole in these compartments ranged from 5.2 to 7.7 hr; therefore, the steady state was reached after 4-5  $t_{1/2}$  (26-40 hr after the regimen), namely, after the two-day treatment. The respective C.V.s of samples from the 3-day treatment were 38.8%, 35.7%, 37.7% and 36.8%, similar to those after 1-day treatment.

The accumulation or multiple dose factor at steady state ( $\text{MDF}_{\text{ss}}$ ) were calculated by the equation of  $\text{MDF}_{\text{ss}} = [1 / (1 - e^{-k\tau})]$ , where k was the repeating elimination rate constants in individual compartments. The  $\text{MDF}_{\text{ss}}$  of Riluzole were similar in plasma, brain, cervical and thoracic spinal cords, 1.27, 1.43, 1.51 and 1.36, respectively, after the 3-day treatment.

#### **4.3.2.2. Cervical Spinal Cord Injured Group**

The Riluzole concentrations after 1-day and 3-day multiple dosing regimen again confirmed the observation of slower Riluzole elimination from the plasma and spinal cords, resulting in greater accumulations as compared with those in uninjured rats (Figures 20-21). The Riluzole concentrations after the same 1-day treatment yielded Riluzole concentrations of 10.16-12.34  $\mu\text{g/g}$  (n=4, CV of 23.0% and 23.7%) in spinal cords of SCI rats, twice of those in uninjured rats, 3.97-4.14  $\mu\text{g/g}$ . The plasma and brain levels were also significantly higher, 1.33  $\mu\text{g/ml}$  and 6.35  $\mu\text{g/g}$  (CV of 6.0% and 19.1%) vs 0.60  $\mu\text{g/ml}$  and 2.17  $\mu\text{g/g}$  in control rats. For 3-day treatment, the Riluzole concentrations in plasma, brain, cervical spinal cord and thoracic spinal cord (n=4 each)

were  $3.40 \pm 0.46 \mu\text{g/ml}$ ,  $13.19 \pm 1.74 \mu\text{g/g}$ ,  $23.02 \pm 3.45 \mu\text{g/g}$  and  $26.48 \pm 3.42 \mu\text{g/g}$ , which were significantly higher than those in the uninjured group ( $1.88 \pm 0.73 \mu\text{g/ml}$ ,  $8.05 \pm 2.87 \mu\text{g/g}$ ,  $14.53 \pm 5.48 \mu\text{g/g}$  and  $15.18 \pm 5.59 \mu\text{g/g}$ , respectively). The respective C.V.s of samples from 3-day treatment were 13.5%, 13.2%, 15.0% and 12.9%.

The  $\text{MDF}_{\text{ss}}$  in cervical and thoracic spinal cords after 3-day treatment were 1.43 and 1.62, respectively, vs  $\text{MDF}_{\text{ss}}$  of 1.27 and 1.43 in uninjured rats.

All in all, the concentrations of Riluzole in plasma, brain, cervical and thoracic spinal cord were significantly higher in acute SCI rats than those in the uninjured control rats after 1-day and 3-day treatments.

### 4.3.3 Three-compartment Model of Riluzole by ADAPT II After

#### Single Dose

The pharmacokinetic model and the derived parameters of Riluzole in each and among the plasma, brain and spinal cord compartments for both controlled and SCI injured groups were tabulated (Table 11). After I.P. administration, Riluzole was absorbed into plasma very rapidly for both groups, with the absorption rate constants ( $k_a$ ) of 1.60 vs.  $2.79\text{hr}^{-1}$  for injured and control groups, respectively. For the control and injured groups, the transferring rate constants between plasma and brain compartments ( $k_{12}$  and  $k_{21}$ ) were 1.97 (SCI injured) vs. 4.06 (uninjured control)  $\text{hr}^{-1}$  and 2.21 (SCI injured) vs. 0.21 (uninjured control)  $\text{hr}^{-1}$ , respectively. Riluzole penetrated across the blood-brain barrier (BBB) more slowly and pumped out of the brain much faster in the SCI injured rats compared to the control rats. Similar results were also observed in the transferring rate constants between plasma and spinal cord compartments ( $k_{13}$  and  $k_{31}$ ), 5.80 (SCI injured) vs. 33.96 (uninjured control)  $\text{hr}^{-1}$  and 3.07 (SCI injured) vs. 2.72 (uninjured control)  $\text{hr}^{-1}$ , respectively. Riluzole penetrated into the spinal cord more slowly across the blood-spinal cord barrier (BSCB) for SCI injured rats, but Riluzole transferred from spinal cord back to plasma compartment with similar rate constants for both groups. Because of the existence of cerebral spinal fluid (CSF), Riluzole could also transfer from the brain into the spinal cord compartment, in view of the flow of CSF (from brain to spinal cord), the amount and rate of Riluzole transferred from spinal cord to the brain would be limited and could be ignored. The transferring rate constant of Riluzole between brain and spinal cord compartments ( $k_{23}$ ) were 0.01 (SCI injured) vs. 6.25 (uninjured control)  $\text{hr}^{-1}$

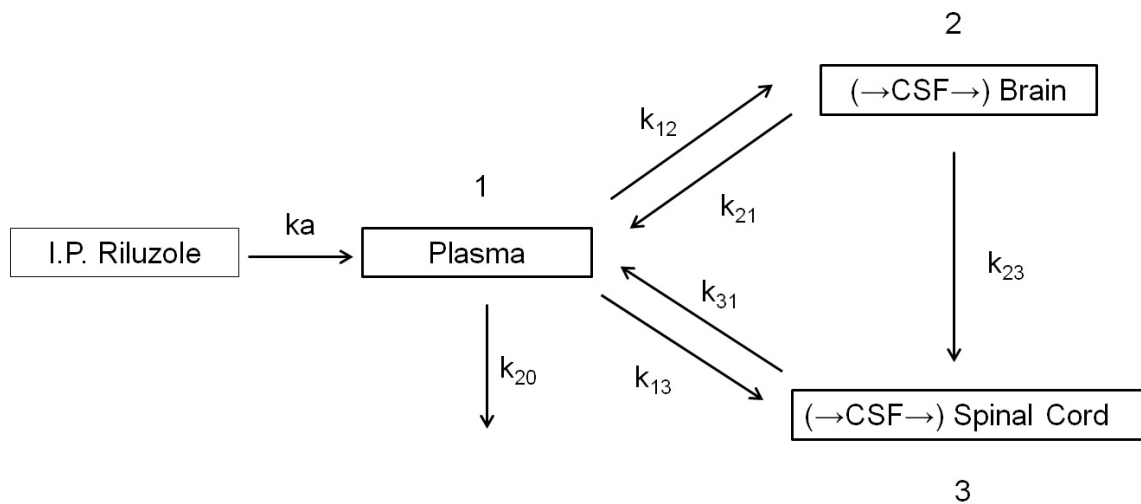


**Table 11 Pharmacokinetic Parameters of Riluzole Derived by ADAPT II Model  
between Uninjured Control and Cervical Spinal Cord Injured (SCI) Rats  
after Single I.P. Administration of 8 mg/kg**

Pharmacokinetic Parameters	Predicted Values	
	Control Group	ASCI Group
$k_a$ ( $hr^{-1}$ )	2.79	1.60
$k_{20}$ ( $hr^{-1}$ )	1.49	0.33
$k_{12}$ ( $hr^{-1}$ )	4.06	1.97
$k_{21}$ ( $hr^{-1}$ )	0.23	2.21
$k_{23}$ ( $hr^{-1}$ )	6.25	0.01
$k_{13}$ ( $hr^{-1}$ )	33.96	5.80
$k_{31}$ ( $hr^{-1}$ )	2.72	3.07
$AUC_{0-\infty}$ plasma ( $\mu g \cdot hr/ml$ )	26.84	23.58
$AUC_{0-\infty}$ brain ( $\mu g \cdot hr/ml$ )	97.93	99.50
$AUC_{0-\infty}$ spinal cord ( $\mu g \cdot hr/ml$ )	167.90	172.7

Ratio of AUC in spinal cord: brain: plasma= 8:4:1 for both control and SCI injured rats

for the injured and control groups. The elimination rate constant of Riluzole from plasma compartment was 4 times slower in the SCI injured rats compared to the control rats, 0.33 (SCI injured) vs.1.49 (uninjured control)  $\text{hr}^{-1}$ , respectively. Overall, Riluzole in the SCI injured rats had slower transferring rate constants from plasma to brain and spinal cord compartments and slower elimination rate constant compared with the control group in 13 hr post SCI injury (acute phase). Riluzole achieved highest exposures in the spinal cord, followed by the brain and plasma, with the  $\text{AUC}_{0-\infty}$  ratio (spinal cord: brain: plasma) was about 8:4:1 for both groups (Table 11).

The predicted concentration-time profiles of Riluzole in the plasma, brain and spinal cord for both control and SCI injured groups after a single I.P. dose of 8 mg/kg were generated using the established three-compartment model by ADAPT II software (Figures 23 & 24). Based on the coefficient of determination ( $R^2$ ) between the observed data and the predicted values, the selected model for both groups adequately described the Riluzole concentrations among the three-compartments (plasma, brain and spinal cord), except the  $R^2$  value (0.561) in the plasma compartment for the injured group, which might be resulting from the insufficient data in the brain compartment, weakening the overall fitting of the model for the injured group.

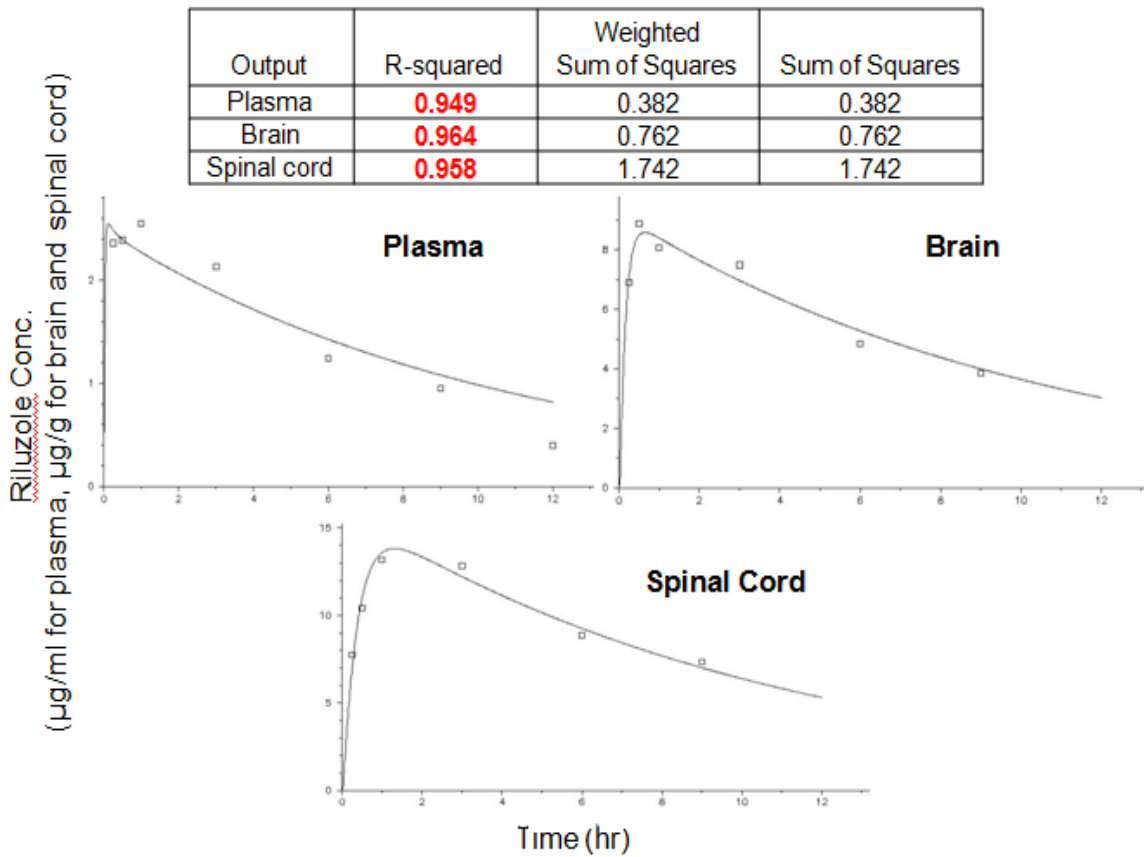


**Figure 20 Model Fitting of Riluzole Concentration vs. Time Profiles in Plasma, Brain and Spinal Cord after Single I.P. Dose of 8 mg/kg for Uninjured Control Group**

**Open Symbol Represented Measured Mean Riluzole Concentrations;**

**Lines Represented the Best-fit Curves Using the Model Fit Parameters**

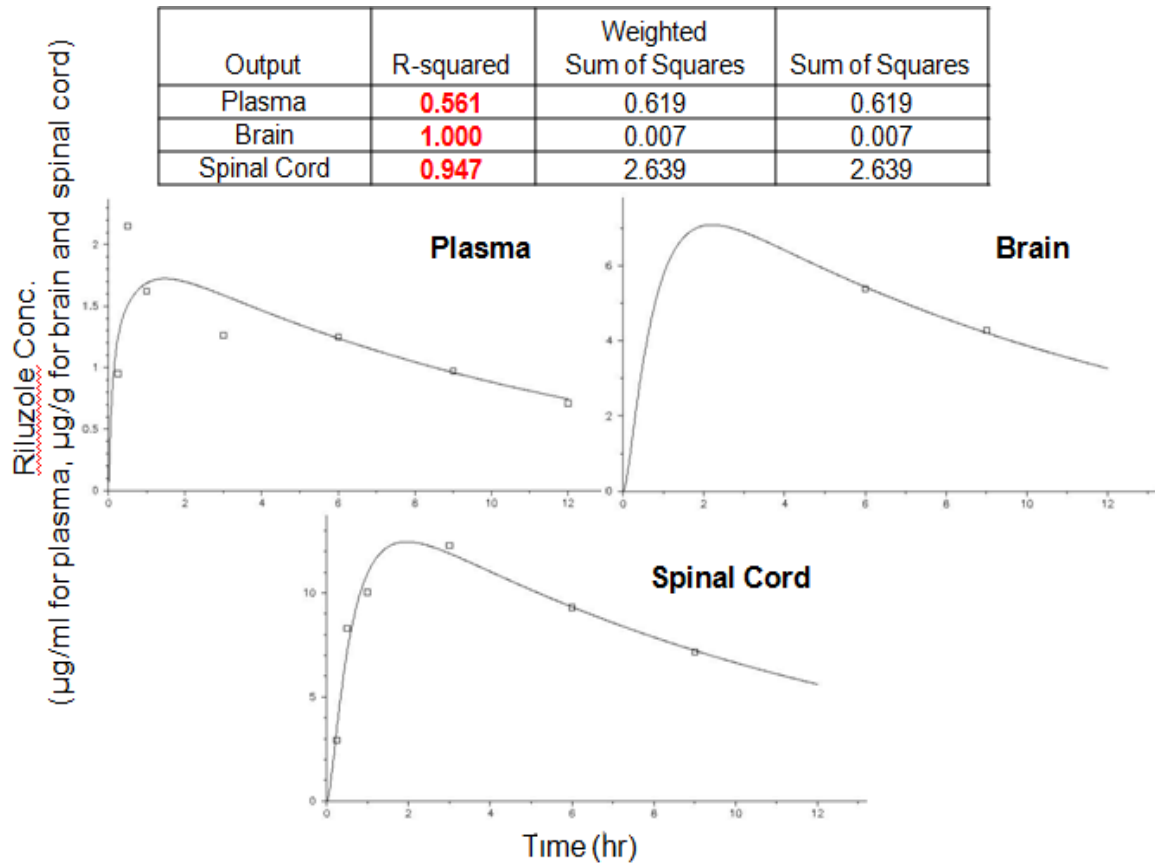


**Figure 21 Model Fitting of Riluzole Concentration vs. Time Profiles in Plasma, Brain and Spinal Cord after Single I.P. Dose of 8 mg/kg for Cervical SCI Group**

**Open Symbol Represented Measured Mean Riluzole Concentrations;**

**Lines Represented the Best-fit Curves Using the Model Fit Parameters**

#### 4.3.4 Evaluations of ADAPT II Model

The established ADAPT model was evaluated by the comparisons of the predicted and observed Riluzole concentrations after multiple I.P. doses (2 and 6 doses) for both uninjured control and SCI injured groups.

The red dots represented the mean observed Riluzole concentrations; the blue dots represented the individual observed Riluzole concentrations; the open squares on the simulated PK profiles represented the predicted concentrations (Figures 25 & 26).

In the control group, the predicted Riluzole concentrations in plasma, brain and spinal cord after 2 and 6 I.P. doses were close to the mean observed values, 0.88 vs. 0.60  $\mu\text{g/ml}$ , 3.27 vs. 2.17  $\mu\text{g/g}$  and 5.73 vs. 4.14  $\mu\text{g/g}$  after 2 doses, and 2.31 vs. 1.88  $\mu\text{g/ml}$ , 8.55 vs. 8.05  $\mu\text{g/g}$  and 14.93 vs. 14.53  $\mu\text{g/g}$  after 6 doses (Figures 25-26 & Table 12).

However, all the predicted Riluzole concentrations in SCI injured rats among these compartments after 2 and 6 I.P. doses were under-estimated by only half of the corresponding mean observed values, 0.83 vs. 1.33  $\mu\text{g/ml}$ , 3.64 vs. 6.35  $\mu\text{g/g}$  and 6.24 vs. 10.16  $\mu\text{g/g}$  after 2 doses, and 2.01 vs. 3.40  $\mu\text{g/ml}$ , 8.55 vs. 13.19  $\mu\text{g/g}$  and 14.90 vs. 23.02  $\mu\text{g/g}$  after 6 doses (Figures 27-28 & Table 13). The accumulation phenomenon was much higher in SCI injured rats than in uninjured rats after multiple doses.

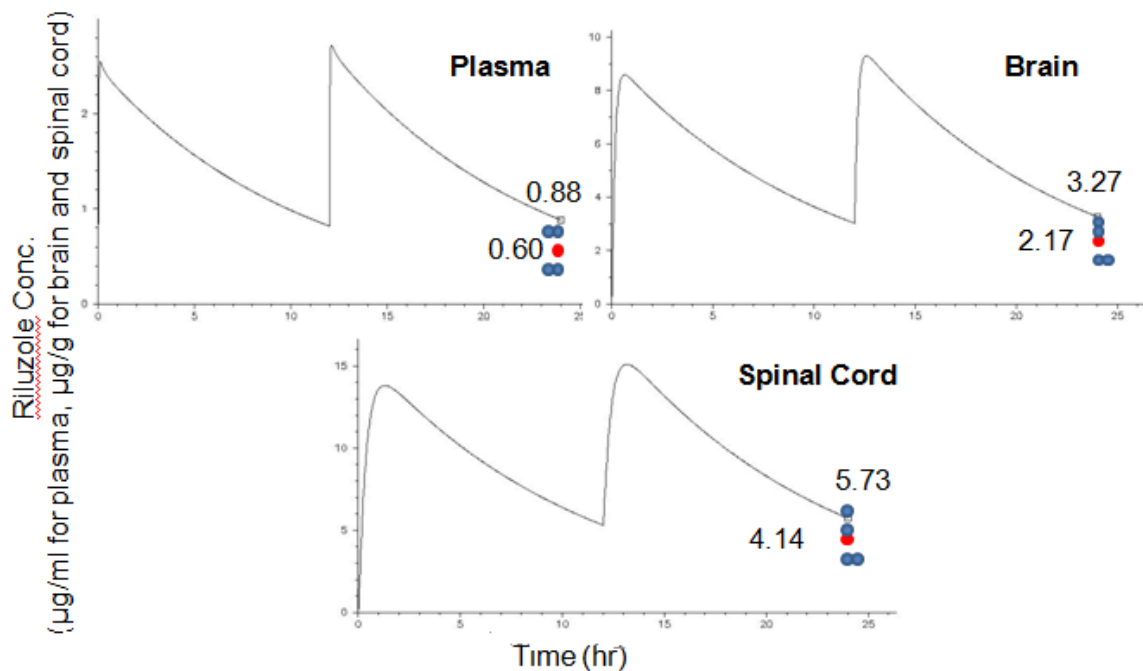


**Figure 22 Predicted Riluzole Concentration Profiles in Plasma, Brain and Spinal Cord after 2 I.P. Doses (8 mg/kg + 6 mg/kg, q 12 hr) for Uninjured Control Group (N =4 at Each Time Point for Observed Concentrations)**

**Red Dots Represented the Mean Observed Riluzole Concentrations with Values; Blue Dots Represented the Individual Observed Riluzole Concentrations; Open Circles on the Profiles Represented the Predicted Concentrations with Values**

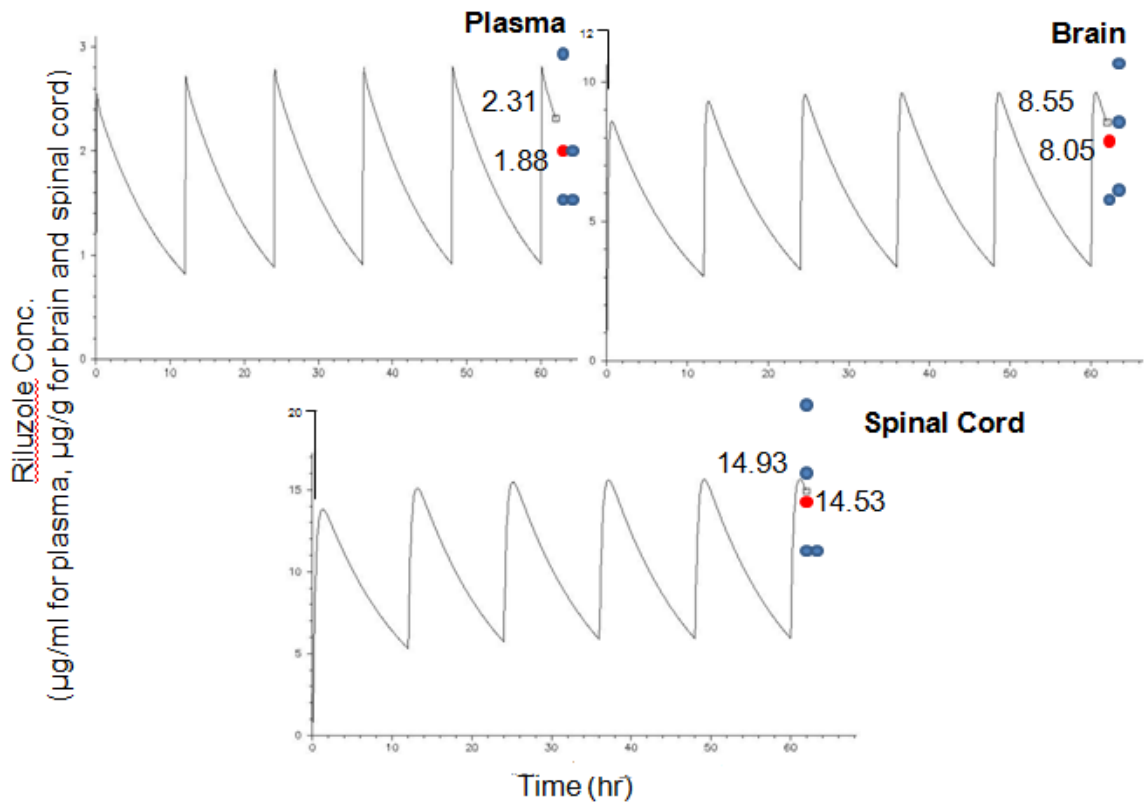


**Figure 23 Predicted Riluzole Concentration Profiles in Plasma, Brain and Spinal Cord after 6 I.P. Doses (First Loading Dose of 8 mg/kg, Followed by 6 mg/kg, q 12 hr) for Uninjured Control Group (N =4 at Each Time Point for Observed Concentrations)**

**Red Dots Represented the Mean Observed Riluzole Concentrations with Values; Blue Dots Represented the Individual Observed Riluzole Concentrations; Open Circles on the Profiles Represented the Predicted Concentrations with Values**

**Table 12 Comparisons of Observed Riluzole Concentrations vs. Predicted Riluzole Concentration by Simulation in Plasma, Brain and Spinal Cord of Uninjured Control Group after 2 and 6 I.P. Doses**

Sampling Time (hr)	Observed Riluzole Concentrations (Predicted Concentrations by Simulation) ( $\mu\text{g/ml}$ or $\mu\text{g/g}$ )		
	Plasma	Brain	Spinal Cord
12 hr post 2nd dose (24 hr post-dosing)	$0.60 \pm 0.18$ (0.88)	$2.17 \pm 0.76$ (3.27)	$4.14 \pm 1.43$ (5.73)
2 hr post 6th dose (62 hr post-dosing)	$1.88 \pm 0.73$ (2.31)	$8.05 \pm 2.87$ (8.55)	$14.53 \pm 5.48$ (14.93)

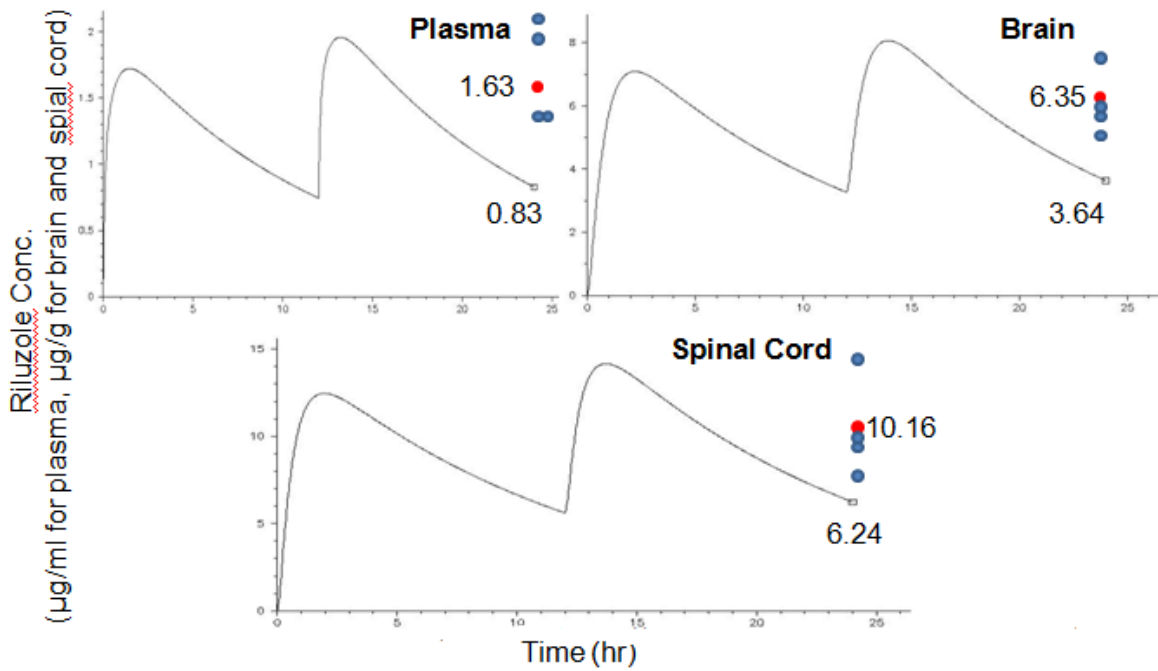


**Figure 24 Predicted Riluzole Concentration Profiles in Plasma, Brain and Spinal Cord after 2 I.P. Doses (8 mg/kg + 6 mg/kg, q 12 hr) for Cervical SCI Group (N =4 at Each Time Point for Observed Concentrations)**

**Red Dots Represented the Mean Observed Riluzole Concentrations with Values; Blue Dots Represented the Individual Observed Riluzole Concentrations; Open Circles on the Profiles Represented the Predicted Concentrations with Values**

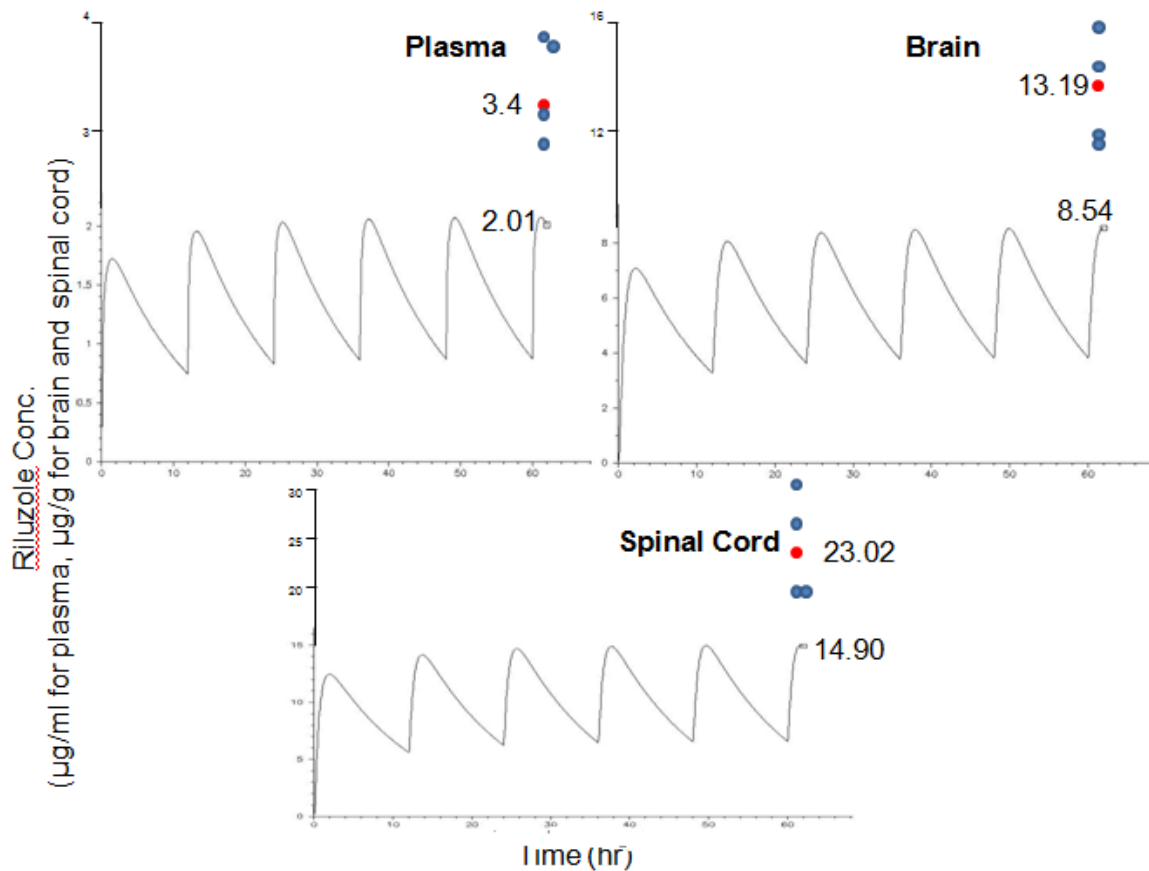


**Figure 25 Predicted Riluzole Concentration Profiles in Plasma, Brain and Spinal Cord after 6 I.P. Doses (First Loading Dose of 8 mg/kg, Followed by 6 mg/kg, q 12 hr) for Cervical SCI Group (N =4 at Each Time Point for Observed Concentrations)**

**Red Dots Represented the Mean Observed Riluzole Concentrations with Values; Blue Dots Represented the Individual Observed Riluzole Concentrations; Open Circles on the Profiles Represented the Predicted Concentrations with Values**

**Table 13 Comparisons of Observed Riluzole Concentrations vs. Predicted Riluzole Concentration by Simulation in Plasma, Brain and Spinal Cord of Cervical SCI Group after 2 and 6 I.P. Doses**

Sampling Time (hr)	Observed Riluzole Concentrations (Predicted Concentrations by Simulation) ( $\mu\text{g/ml}$ or $\mu\text{g/g}$ )		
	Plasma	Brain	Spinal Cord
12 hr post 2nd dose (24 hr post-dosing and 25 hr post-injury)	1.63 $\pm$ 0.40 (0.83)	6.35 $\pm$ 1.21 (3.64)	10.16 $\pm$ 2.34 (6.24)
2 hr post 6th dose (62 hr post-dosing and 63 hr post-injury)	3.40 $\pm$ 0.46 (2.01)	13.19 $\pm$ 1.74 (8.54)	23.02 $\pm$ 3.45 (14.90)

The transferring rate constants among compartments might not be the confounding factors due to the similar proportional under-estimation by 50% of the predicted concentrations. Therefore, we hypothesized that the under-estimations of the predicted Riluzole concentrations in SCI injured rats might be caused by the slower elimination rate constant from the central plasma compartment, of which the impairment became more evident from 13 hr to 63 hr post-injury after multiple doses. In order to verify our hypothesis, we selected a decrease the elimination rate constant of the half value ( $k_{20}$ ,  $0.33/2 = 0.17$ ) and kept all other parameters unchanged. The resulting predicted Riluzole concentrations after the modification were much closer to the mean observed values for both 2- and 6-dose treatments, 1.65 vs. 1.33  $\mu\text{g/ml}$ , 7.12 vs. 6.35  $\mu\text{g/g}$  and 12.29 vs. 10.16  $\mu\text{g/g}$  after 2 doses, 3.36 vs. 3.40  $\mu\text{g/ml}$ , 14.17 vs. 13.19  $\mu\text{g/g}$  and 24.71 vs. 23.02  $\mu\text{g/g}$  after 6 doses (Figures 29-30 & Table 14).

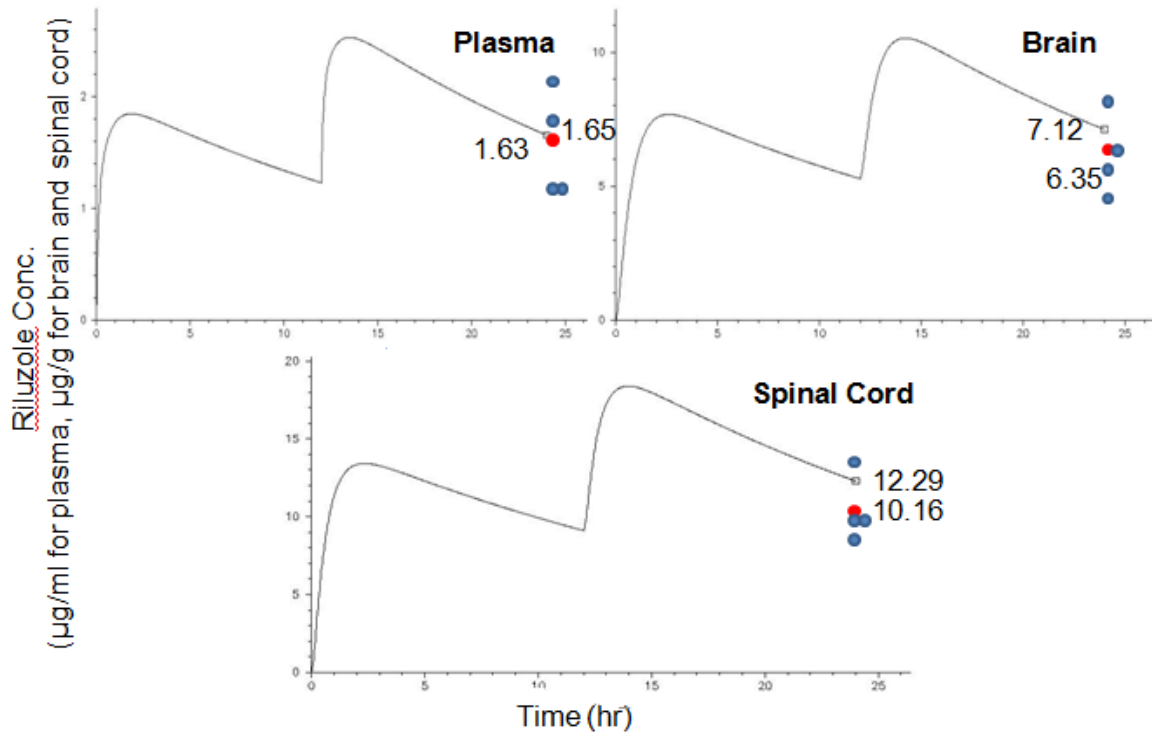


**Figure 26 Predicted Riluzole Concentration Profiles in Plasma, Brain and Spinal Cord after 2 I.P. Doses (8 mg/kg + 6 mg/kg, q 12 hr) for Cervical SCI Group with Decreased Elimination Rate Constant to Half of the Value ( $k_{20} = 0.33/2 = 0.17$ ) (N =4 at Each Time Point for Observed Concentrations)**  
**Red Dots Represented the Mean Observed Riluzole Concentrations with Values; Blue Dots Represented the Individual Observed Riluzole Concentrations; Open Circles on the Profiles Represented the Predicted Concentrations with Values**

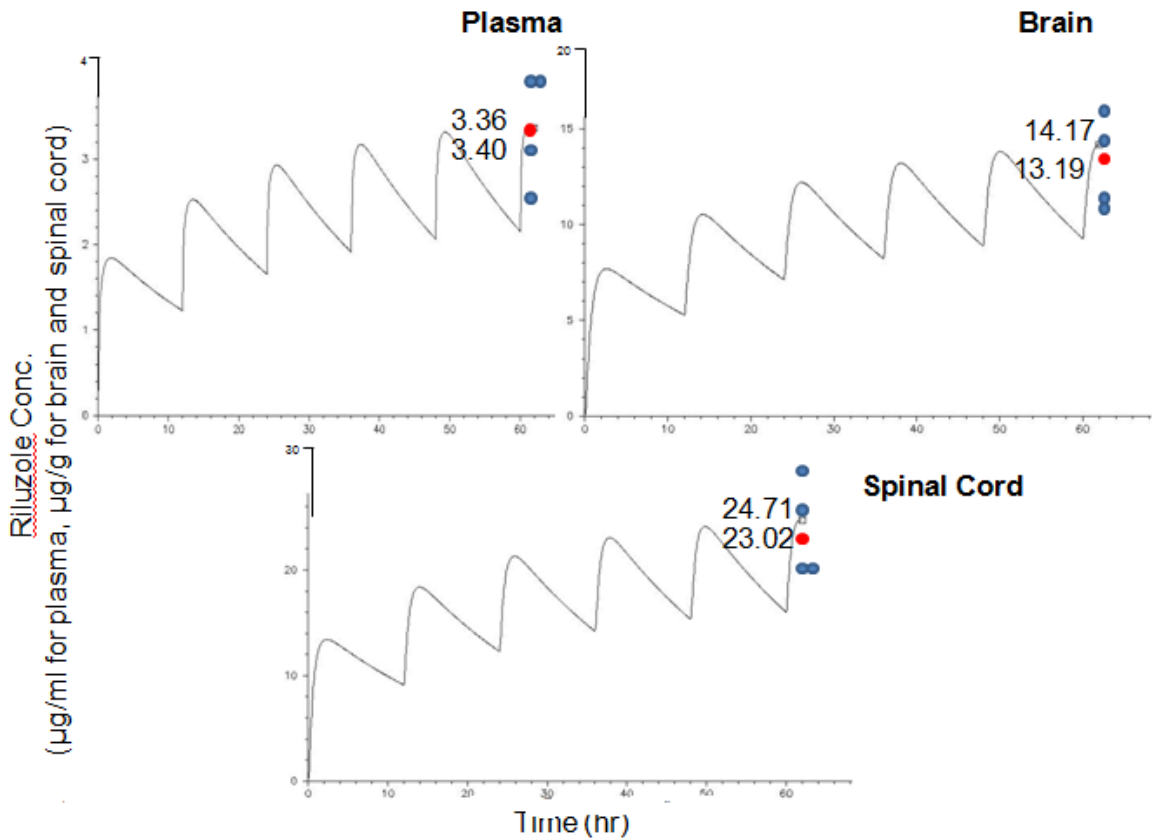


**Figure 30 Predicted Riluzole Concentration Profiles in Plasma, Brain and Spinal Cord after 6 I.P. Doses (First Loading Dose of 8 mg/kg, Followed by 6 mg/kg, q 12 hr) for Cervical SCI Group after Decreased Elimination Rate Constant to Half of the Value ( $k_{20}=0.33/2 = 0.17$ ) (N =4 at Each Time Point for Observed Concentrations)**

**Red Dots Represented the Mean Observed Riluzole Concentrations with Values; Blue Dots Represented the Individual Observed Riluzole Concentrations; Open Circles on the Profiles Represented the Predicted Concentrations with Values**

**Table 14 Comparisons of Observed Riluzole Concentrations vs. Predicted Riluzole Concentrations by Simulation in Plasma, Brain and Spinal Cord of Cervical SCI Group after 2 and 6 I.P. Doses with Decreased Elimination Rate Constant to Half of the Value ( $k_{20} = 0.33/2 = 0.17$ )**

Sampling Time (hr)	Observed Riluzole Concentrations (Predicted Concentrations by Simulation) ( $\mu\text{g/ml}$ or $\mu\text{g/g}$ )		
	Plasma	Brain	Spinal Cord
12 hr post 2nd dose (24 hr post-dosing and 25 hr post-injury)	1.63 $\pm$ 0.40 (1.65)	6.35 $\pm$ 1.21 (7.12)	10.16 $\pm$ 2.34 (12.29)
2 hr post 6th dose (62 hr post-dosing and 63 hr post-injury)	3.40 $\pm$ 0.46 (3.36)	13.19 $\pm$ 1.74 (14.17)	23.02 $\pm$ 3.45 (24.71)

#### **4.3.5 Correlations of Riluzole Concentrations in Brain and Spinal Cord with Concentrations in Plasma**

Linear regression in SYSTAT program was used to establish the correlations of Riluzole concentrations in brain and spinal cord with those in plasma. The Riluzole concentrations in brain and spinal cord exhibited good correlations with those in plasma after single and multiple I.P. doses, based on the p values ( $p < 0.05$ ) (Figures 31 & 32). The Riluzole concentrations in the plasma could be used as a substituted measure to predict the Riluzole concentrations in the brain and spinal cord compartments in the rat model. We could calculate Riluzole concentrations in the brain and spinal cord based on plasma samplings and the established correlation equations (Figures 31 & 32). The results provided the rationale that the plasma concentrations monitored in the phase I clinical trial were meaningful and relevant for clinical efficacy outcomes from Riluzole treatment.

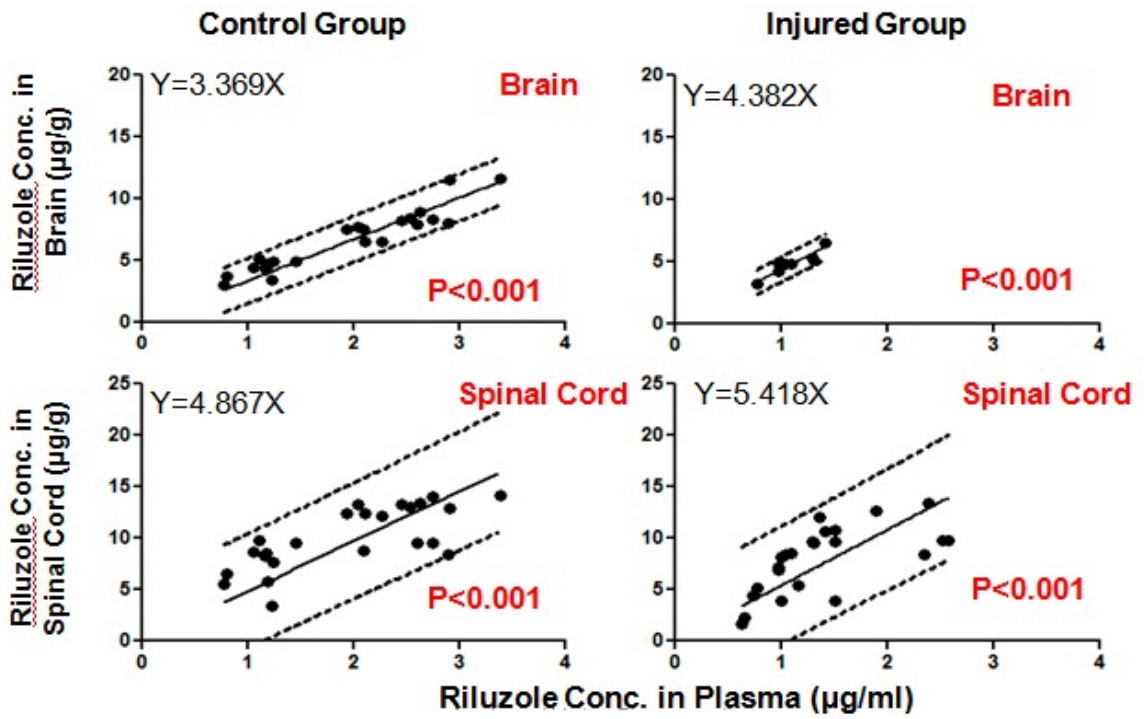


**Figure 31 Correlations of Riluzole Concentrations in Brain and Spinal Cord with Plasma Concentrations for both Control and Injured Groups after Single I.P. Dose of 8 mg/kg**

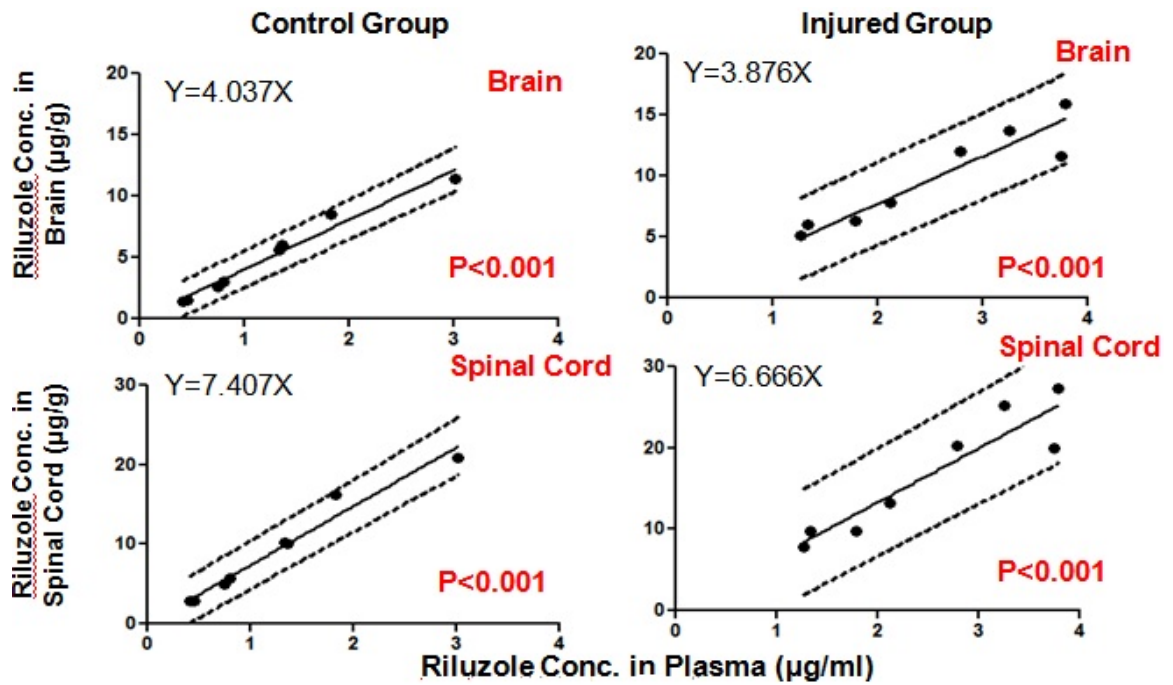


**Figure 27 Correlations of Riluzole Concentrations in Brain and Spinal Cord with Plasma Concentrations for Both Control and Injured Groups after Multiple I.P. Doses (First Loading Dose of 8 mg/kg, Followed by 6 mg/kg, q 12 hr)**

## **4.4 Phase I Clinical Trial of Riluzole in Acute Spinal Cord**

### **Injured Patients**

Thirty-six (36) SCI patients were enrolled between April 12, 2010 to June 20, 2011 and receive 50 mg Riluzole twice daily for 28 doses. The first dose was administered at  $8.7 \pm 2.2$  hr post injury. Thirty-five (35) patients completed the 2-week regimen. One patient had Riluzole administration stopped on Day 7 as the patient had a moderate elevation of Gamma Glutamyl Transpeptidase (GGT) on that day. This patient had received a large number of medications and a definite relationship of the elevated GGT to Riluzole could not be established. Blood tests at 6 months revealed normal liver enzymes (patient ID: R02-002).

#### **4.4.1 Patient Demographics**

The basic demographics of the subjects with plasma samples available and evaluable for Day 3, Day 14 and both days are summarized in Table 15. The ages of the patients were  $39.4 \pm 18.3$  (18-69) years old, with body weights of  $83.0 \pm 16.9$  kg and heights of  $68.7 \pm 4.2$  inches. Among the 35 patients receiving 28 doses of Riluzole, 6 were female. One-third of the patients were smokers. The AIS scores of the patients were A (52.8%), B (25%) or C (22.2%). The neurological injury levels were C4-8 (77.8%), T1-6 (13.9%) or T7-T12 (8.3%).

**Table 15 Demographics of Patients**

Characteristic	Value*		
	Day 3	Day 14	Total
No. of patients	33	32	36
Sex			
Male	28	26	30
Female	5	6	6
Smoking status			
Smoking	11	9	11
Non-smoking	22	23	25
Age (yrs)			
Mean $\pm$ SD	41.15 $\pm$ 18.21	39.63 $\pm$ 18.22	39.44 $\pm$ 18.34
Range	18-69	18-68	18-69
Weight (kg)			
Mean $\pm$ SD	81.22 $\pm$ 13.66	83.33 $\pm$ 17.79	83.01 $\pm$ 16.90
Range	55.69-113.4	55.69-113.4	55.69-113.4
Height (in)			
Mean $\pm$ SD	68.55 $\pm$ 4.29	68.42 $\pm$ 4.33	68.69 $\pm$ 4.23
Range	62-75	62-75	62-75
ASIA Impairment			
Scale grade			
A			19 (52.8)
B			9 (25.0)
C			8 (22.2)
SCI Level			
Cervical 4-8			28 (77.8)
Thoracic 1-6			5 (13.9)
Thoracic 7-12			3 (8.3)

\*Values represent the number of patients (%) unless specified otherwise.

## 4.4.2 Distinct Alterations of Riluzole Pharmacokinetics in SCI

### Patients during Two-week Period Post-injury

The plasma profiles of Riluzole on Day 3 and Day 14 were constructed for individual patients as represented by those of Subject R07-05 (Figure 33). The peak concentration ( $C_{max}$ ) and trough concentration ( $C_{min}$ ) were derived from the quantified samples. The  $C_{max}$  (Mean  $\pm$  S.E.) achieved with the 50 mg BID dose varied significantly among subjects,  $128.86 \pm 14.03$  (23.86-409.16) ng/ml (n=32) on Day 3, and  $76.46 \pm 15.04$  (8.51-316.97) ng/ml (n=27) on Day 14 (Figure 34A). The  $C_{min}$  were of large inter-subject variability as well,  $45.40 \pm 6.97$  (7.08-183.77) ng/ml on Day 3 and  $19.09 \pm 2.67$  (2.78-61.18) ng/ml on Day 14 (Figure 34B). The declines of  $C_{max}$  and  $C_{min}$  on Day 14 from those of Day 3 were significant by nonparametric test ( $p < 0.05$ ), and consistently observed in individual patients from all clinical sites. The extents of reduction were 68.6% and 56.5% for  $C_{max}$  and  $C_{min}$ , respectively.

The systemic exposures of Riluzole from the treatment,  $AUC_{0-12}$  (truncated for each dosing interval of 12 hr) were calculated from individual plasma profiles using the trapezoidal rule. The  $AUC_{0-12}$  were  $982.03 \pm 111.18$  ng\*hr/ml and  $521.01 \pm 87.32$  ng\*hr/ml for Day 3 and Day 14, respectively, and exhibited the same trend of decline as in  $C_{max}$  and  $C_{min}$  for Day 14 from Day 3 on the same dose basis (Figure 34C).

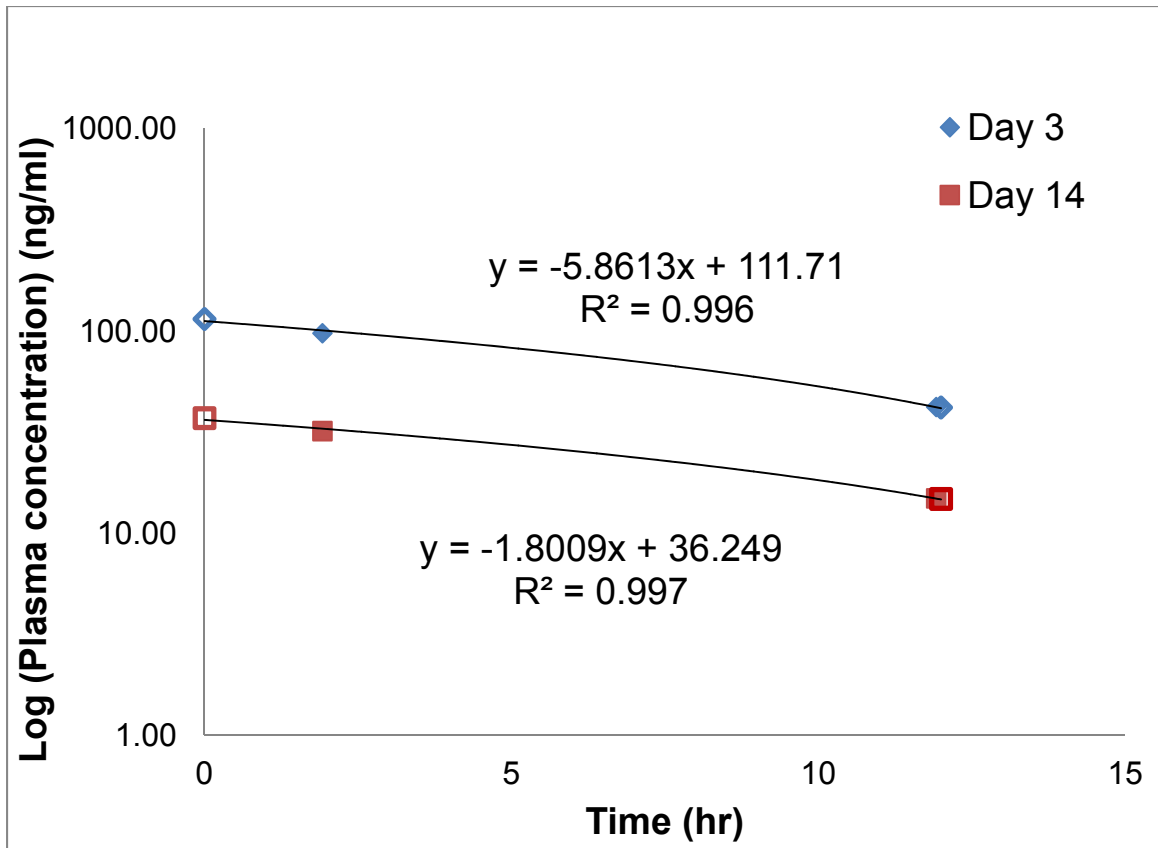


**Figure 28 Typical Pharmacokinetic Profiles of Riluzole in Human Plasma Samples for Day 3 and Day 14**

Riluzole dose of 50 mg was given at 0 Time. Plasma concentrations of Riluzole were shown in a blood sample taken 2 Hours after dose (Peak Value) and in blood sample taken at 12 hours after dose, prior to the next dose (Trough Value)

**Open Symbols: Calculated Values; Solid Symbols: Measured Values**

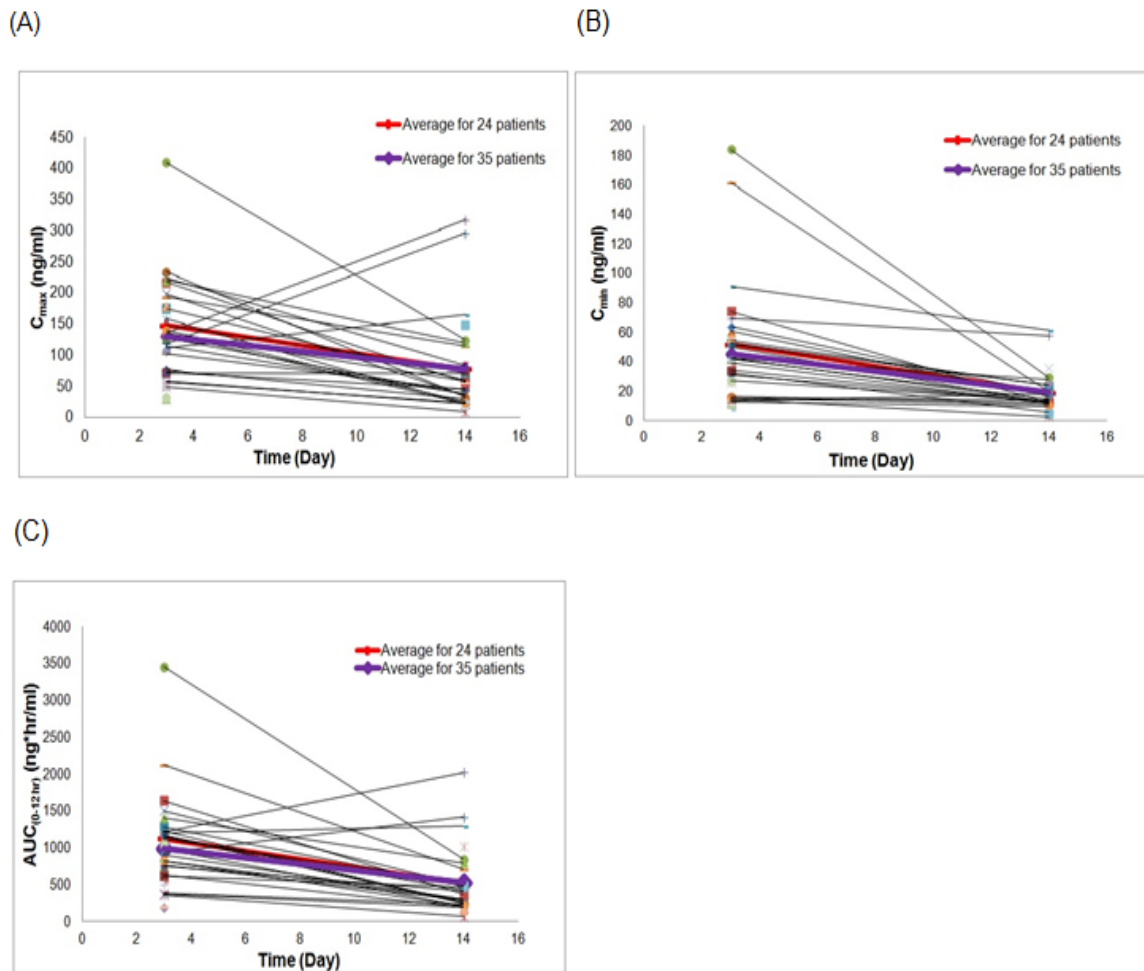


**Figure 29 Spaghetti Plots of (A)  $C_{max}$ , (B)  $C_{min}$  and (C)  $AUC_{0-12}$  on Day 3 and Day 14**

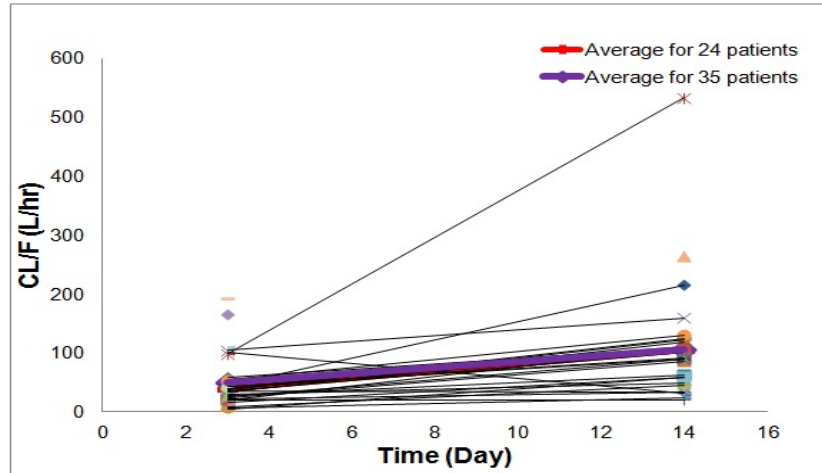
**( $C_{max}$  and  $C_{min}$  exhibited the same trend as  $AUC_{0-12}$  from Day 3 to Day 14 on the same dose basis, twenty-four patients had both Day 3 and Day 14 data available)**

**Note: Symbols without Lines Connecting Days 3 and 14 have Values only for Day 3 or Day 14**

The pharmacokinetic parameters of clearance (CL/F), volume of distribution (V/F) and biological half-life ( $t_{1/2}$ ) were derived using standard pharmacokinetic equations in Method 3.2.4.5.2. The CL/F was  $49.47 \pm 7.77$  (3.82-192.23) L/hr on Day 3, but significantly increased on Day 14 to  $106.20 \pm 19.80$  (20.66-533.58) L/hr (Figure 35-A). The V/F was  $557.06 \pm 73.80$  (120.8-2046.3) L and  $1297.88 \pm 218.92$  (129.75-5718.99) L for Day 3 and Day 14, respectively (Figure 35-B). The  $t_{1/2}$  is affected by the alterations in CL/F and V/F independently, as  $t_{1/2} = 0.693 V/CL$ . As a result, the net effect on  $t_{1/2}$  was nil, due to the increases in both CL/F and V/F offsetting each other with the comparable magnitudes. The  $t_{1/2}$  remained as 10.61-11.91 hr on Day 3 and Day 14 (Table 16). The higher  $C_{max}$ ,  $C_{min}$  and  $AUC_{0-12}$  observed on Day 3 as compared with those on Day 14 were resulted from the lower CL/F and smaller V/F on Day 3.

In comparing the pharmacokinetic parameters of Riluzole in SCI patients with those in healthy volunteers (Table 16), the  $C_{max}$  on Day 3 and Day 14, as well as  $AUC_{0-12}$  on Day 14 were lower than those in healthy subjects. However, it may be difficult to determine the cause of this difference due to the different doses given, 9 doses (Le Liboux A et al., 1997) and 20 doses (Le Liboux A et al., 1999) in healthy volunteers versus a maximum of 6 doses on Day 3 and 28 doses on Day 14 in the current trial.

(A)



(B)

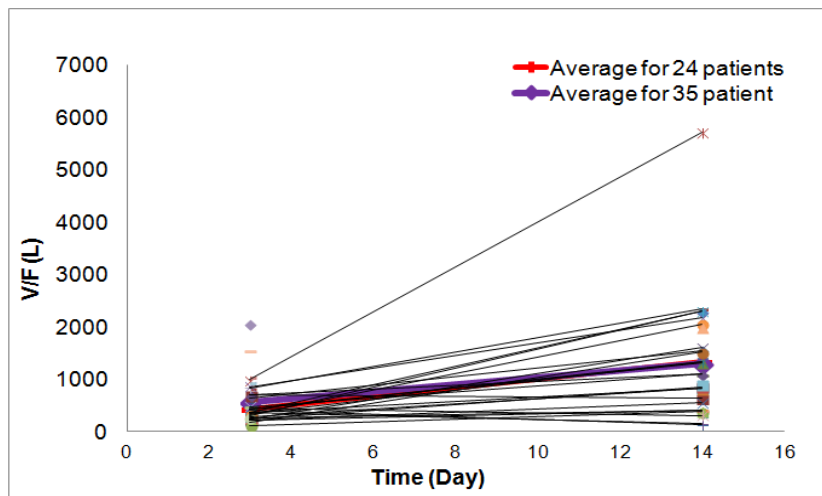


**Figure 30 Spaghetti Plots of (A) Clearance (CL/F) and (B) Volume of Distribution**

**(V/F) on Day 3 and Day 14**

**(Twenty-four patients had both Day 3 and Day 14 data available)**

**Symbols without Lines Connecting Days 3 and 14 have Values only for**

**Day 3 or Day 14**

**Table 16 Pharmacokinetic Parameters of Riluzole in Spinal Cord Injured Patients and Healthy Volunteers\***

Parameters	Spinal Cord Injured Patients Individual Estimation		Healthy Volunteers		
	Day 3 (n=32)	Day 14 (n=27)	White Individuals (n=12)†	Young Individuals (n=18) ‡	Elderly Individuals (n=18) ‡
Dose	50 Bid	50 Bid	50 Bid	50 Bid	50 Bid
Sex (M/F)	28/4	23/4	All male	9/9	9/9
Mean Age (yrs)	41.15 ± 3.17	39.63 ± 3.22	18-40	18-30	70-82
C <sub>max</sub> (ng/ml)	128.86 ± 14.03 (10.9%)	76.46 ± 15.04£ (19.7%)	173 ± 21	244 ± 33	271 ± 29
AUC <sub>0-12 hr</sub> (ng*hr/ml)	982.03 ± 111.18 (11.3%)	521.01 ± 87.32£ (16.8%)	654 ± 81	869 ± 110	1029 ± 95
AUC <sub>0-∞</sub> (ng*hr/ml)	2101.99 ± 441.09 (21.0%)	807.83 ± 111.26£ (13.8%)			
CL/F (L/hr)	49.47 ± 7.77 (15.7%)	106.20 ± 19.80£ (18.6%)		71.35 ± 7.33	59.32 ± 6.99
k (hr <sup>-1</sup> )	0.095 ± 0.009 (9.3%)	0.101 ± 0.010 (9.7%)			
t <sub>1/2</sub> (hr)	11.91 ± 2.18 (18.3%)	10.61 ± 2.23 (21.0%)	14.7 ± 3.5	49.03 ± 10.93	40.30 ± 8.84

\* Mean Values are ± SE;

When this construction is followed by a value in parentheses, the value is the relative standard error (the standard error divided by the mean)

Abbreviations: AUC<sub>0-∞</sub>= the area under the curve (calculated by Dose/[CL/F]; BID= twice daily; CL/F= apparent oral clearance; k= elimination rate constant; RES= relative standard error (the standard error divided by the mean and expressed as a percentage); V/F= apparent volume of distribution

£ Statistically difference between Day 3 and Day 14 using the nonparametric test (sign), p<0.05

† Based on data from Le Liboux et al, 1997 (Samplings on Day 13)

‡ Based on data from Le Liboux et al, 1999 (Samplings on Day 5)

### 4.3 Individual and Population Pharmacokinetic Parameters

The individual PK parameters were estimated using the two concentration-time data on each day (Day 3 and Day 14) to obtain the elimination rate constant and other parameters using the equations described in Method 3.2.4.5.2., and compared with those from final population PK model (Table 17).

The population PK model was best represented by a one-compartment first-order absorption and elimination model that included inter-individual and intra-individual variability. The parameter estimates given by this model are summarized in Table 17. The population mean parameter estimates were in good agreement with the parameters derived using individual estimation for CL/F (60.4 vs. 50.0 L/hr), V/F (663 vs. 557 L), and the further derived half-life (7.29 vs. 11.91 hrs) on Day 3, as well as CL/F (148 vs. 106 L/hr), V/F (2080 vs. 1298 L), and the further derived half-life (9.76 vs. 10.61 hrs) on Day 14. The absorption constant ( $k_a$ ) proved to be difficult to estimate. Fixing  $k_a$  to values from 0.5 to 100  $\text{hr}^{-1}$  did not affect the estimates of the other parameters and the fit of model, indicating that those values are equally probable, based on the available data. Therefore,  $k_a$  was fixed to 5  $\text{hr}^{-1}$  (Bruno R et al., 1997).

The basic one-compartment pharmacokinetic model that incorporated inter-individual and intra-individual variability was retained for covariate model building. The covariates that were introduced into the clearance model did not significantly improve the fit of the

**Table 17 Comparison of Population and Individual Estimated Pharmacokinetic Parameters of Riluzole for Day 3 and Day 14\***

Parameters	Population Pharmacokinetics Mean ± SE (RSE%)		Individual Estimation Mean ± SE (RSE%)	
	Day 3 (n=33)	Day 14 (n=32)	Day 3 (n=32)	Day 14 (n=27)
C <sub>max</sub> (ng/ml)			128.86 ± 14.03 (10.9%)	76.46 ± 15.04† (19.7%)
AUC <sub>0-∞</sub> (ng*hr/ml)	827.81	337.84	2101.99 ± 441.09 (21.0%)	807.83 ± 111.26† (13.8%)
CL/F (L/hr)	60.4 ± 6.24 (10.3%)	148 ± 25.5 (17.2%)	49.47 ± 7.77 (15.7%)	106.20 ± 19.80† (18.6%)
V/F (L)	663 ± 103 (16.3%)	2080 ± 947 (45.5%)	557.06 ± 73.80 (13.2%)	1297.88 ± 218.92† (16.9%)
ka (hr <sup>-1</sup> )	5‡	5‡		
k (hr <sup>-1</sup> )	0.095	0.071	0.095 ± 0.009 (9.3%)	0.101 ± 0.010 (9.7%)
t <sub>1/2</sub> (hr)	7.29	9.76	11.91 ± 2.18 (18.3%)	10.61 ± 2.23 (21.0%)
ω <sub>CL</sub> (%)	20.0% ± 8.13% (40.6%)	41.7% ± 23.6% (56.6%)		
ω <sub>V</sub> (%)	0.13 % ± 0.11% (79.1%)	0.02% ± 0.01% (37.2%)		
σ <sub>Proportional error</sub> (%)	11.8% ± 2.27% (19.2%)	20.6% ± 5.19% (25.2%)		
σ <sub>Additive error</sub> (ng/ml)	13.8 ± 11.9 (86.2%)	2.43 ± 3.24 (133%)		

\* Mean Value are ± SE;

When this construction is followed by a value in parentheses, the value is the relative standard error (the standard error divided by the mean and expressed as a percentage);  
Abbreviations: ka=absorption rate constant; ω=inter-individual variability; σ=residual variability;

† Statistical difference between Day 3 and Day 14 using Nonparametric test (sign),  
p<0.05;

‡ Fixed parameter.

basic model (objective function values, OFV>7.8; P<0.005) after forward and backward steps. The tested covariates included gender, body weight, smoking status, age and creatinine clearance. When added to the volume of distribution model, no covariates significantly improved the fit (Table 18).

The results of Riluzole population PK model evaluation revealed that the final model provided a reliable description of the data with good precisions of the parameter estimates. The stratified nonparametric bootstrap procedure resulted in 95% CIs for population PK parameter estimates, which are summarized in Table 19.

The diagnostic plots from the fit of the final model are presented for both Day 3 and Day 14 (Figure 36), which suggested that the current sampling schedule (2 blood samples for peak and trough concentrations, respectively) was adequate to characterize the PK of Riluzole for future clinical trial in SCI patients.

#### **4.4.4 Plasma Protein Binding**

Retrospectively, the plasma samples of ten patients were re-assayed for free fractions (fu) of Riluzole. The fractions unbound were comparable between Day 3 and Day 14,  $6.18 \pm 1.33\%$  and  $9.57 \pm 3.08\%$ , respectively, and could not be accounted for the significantly larger V/F on Day 14.

**Table 18 Forward and Backward Steps for Covariate Model of Riluzole**

Model	Test	Base OFV	New OFV	Test Value		Goal	Significant?
CLWT	OFV	424.486	421.509	2.977	<	3.8	No!
CLAGE	OFV	424.486	424.432	0.054	<	3.8	No!
CLSEX	OFV	424.486	419.523	4.963	>	3.8	Yes!
CLSMK	OFV	424.486	424.260	0.226	<	3.8	No!
VWT	OFV	424.486	421.304	3.182	<	3.8	No!
VAGE	OFV	424.486	424.352	0.134	<	3.8	No!
VSEX	OFV	424.486	423.725	0.761	<	3.8	No!
VSMK	OFV	424.486	422.309	2.177	<	3.8	No!

Parameter-covariate relation chosen in this forward step: CL-SEX  
Parameter-covariate relation chosen in this backward step: NONE

Forward inclusion ( $p < 0.05$ , 3.8)  
Backward elimination ( $p < 0.005$ , 7.8)  
Continuous (Age, BW) and Categorical (SEX, SMK)

**Table 19 Pharmacokinetic Parameters of Riluzole in Acute SCI Patients for Day 3  
and Day 14**

Parameters	Population Pharmacokinetics			
	Day 3		Day 14	
	Mean $\pm$ SE (RSE%)	Bootstrap 95% CI	Mean $\pm$ SE (RSE%)	Bootstrap 95% CI
No.	33	33	32	32
$C_{max}$ (ng/ml)				
$AUC_{0-\infty}$ (ng*hr/ml)	827.81		337.84	
CL/F (L/hr)	60.4 $\pm$ 6.24 (10.3%)	59.4 (47.4 to 71.4)	148 $\pm$ 25.5 (17.2%)	133 (95.4 to 171)
V/F (L)	663 $\pm$ 103 (16.3%)	553 (391 to 715)	2080 $\pm$ 947 (45.5%)	1650 (523 to 2780)
$k_a$ (hr <sup>-1</sup> )	5‡	5‡	5‡	5‡
$k$ (hr <sup>-1</sup> )	0.095		0.071	
$t_{1/2}$ (hr)	7.29		9.76	
$\omega_{CL}$ (%)	20.0% $\pm$ 8.13% (40.6%)	14.5% (1.56 % to 27.4%)	41.7% $\pm$ 23.6% (56.6%)	33.9% (2.93% to 64.9%)
$\omega_V$ (%)	0.13 % $\pm$ 0.11% (79.1%)	0.16% (-0.009% to 0.3%)	0.02% $\pm$ 0.01% (37.2%)	0.006% (0.002% to 0.01%)
$\sigma_{Proportional\ error}$ (%)	11.8% $\pm$ 2.27% (19.2%)	14.4% (8.68% to 20.1%)	20.6% $\pm$ 5.19% (25.2%)	18.2% (11.8% to 24.6%)
$\sigma_{Additive\ error}$ (ng/ml)	13.8 $\pm$ 11.9 (86.2%)	30.1 (-63.4 to 124)	2.43 $\pm$ 3.24 (133%)	2.57 (-5.68 to 10.8)

Mean Value are  $\pm$  SE;

When this construction is followed by a value in parentheses, the value is the relative standard error (the standard error divided by the mean and expressed as a percentage);

Abbreviations:  $k_a$ =absorption rate constant;  $\omega$ =inter-individual variability;  $\sigma$ =residual variability;

‡ Fixed parameter.

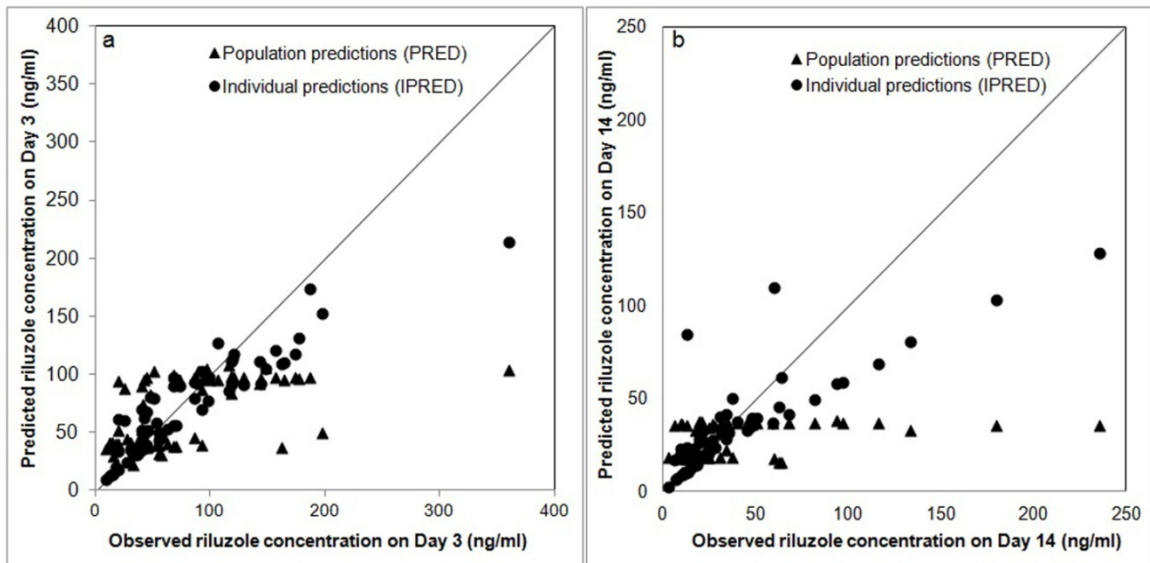


**Figure 31 Goodness Fit of Plots. Population PK Predicted and Individual PK Predicted Riluzole Concentrations vs. Observed Riluzole Concentrations on (a) Day 3 and (b) Day 14**

**The Line of Identity (solid black) is included as a Reference**

#### **4.4.5 Safety Data**

A summary of the findings is given here:

##### ***Medical Complications***

The incidence and types of medical complications in the phase I study group were similar to those without receiving Riluzole in a comparable group of patients who were matched for demographic and injury characteristics, whose clinical courses were recorded in the NACTN Registry of SCI patients admitted to the NACTN clinical centers. In the present study the number of complications by organ/system within 30 days of admission was: Pulmonary-16 in 11 patients; Infections including pneumonia-19 in 14; Cardiovascular-5 in 5; Gastrointestinal-5 in 4; Skin-5 in 4; Hematological-9 in 7; Psychiatric-6 in 5; and Neurological-5 in 5 patients.

##### ***Liver Enzyme Elevations***

An elevation of ALT, AST, or GGT, singly or in combination, occurred on one or more of the 4 days on which liver enzyme levels were monitored. Elevations were classified as mild (> ULN to 2.5 times ULN), moderate (> 2.5 to 5 times ULN), or severe (> 5 to 20 times ULN). The highest level obtained was used to classify the severity of elevation for each patient. For each of these enzymes, mild and moderate elevations occurred in the following proportions: ALT: mild 42%, moderate 28%; AST: mild 44%, moderate 19%; GGT: mild 36%, moderate 14%; ALP: mild 14%, moderate 3%. A severe elevation of ALT (6 times the ULN) occurred in 1 patient, of AST (5.5 times the ULN) in another, and of GGT (7 times the ULN) in a third patient; all returned to normal at the 3- and 6-month

follow-up examinations. The levels fluctuated over the 14-day course in individual patients; even if they were elevated on 1 of the days of monitoring, the levels did not necessarily continue to increase. There was mild elevation of bilirubin in 4 patients and moderate elevation in 1 patient.

#### **4.4.6 Efficacy Evaluations**

The efficacy outcomes were evaluated from three variables, first-dosing time of Riluzole (post-injury time), ASIA impairment scale and spinal cord injury position.

The motor function had been significantly improved at 3- and/or 6-month of follow-up examinations and the sensory function at 6-month follow-up examination after 2-week Riluzole treatment. The improvements of motor and sensory scores between 3-month and 6-month follow-ups were not significantly different (Figure 37).

The improvements of motor and sensory scores at the last follow-up examination (3-month or 6-month follow-ups) were no statistical difference when Riluzole was administrated between different time intervals within 12 hrs since injury (Figure 38), which provided the evidence that the first dosing time of Riluzole at any time within 12 hrs since injury had no effects on the efficacy outcomes. Most of the patients with AIS A had less, no or even worse improvements of motor/sensory scores.

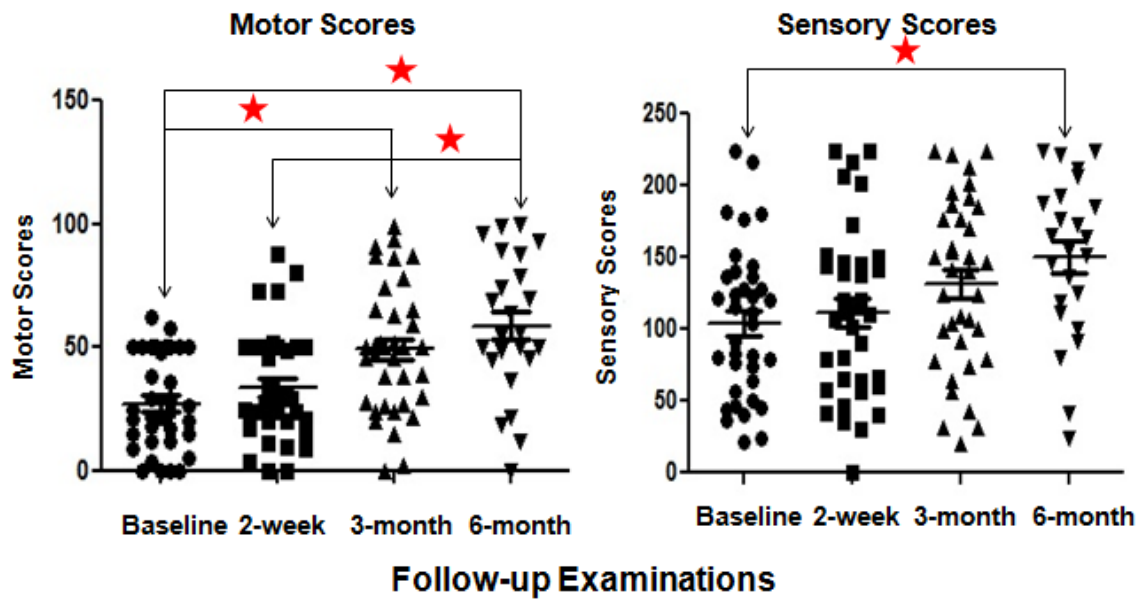
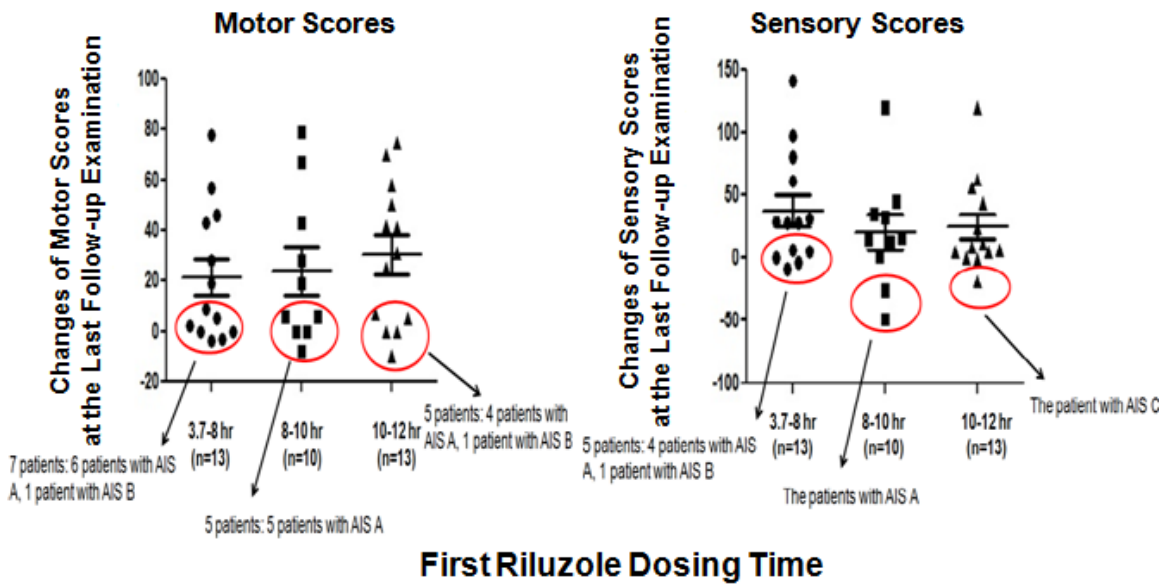


Figure 32 Scatter Plots of Motor and Sensory Scores vs. Follow-up Examination

(\*Nonparametric Kruskal-Wallis test, Significance level  $p < 0.05$ ;  $N = 36$ , except 6-month follow-up examination  $N = 24$ )



**Figure 33 Scatter Plot of the Changes of Motor and Sensory Scores at the Last Follow-up Examination (3- month or 6-month follow-ups) vs. First Riluzole Dosing Time (Post-injury Time)**

The ASIA impairment scale had significant effects on the improvements of motor scores, not on the sensory scores (Figure 39). The improvements of motor scores at the last follow-up examination (3-month or 6-month follow-ups) for the patients with AIS A were statistically lower than those of patients with AIS B or C. The spinal cord injury with AIS A level is in an extremely severe condition, the patients have no motor or sensory function preserved in the sacral segments S4-S5, which is very difficult to treat and get recovery. From this point, we might stratify the patients into two groups, AIS A group, and combined AIS B and C group for PK-PD correlations.

The spinal cord injury position also affected the improvements of motor scores significantly. The improvements of motor scores in patients with thoracic spinal cord injury were significantly less than those of patients with cervical spinal cord injury (Figure 40). Therefore, we stratified the patients into two groups, cervical injured group and thoracic injured group, for PK-PD correlations.

Statistical tests were performed by nonparametric Kruskal-Wallis test, at a significance level  $p < 0.05$ .

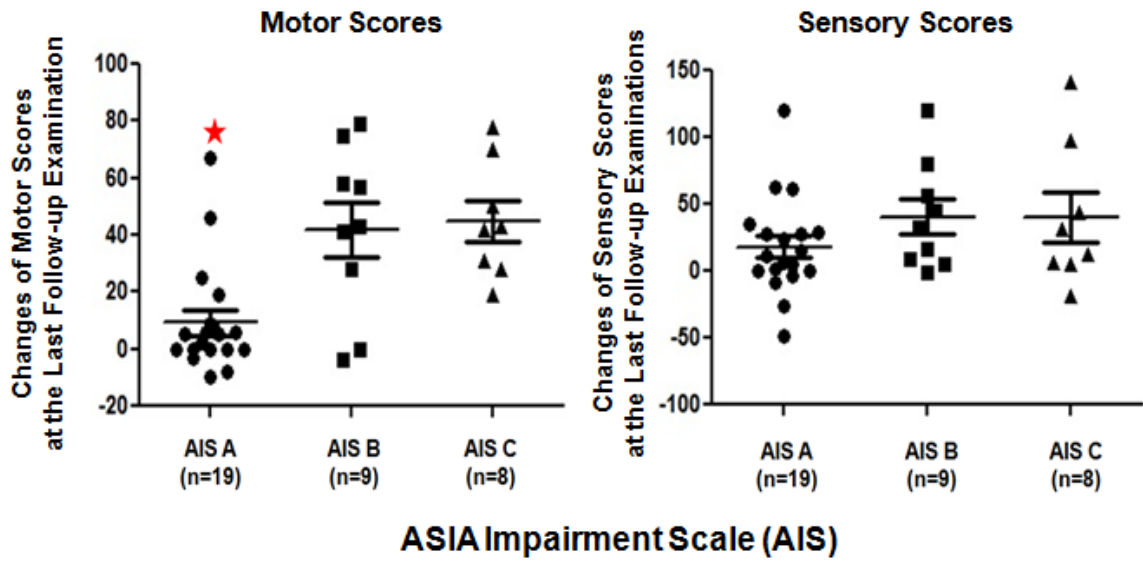


**Figure 34 Scatter Plots of the Changes of Motor and Sensory Scores at the Last Follow-up Examination (3-month or 6-month follow-ups) vs. ASIA Impairment Scale (AIS)**

(\*Nonparametric Kruskal- Wallis test, Significance level  $p < 0.05$ )

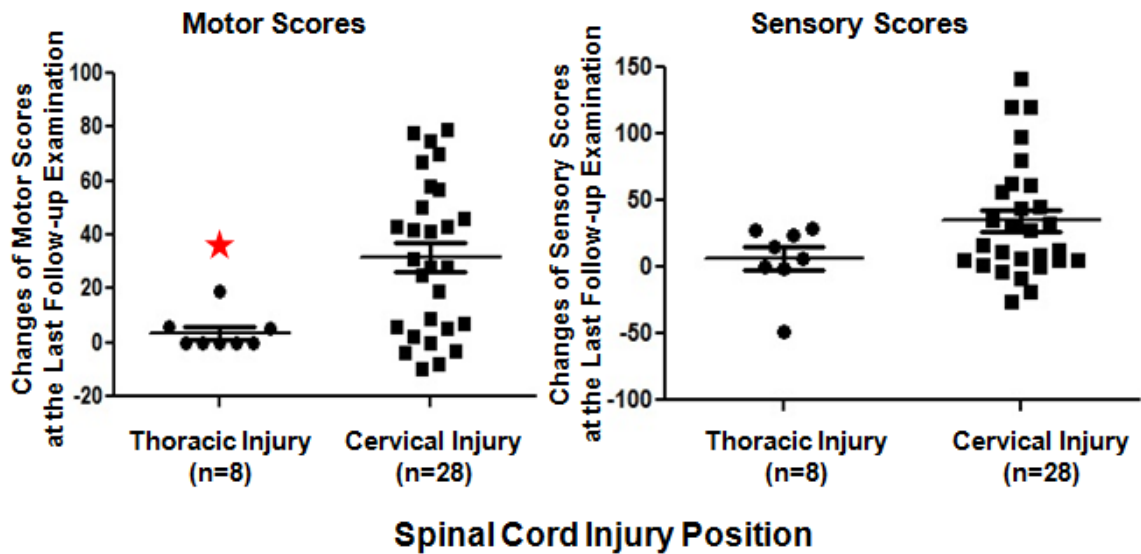


**Figure 40 Scatter Plots of the Changes of Motor and Sensory Scores at the Last Follow-up Examination (3-month or 6-month follow-ups) vs. Position of Spinal Cord Injury**

(\*Nonparametric Kruskal- Wallis test, Significance level  $p < 0.05$ )

#### **4.4.7 Pharmacokinetic/pharmacodynamic (PK/PD) Correlations**

Multiple PK/PD correlations, using increases in motor scores (maximal, 3-month or 6-month follow-ups) for efficacy with PK values ( $C_{max}$ ,  $C_{max}/\text{body weight}$ ,  $AUC_{0-12}$ ,  $AUC_{0-12}/\text{body weight}$ ) (Table 20) were attempted. A similar approach was employed for toxicity (maximal, Day 3 or Day 14 ULN ratio of ALT or AST) (Table 20).

The changes of motor and sensory scores at 3-month follow-up had good correlations with Day 3 AUC/kg within the range of 90% percentile of  $AUC_{0-12}/\text{kg}$  (3.40-25.03 ng\*hr/ml/kg) in 20 patients with cervical injury (Figure 41). No relationship was found between elevation of enzymes and  $AUC_{0-12}/\text{kg}$  (Figure 42). The establishments of PK-PD correlation may be used to predict the potential PD outcomes in future clinical trials.

**Table 20 Attempts of PK-PD Correlations (p < 0.05 indicates correlation established)**

Subjects	Efficacy	PK Parameters (Day 3 or Day 14)	Enzyme Levels
	3-month Change of Motor Scores	$C_{max}$	Maximal ULN Ratio of ALT
	3-month Change of Sensory Scores	$C_{max}/\text{body weight}$ (kg, day 0)	Day 3 ULN Ratio of ALT
Patients with Cervical Injury	6-month Change of Motor Scores	$AUC_{0-12}$	Day 14 ULN Ratio of ALT
	6-month Change of Sensory Scores	$AUC_{0-12}/\text{body weight}$ (kg, day 0)	Maximal ULN Ratio of AST
	Maximal Change of Motor Scores		Day 3 ULN Ratio of AST
	Maximal Change of Sensory Scores		Day 14 ULN Ratio of AST

:Correlation Established

## Patients with cervical injury

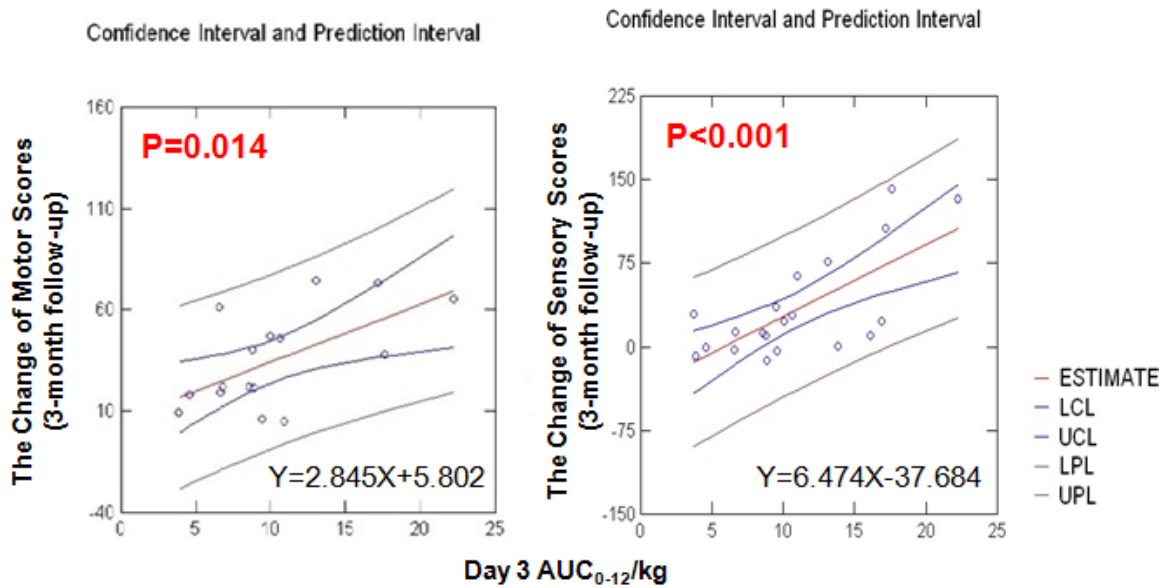


Figure 35 PK-PD Correlations of Change of Motor and Sensory Scores at 3-month Follow-up with Riluzole Day 3  $AUC_{0-12}/kg$  (N = 16 for Correlation of Change of Motor Score; N = 20 for Correlation of Change of Sensory Score)

## Patients with cervical injury

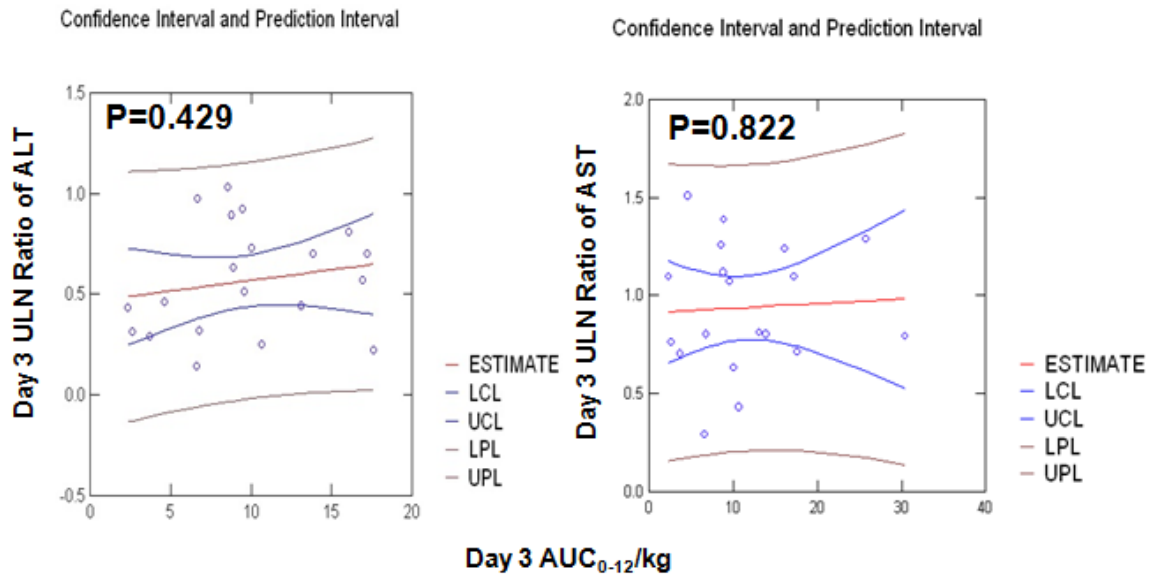


Figure 36 Correlations of Day 3 ULN Ratios of ALT and AST with Riluzole Day 3 AUC<sub>0-12</sub>/kg (N =20)

## DISCUSSION

Acute spinal cord injury (SCI) is a complex disorder involving a sudden traumatic insult to the spinal cord resulting in deficits to ambulatory, sensory and autonomic functions depending on the neurological level and completeness of lesion (Sekhon LH and Fehlings MG, 2001). At present, it is widely accepted that two major pathophysiological events account for the neurological deficits associated with acute SCI: primary and secondary injurious events (Tator CH, 1995; Tator CH and Fehlings MG, 1991). Primary mechanisms, including forces of compression, contusion, shear, distraction and dislocation, are not amenable to therapy. However, with the onset of delayed secondary processes, a therapeutic window exists for intervention. Secondary processes associated with acute SCI include edema, ischemia, inflammation, excitotoxicity, disturbances to ionic homeostasis and apoptosis. In the immediate period (primary) after traumatic spinal cord injury (SCI), a variety of secondary injury mechanisms combine to gradually expand the initial lesion size, potentially leading to diminished neurological outcomes at long-term follow-up.

Most therapeutic interventions that have been hypothesized to improve neurological outcomes after SCI fall into one of two broad categories with respect to mechanisms of action. The first group of therapies aims to promote regeneration of neural tissue within the spinal cord post-injury. Such therapies include emerging drug treatments such as Cethrin, as well as stem cell implantation therapies (Fehlings MG et al., 2011; Hawryluk GW et al., 2008; Rowland JW et al., 2008). The second group of treatments, instead of

generating new tissue, operate to protect viable spinal cord tissue early on after the injury by mitigating the evolution of secondary injury events. GM-1 (Sygen), have been the subject of the largest clinical trials in SCI performed to date (Bracken MB et al., 1984, 1990 and 1997; Geisler FH et al., 2001). Although treatments from both described categories have shown exceptional promise at the preclinical stages of investigation, none have been proven to be uniformly effective in the treatment of human patients with SCI (Hawryluk GW et al., 2008).

Riluzole, a benzothiazole drug, which has neuroprotective properties gleaned from preclinical literatures, falls into the second category of therapies, based on its sodium channel blockade and mitigation of glutamatergic toxicity, is currently an approved drug that attenuates the extent of neuronal degeneration in patients with amyotrophic lateral sclerosis (ALS). Moreover, several preclinical SCI studies have associated Riluzole administration with improved functional outcomes and increased neural tissue preservation (Schwartz G and Fehlings MG, 2002; Tator CH and Koyanagi I, 1997).

In a 2001 study by the Fehlings group, the effects of Riluzole were compared with phenytoin, CNS5546A (a novel sodium channel-blocking compound), and a control compound in rats with severe compression-induced cervical SCI (Schwartz G and Fehlings MG, 2001). At 6 weeks' follow-up, while rats in all treatment groups demonstrated some degree of recovery, those in the Riluzole treated group experienced a significantly larger degree of functional recovery as compared to other treatment

groups. Also in comparison to the other groups, the Riluzole-treated animals exhibited a significantly reduced area of tissue cavitation at the injury epicenter on postmortem histological analysis. Riluzole's neuroprotective effects are due to its combined ability to prevent sodium and calcium influxes as well as to block the synaptic release of excitotoxic glutamate.

Based on these findings, Riluzole has attracted considerable interest as a potential neuroprotective drug for the treatment of SCI. Currently, a Phase I trial evaluating the safety and pharmacokinetic profile of Riluzole in human SCI patients was recently completed by the North American Clinical Trials Network (NACTN) for the treatment of SCI.

Thirty-six patients enrolled in the clinical trial received Riluzole 50 mg every 12 hours for a total of 28 doses, with treatment initiated within 12 hours of injury. The 12-hour drug window, as well as the 2-week duration of therapy, was chosen based on a desire to match the period of drug administration to the known period of sodium- and glutamate-induced secondary injury after SCI (several minutes after injury until 2 weeks after injury).

The only available formulation of Riluzole on the market is coated-film tablet (Rilutek®). However, spinal cord injury causes severe outcomes; more than 50% of injuries result in quadriplegia, a total loss of sensation and function below the injury level. Some patients enrolled in this clinical study have lost or impaired swallow function during the early

stage of injury, and needed to receive the Riluzole paste by nasogastric tubing instead of oral tablet. It was unknown whether this change in formulation or administration would affect the bioavailability of Riluzole in these patients. Based on the FDA guidance, the change in formulation or route of administration might alter the PK of studied compound. Meanwhile, nonclinical evaluations of the previously approved drug products were generally adequate for evaluating these changes. Therefore, the effect of alterations in formulation or administration was investigated in animal models.

As SCI is a catastrophic affliction that result in not only in motor and sensory impairments, but also in major metabolic and systemic alterations (Guizar-Sahagun G et al., 1998). Hence, SCI may change the kinetics of drug absorption, distribution, metabolism and elimination (Segal JL and Brunnemann SR, 1989). Clinical reports on drug kinetics in SCI are often anecdotal, because it is extremely difficult to perform systematic pharmacokinetic studies in SCI patients. This difficulty is due to the significant inter-individual variability in extent and location of injury. Therefore, the use of experimental models appears to be a suitable strategy for understanding the pharmacokinetic alterations resulting from SCI, as well as pathophysiological mechanisms involved. Cervical spinal cord injured and uninjured control rats were used to investigate the influence of SCI on Riluzole PK.

In view of the multiple neuroprotective mechanisms and promising preclinical results, to initiate the translation investigation of this therapy to the clinics for SCI patients, we have

undertaken an open-label Phase I trial to define the safety, pharmacokinetic profile and preliminary pharmacodynamics of Riluzole in this population.

This project was unique in three perspectives:

First, the study demonstrated the Riluzole concentration profiles and exposure levels of Riluzole in different compartments of plasma, brain and spinal cord. The investigation is the first study to investigate the PK of Riluzole in the spinal cord of healthy and spinal cord injured rats.

Secondly, we are the first group researchers to correlate Riluzole concentrations in central nervous tissues with those in plasma in rats. The established correlations provided the rationale for monitoring the Riluzole concentrations in human plasma samples collected in the clinical trial.

The last but the most important aspect is that this is the first characterization of Riluzole Pharmacokinetics in SCI patients. The results accomplished would be used to guide future clinical trials.

## 5.1 HPLC Assay

A specific, accurate and precise HPLC method with UV detection was developed and validated for the quantification of Riluzole in rodent and human biomatrix samples. The method requires only a small volume (100  $\mu$ l or 200  $\mu$ l) of various biomatrix samples, and the assay sensitivities at the concentration of 7.8 ng/ml for plasma and CSF samples and 31.25 ng/g for rat brain and spinal cord samples are sufficient for preclinical and clinical studies.

The HPLC-UV method developed by Van Kan HJ et al., 2004 needed a large volume of human plasma (500  $\mu$ l) and LLOQ was 20 ng/ml for the determination of Riluzole in human plasma or serum. Le Liboux et al. developed HPLC-UV ((Le Liboux et al., 1997) and LC/MS/MS methods (Le Liboux et al., 1999) for the quantifications of Riluzole in human plasma and urine. The HPLC method also required a large volume of human plasma (1 ml), and the solid-phase extraction was less convenient than a liquid-liquid extraction. The LLOQ of 0.5 ng/ml was achieved with the LC/MS/MS method. However, the inter-day precision is large, ranging from 11% to 20%. Our method has an LLOQ of 7.8 ng/ml and uses liquid-liquid extraction with coefficients of variation of < 9% for human plasma samples.

The HPLC-UV method (Colovic M et al., 2004) was developed for the quantification of Riluzole in mouse plasma and central nervous system tissues used the solid-phase extraction, which was not as convenient as liquid-liquid extraction with small quantities of

available samples. Furthermore, our method had lower LLOQ value of 7.8 ng/ml for rat plasma samples and 31.25 ng/g for brain and spinal cord samples. The HPLC-UV method (Maltese A et al., 2004) developed only for quantification of Riluzole in rat brain and did not use I.S. which might cause more variations and errors during the quantification. Moreover, our method had better recoveries compared to the method of Maltese A et al.. Overall, our method broadened the range of pharmacokinetic applications, including rat plasma, brain and spinal cord. The method we developed had an LLOQ of 7.8 ng/ml for plasma samples and 31.25 ng/g for other biological matrixes, and uses liquid-liquid extraction with coefficients of variation of < 4% for all the samples.

To our knowledge, this is the first assay method developed for the quantification of Riluzole in human CSF and the investigation of the influence of CSF protein levels on the quantification of Riluzole. The solid-phase extraction is adopted for CSF samples, which showed higher recoveries comparing to the liquid-liquid extraction with an LLOQ of 7.8 ng/ml and coefficients of variation of < 13%. Our results demonstrated that the CSF protein (22-1,345 mg/dl) has no effects on the recovery and accuracy of Riluzole quantification.

In patients with ALS Riluzole, serum concentrations are in the range of 10-500 ng/ml with a standard drug regimen of 50 mg twice daily (Le Liboux A et al., 1997; Van Kan HJ et al., 2004). The present assay has been successfully employed for the quantification of Riluzole in plasma samples of 36 acute SCI patients who have been treated with a dosing regimen of 50 mg orally or by NG twice daily.

## 5.2 Different Formulations of Riluzole in Rats

Since the pharmacokinetic behaviors of acute SCI patients might be affected by both the change of formulations (oral tablet and nasogastric paste) and spinal cord injury. It was difficult for us to investigate these two factors separately in the patients. Therefore, we attempted to clarify the formulation issue in the animal model.

As we expected, the change of formulations indeed influenced the pharmacokinetics (bioavailability) of Riluzole. The AUC/dose of Riluzole in crushed tablet and paste were lower (12-18%) but comparable, so the change in Riluzole formulation/administration used in the current clinical trial might not be of a concern about affecting its bioavailability in acute SCI patients. The AUC/dose of Riluzole in crushed paste with glycerin, oral suspension and solution groups were significantly higher (42-75%) than those in crushed tablet and paste groups (12-18%). One possible explanation is that Riluzole could be greatly absorbed into GI tract to achieve the higher bioavailability by promoting the wetting and dissolution of the lipophilic Riluzole by glycerin or the commercial suspension vehicle which consists of solubilizing agents and propylene glycol. Riluzole had higher drug exposures and lower variabilities in oral suspension and solution groups. The suspension vehicle is commercially available, and the oral suspension may have potential uses for the clinical patients in order to increase the compliance and achieve a consistent drug administration to achieve the exposures with less variability.

The clinical records of Riluzole administrations in acute SCI patients further confirmed that the Riluzole exposures ( $AUC_{0-12}$  and  $AUC_{0-\infty}$ ) for the patients receiving oral tablet and nasogastric paste were comparable with no statistical differences (Tables 20 & 21). Therefore, the bioavailability of Riluzole given by oral tablet and NG paste would not be an issue for the current and later clinical trials.

The alteration of formulation/administration would change the bioavailability of Riluzole, nevertheless, intrinsic pharmacokinetic characteristics of Riluzole were unaffected, since the clearance ( $CL/F$ ) and volume of distribution ( $V/F$ ) were of no significant differences among the six groups (oral groups: crushed tablet, crushed paste, crushed paste with glycerin, suspension and solution; i.v.: solution).

**Table 21 Comparisons of Riluzole Exposures (AUC<sub>0-12</sub>) for the Patients Taking Oral Tablet, Nasogastric Paste and Mixture of Tablet and Paste**

P.O. Group				N.G. Group				P.O. and N.G. Groups				
ID	Total Doses	AUC <sub>0-12</sub>		ID	Total Doses	AUC <sub>0-12</sub>		ID	NG Dose	Total Doses	AUC <sub>0-12</sub>	
		Day 3	Day 14			Day 3	Day 14				Day 3	Day 14
R07-0002	27	614.18	465.96	R07-0005	27	903.04	301.08	R07-0001	1st	27	632.79	191.91
R07-0003	28	759.01	291.78	R07-0009	28	387.05	236.23	R07-0006	2nd-28st	28	1174.63	254.45
R07-0004	28	1222.24	250.32	R07-0010	28	826.90		R07-0008	2nd-28st	28	920.29	1414.96
R07-0007	28	538.74		R10-0006	28	1502.16	490.47	R07-0011	2nd-7st,15st-28st	28	190.30	
R10-0001	27	817.83	305.87	R10-0011	27	947.26		R10-0004	1st-10st	28	1284.94	480.53
R10-0002	28		468.78	R05-0002	27	1204.02	1291.44	R10-0005	1st-20st	28	1142.65	421.63
R10-0003	28	751.00	405.23	R06-0001	28	372.24	185.33	R10-0008	7st-16st	28		152.04
R10-0007	27	357.55	63.91	R06-0003	28	203.87		R10-0010	19st, 21st-26st	28	1207.03	2015.10
R10-0009	28	3452.97	843.39					R05-0004	1st-8st	28	1160.00	239.83
R10-0012	28		1014.44					R05-0005	2nd-13st	27	1635.79	365.12
R10-0013	27							R02-0002	3st-12st	14	498.82	
R05-0001	27	1046.93										
R05-0003	26	2121.10	707.84									
R06-0002	28	976.04	208.37									
R02-0001	28	1408.28	794.80									
R02-0003	28	346.88										
R04-0001	28	818.32	206.38									
N		14	13			8	5				10	9
Mean		1087.93	463.62			793.32	500.91				984.72	615.06
SD		821.43	290.32			446.86	456.79				428.22	650.21

One-way ANOVA, Tukey's test, significance level, P<0.05; Non-parametric test, significance level, P<0.05

**Table 22 Comparisons of Riluzole Exposures (AUC<sub>0-∞</sub>) for the Patients Taking Oral Tablet, Nasogastric Paste and Mixture of Tablet and Paste**

P.O. Group				N.G. Group				P.O. and N.G. Groups				
ID	Total Doses	AUC <sub>0-∞</sub>		ID	Total Doses	AUC <sub>0-∞</sub>		ID	NG Dose	Total Doses	AUC <sub>0-∞</sub>	
		Day 3	Day 14			Day 3	Day 14				Day 3	Day 14
R07-0002	27	1167.37	556.94	R07-0005	27	1399.83	493.12	R07-0001	1st	27	1081.82	231.42
R07-0003	28	844.16	456.11	R07-0009	28	495.09	1588.47	R07-0006	2nd-28st	28	1247.43	400.07
R07-0004	28	1453.26	420.13	R07-0010	28	1261.74		R07-0008	2nd-28st	28	1415.84	1462.40
R07-0007	28	3483.02		R10-0006	28	1902.40	562.47	R07-0011	2nd-7st,15st-28st	28	302.04	
R10-0001	27	1311.17	405.61	R10-0011	27	2015.20		R10-0004	1st-10st	28	1813.13	790.48
R10-0002	28		832.49	R05-0002	27	6921.63	2035.72	R10-0005	1st-20st	28	2037.30	581.77
R10-0003	28	3084.62	847.02	R06-0001	28	477.31	312.26	R10-0008	7st-16st	28		188.88
R10-0007	27	504.59	93.71	R06-0003	28	260.10		R10-0010	19st, 21st-26st	28	2455.05	2420.44
R10-0009	28	6208.14	1097.84					R05-0004	1st-8st	28	2171.94	1472.26
R10-0012	28		1310.75					R05-0005	2nd-13st	27	2467.89	461.94
R10-0013	27							R02-0002	3st-12st	14	919.48	
R05-0001	27	1205.13										
R05-0003	26	13100.01	841.77									
R06-0002	28	1163.18	543.37									
R02-0001	28	1716.22	1020.50									
R02-0003	28	454.32										
R04-0001	28	923.42	383.47									
N		14	13			8	5				10	9
Mean		2615.62	677.67			1841.66	998.41				1591.19	889.96
SD		3385.36	344.49			2156.30	764.91				716.62	746.86

One-way ANOVA Tukey's test, significance level, P<0.05; Non-parametric test, significance level, P<0.05

## 5.3 Impacts of SCI on Riluzole Pharmacokinetics in Rats

### 5.3.1 Single I.P. Dose of Riluzole

Brain and plasma pharmacokinetics of Riluzole have been reported (Milane A et al., 2009). Plasma and brain kinetic profiles were similar for the three doses of Riluzole tested (5, 10 and 20 mg/kg). Intracerebral entry of Riluzole was rapid ( $t_{max}$  of 5-30 minutes in brain and plasma) and was directly dependant on plasma concentration (Figures 43 & 44). The relations between plasma and brain AUCs (Figures 43 & 44) is shown that the  $AUC_{0-t, brain/plasma} = 2.77, 2.45$  and  $2.14$  at the dose levels of 5, 10 and 20 mg/kg, respectively.

In our study, after a single I.P. administration, Riluzole exhibited higher concentrations in cervical and thoracic spinal cords, followed by in brain and plasma, the ratio of  $AUC_{0-\infty, spinal\ cord} / AUC_{0-\infty, brain} / AUC_{0-\infty, plasma} = 8:4:1$ , Riluzole concentrations in plasma and brain and AUC ratio of brain/plasma had the similar trends with those of Milane A et al., 2.14-2.77. However, Riluzole concentrations in plasma and brain reached  $C_{max}$  more slowly (0.57 and 0.71 hrs in brain and plasma for the control group; 0.90 hrs in plasma for SCI group) compared to those reported by Milane A et al. ( $t_{max}$  of 5-30 minutes in brain and plasma).

This is the first study to investigate the pharmacokinetics of Riluzole in the spinal cord. Riluzole in spinal cords had the highest concentrations and exposures, which further

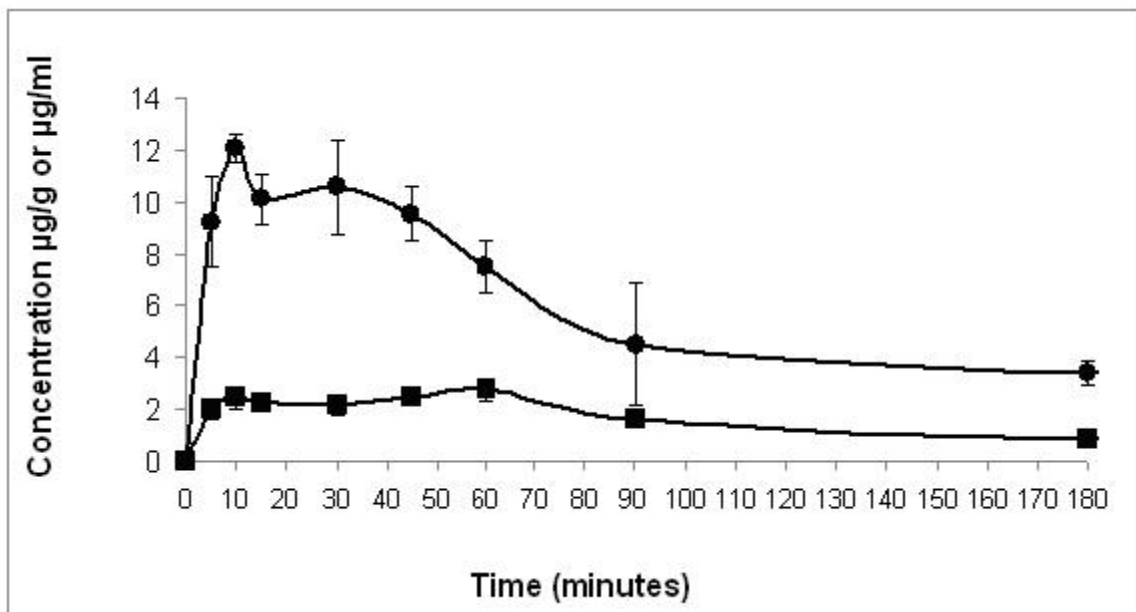


**Figure 37 Plasma and Brain Pharmacokinetic Profiles of Riluzole Given by I.P.**

**Route to CF1 mdr1a (+/+) Mice (10 mg/kg; n=3 mice per time point, Mean ± SD)**

**Brain Concentration (round shape) in µg/g and Plasma Concentration (square shape) in µg/ml (Milane A et al., 2009)**

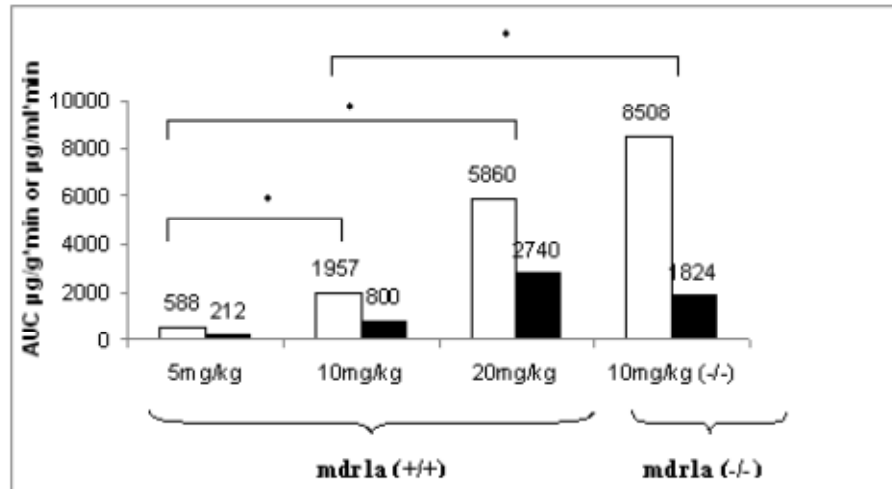


**Figure 38 Brain and Plasma AUC<sub>0-∞</sub> Achieved After Administration of Riluzole (5, 10, 20 mg/kg) by I.P. Route to CF1 mdr1a (+/+) Mice and at 10 mg/kg by I.P. Route to CF1 mdr1a (-/-) Mice (n=27 mice/dose) Brain AUC<sub>0-∞</sub> (white shape) and Plasma AUC<sub>0-∞</sub> (black shape) (Milane A et al., 2009)**

confirmed that Rilzuole have great potential with a favorable drug distribution to the site of action (spinal cords) for its therapeutic effect in patients with spinal cord injury.

As reported in the literatures, the blood-brain barrier (BBB) and blood-spinal cord barrier (BSCB) tightly regulate the blood-central nervous system (CNS) molecular exchange required for normal neuronal function (Zlokovic BV, 2008, 2011). In contrast to the highly permeable capillaries in the systemic circulation (Mann GE et al., 1985), blood-CNS vascular barriers are formed by continuous endothelial cells with tight junction protein complexes and low rates of vesicular transport (Winkler EA et al., 2011). This largely prohibits transport of large molecules and polar solutes without specific transport systems (Zlokovic BV and Apuzzo ML, 1997; Zlokovic BV, 2011). The BBB and BSCB are functionally similar; however, many differences have been identified (Table 23) (Bartanusz V et al., 2011). For example, the rodent BSCB has heightened permeability to mannitol and inulin (Daniel PM et al, 1985; Prockop LD et al., 1995), interferons (Pan W et al., 1997a), albumin, sucrose, and tumor necrosis factor  $\alpha$  (Pan W et al., 1997b). The source of these permeability changes is largely unknown, although reduced tight junction protein expression in the spinal cord has been reported (Ge S and Pachter JS, 2006).

Riluzole is a substrate of P-glycoprotein and lipophilic compound, with log P value of 3.5 and molecular weight of 234 (Milane A et al., 2007), which could penetrate into brain and spinal cord across the BBB and BSCB. White matter is one of the two components of the central nervous system and consists mostly of glial cells and myelinated axons. Myelin is

**Table 23 Morphological and Physiological Differences between the BBB and BSCB (Bartanusz V et al., 2011)**

Feature	Difference from BBB
Glycogen deposits	Present only on BSCB microvessels
Permeability	Increased to tracer: Increased to tracers: [3H]-D-mannitol, [14C]-carboxyl-inulin; increased to cytokines: interferon- $\alpha$ , interferon- $\gamma$ , tumor necrosis factor- $\alpha$
Transporter molecules	Decreased: P-glycoprotein
Tight junction protein expression	Decreased: ZO-1, occludin
	Decreased: VE-cadherin, $\beta$ -catenin

BBB=blood-brain barrier; BSCB=blood-spinal cord barrier; VE=vascular endothelial

composed largely of lipid tissue veined with capillaries. White matter forms the bulk of the deep parts of the brain and the superficial parts of the spinal cord. Meanwhile, BSCB is more permeable and has less P-gp expression than the BBB as reported. All in all, Riluzole may have high affinity and more chance to permeate into spinal cord than brain, which is consistent with our observations. Riluzole exhibited higher concentrations in cervical and thoracic spinal cords, followed by those in brain and plasma.

### 5.3.2 Multiple I.P. Doses of Riluzole

Acute spinal cord injury did not apparently influence the pharmacokinetics of Riluzole after a single I.P. dose. However, after multiple I.P. doses (2 and 6 doses), Riluzole exhibited significantly higher concentrations in plasma, brain and spinal cords in the cervical SCI rats compared to those in the uninjured control group. Two possible reasons accounted for this change were speculated as follows:

As reported in the literatures, in the uninjured CNS, the BBB functions as a highly selective filter limiting the transport of compounds both into and out of the CNS parenchyma. Following SCI there is a marked increase in BBB permeability due to both direct mechanical disruption by the primary injury and the effects on endothelial cells by numerous inflammatory mediators and other compounds (Rowland JW et al., 2008). For blood-spinal cord barrier (BSCS), leakage of the barrier to luciferase after spinal cord injury exhibits a biphasic temporal pattern. The most robust leakage occurs within the first several hours after injury and likely reflects direct damage to blood vessels. By 24 hr post-injury, there is a significant reduction in leakage relative to the earlier time points. At 3 days after injury, however, there is a significant increase in leakage relative to that measured at 24 hr. This more delayed time period has been shown by others to coincide with the loss of expression of endothelial barrier antigen, an indicator of barrier dysfunction (Perdiki et al., 1998). Therefore, Riluzole could be much easier to permeate into brain and spinal cord through BBB and BSCB after SCI.

Furthermore, Riluzole is mainly metabolized by CYP1A2 in the liver. Hepatic clearance ( $CL_H$ ) related to drug metabolism has been reported to decrease in SCI patients for phenacetin (Vertiz-Hernandez A et al., 2007), methylprednisolone (Segal JL et al., 1998) and cyclosporine A (Garcia-Lopez P et al., 2007; Ibarra A et al., 1996). The underlying causes can be a reduced MVBF in liver (Cruz-Antonio L et al., 2006), enzyme synthesis or protein binding (Shargel L W-PS and Yu A, 2005) singly and in combination. The reduction of hepatic clearance may slow the elimination of Riluzole out of body. In SCI, reductions in the MVBF in the liver, spleen and skeletal muscle occur in the acute phase of SCI and peaks at ~24 h after the injury. The reduction is more pronounced after a high thoracic complete lesion above T6 than a low one. These alterations are likely due to a redirection of blood flow to maintain an adequate perfusion of the brain and heart (Cruz-Antonio L et al., 2006).

Overall, the significantly higher concentrations of Riluzole in plasma, brain and spinal cords after SCI may be due to the increased permeability of BBB and BSCB and slower elimination caused by impaired hepatic clearance.

Three-compartmental model was established using ADAPT II software to elaborate the transferring kinetics of Riluzole among plasma, brain and spinal cord compartments. The simulation results also suggested that slower elimination of Riluzole due to impaired hepatic clearance might be the reason to cause higher concentrations post-injury after multiple I.P. doses. The observed concentrations of Riluzole were all almost double the values of the predicted ones using the parameters from the model established using the

drug profiles in various compartments after a single dose in SCI rats. The potential changes in transfer rate constants among these three compartments might not be the case. After we decreased the elimination rate constant of Riluzole from plasma to half of the predicted value based on single dose, with all other parameters being kept the same derived from the single dose, the predicted Riluzole concentrations were much closer to those observed values with 2 and 6 I.P. doses. The simulation results also suggested that the spinal cord injury is a progressive disease, which affected the PK of Riluzole with different dynamics during the course of 3-day treatment.

### **5.3.3 Correlations of Riluzole Concentrations in Central Nervous Tissues with Those in Plasma**

We are the first one to correlate Riluzole concentrations in central nervous tissues with those in plasma. Riluzole concentration in brain and spinal cord had good correlations with those in plasma, providing the rationale that human plasma samples collected in the clinical trial were sufficient since the plasma is an indicator of exposures in brain and spinal cord. If the pharmacological effect or toxicity of Riluzole is correlated to brain and spinal cord concentrations in patients, plasma concentrations could be used to predict the brain and spinal cord concentrations and further the efficacy or toxicity.

## 5.4 Phase I Clinical Trial of Riluzole in Acute SCI

### Patients

#### 5.4.1 Distinct Alteration of Riluzole Pharmacokinetics in Acute SCI Patients

Riluzole pharmacokinetics in SCI was distinguished from those in ALS, as well as SMA in children. The  $C_{max}$  and  $AUC_{0-\infty}$  in SCI patients on the same dose basis did not achieve the comparable levels as in ALS patients, but were lower (128.8 ng/L and 827.8 ng\*hr/ml on Day 3, and 76.5 ng/ml and 337.8 ng\*hr/ml on Day 14) compared with those in patients with ALS (231 ng/ml and 3409 ng\*hr/ml) and SMA (371 ng/ml and 2257 ng\*hr/ml). The decreased bioavailability (F) in SCI may be due to the reduced GI absorption (Fealey RD et al., 1984; Guizar-Sahagun G et al., 2004; Segal JL et al., 1986; Stone JM et al., 1990). The apparent clearance (CL/F) and volume of distribution (V/F) in the SCI population, 60.4-148 L/hour and 663-2080 L, were substantially higher than those in the ALS population (25.9 L/hour and 361 L) and SMA patients (22.2 L/hour and 299 L) (Table 24).

The difference of CL between Day 3 and Day 14 post-SCI may result from the following potential causes:

- 1) Impaired hepatic metabolic clearance shortly after the early acute phase ( $\leq 48$  hours) on Day 3, due to the decreased hepatic microvascular blood flow and hepatocyte gene expression (Vertiz-Hernandez A et al., 2007). Riluzole is an intermediate hepatic

**Table 24 Comparison of Population Pharmacokinetic Parameters in Acute Spinal Cord Injured Patients versus Patients with Amyotrophic Lateral Sclerosis (ALS) and Spinal Muscular Atrophy (SMA)**

Parameters	PopPK in SCI Patients		ALS†	SMA‡
	Day 3	Day 14		
Dose	50 Bid	50 Bid	50 Bid	50 QD
No.	33	32	169/179	13
Sex	28 M+5 F	26 M+6 F		4 M+9 F or 5 M+8 F
Age	41.15 ± 3.17	39.63 ± 3.22	55.0 ± 0.9	9-17
C <sub>max</sub> (ng/ml)	128.86 ± 14.03** (10.9%)	76.46 ± 15.04** (19.7%)	231 ± 5	371 ± 62 (N)
AUC <sub>0-∞</sub> (ng*hr/ml)	827.81	337.84	3409 ± 220 (70 kg) 48.70 ± 3.15 (AUC/kg)	2257 ± 444 (N) (0-24 hr)
CL/F (L/hr)	60.4 ± 6.24 (10.3%)	148 ± 25.5 (17.2%)	25.9 ± 1.13 51.4 (7.2%)	22.15 (N)
V/F (L)	663 ± 103 (16.3%)	2080 ± 947 (45.5%)	361 (10.1%)	299 ± 54 (C)
t <sub>1/2</sub> (hr)	7.29	9.76	4.93	9.8 ± 1.3 (N)
T <sub>max</sub> (hr)				1 (1-5) (N)

\*Mean Values are ± SE;

CL/F, apparent oral clearance; V/F, apparent volume of distribution; AUC<sub>0-∞</sub>, the area under the curve, calculated by Dose/(CL/F); C<sub>max</sub>, peak concentration; t<sub>1/2</sub>, half life;

\*\*From individual estimation.

N: The parameters calculated by non-compartmental model; C: The parameters calculated by compartmental model.

†: Bruno R et al., 1997; Groeneveld GJ et al., 2003

‡: Abbara C et al., 2011

extraction drug whose hepatic metabolism would be decreased by a lower hepatic blood flow, similar to methylprednisolone and cyclosporine A.

2) Concomitant medications that are CYP 1A2 substrates, inducers, or inhibitors would affect the metabolism of Riluzole by CYP 1A2. However, it was unlikely that any significant drug-drug interaction was accountable for the observed CL difference. After screening the medication charts of the patients, 21 medications were identified, namely, acetaminophen, fentanyl, oxycodone, Percocet, gabapentin, methylprednisolone, morphine, aspirin, tramadol, pregabalin, lorazepam, diphenhydramine, propofol, methadone, hydromorphone, ibuprofen, lidocaine, MS Contin, meperidine, Norco, and Vicodin. Nevertheless, among the first 6 medications that were used by more than 5 patients, only acetaminophen is a known substrate of CYP 1A2. Acetaminophen was used by 6 patients on both Day 3 and Day 14.

The difference of V between Day 3 and Day 14 may have the following potential causes:

1) Fluid imbalance during the first 14 days. However, no apparent net gain in body fluid on Day 14 was recognized, based on patients' fluid intake and output records.

2) Decreased protein binding of riluzole that would result in volume of distribution (V/F) increase on Day 14. Riluzole is 96% bound to plasma proteins, mainly to albumin and lipoproteins over the clinical concentration range. Retrospectively, the plasma samples obtained in 10 patients were reassayed for free fractions of Riluzole. The fractions unbound were comparable between Day 3 and Day 14 (mean  $\pm$  SE) 6.18%  $\pm$  0.42% and

9.57% ± 1.09%, respectively) and could not account for the significantly larger V on Day 14.

The individual and population pharmacokinetic models were developed and validated with the observed concentrations. For future clinical trials, the population pharmacokinetic model can be used. The current protocol of sampling blood on Days 3 and 14 is adequate to refine the SCI population-specific pharmacokinetics. The present study suggests that dosing regimen modification may be possible based on the pharmacokinetic modeling and monitoring of plasma levels of Riluzole.

## 5.4.2 Pharmacodynamics of Riluzole

ASIA impairment scale (AIS) A is the most severe condition that, no motor or sensory function preserved in the sacral segments S4-S5. The patients with AIS A had less chance to get recovery compared to the patients with AIS B and C.

The likelihood and degree of neurologic recovery depends in part upon the anatomic region of the spinal cord injury. For example, (T1-T5) are more often complete injury with less potential for meaningful neurologic recovery, believed to be due to the tenuous blood supply in this region as well as the injury mechanism due to the stability of the chest wall and spinal column in the region (Harrop JS et al., 1976). Therefore, the patients with thoracic injury may have less opportunity to recover because of the severity of injury, which is consistent with our observations; the patients with cervical injury had better treatment outcomes after Riluzole treatment in the current clinical trial compared to the ones with thoracic injury.

The motor and sensory functions had been significantly improved at 3 and/or 6-month follow-up examinations after the 14-day Riluzole treatment. The neurological and functional outcomes of enrolled participants still need to be compared with those of matched patients from the NACTN registry, in order to verify the effectiveness of Riluzole treatment.

Toxicity is the primary concern in the phase I clinical trial. Throughout the course of this study, adverse events were carefully monitored for each patient. Particular care was made to track adverse events previously associated with Riluzole administration in the ALS literature, particularly the hepatotoxicity. Liver enzyme tests were repeated on admission and Day 3, 7, 10 and 14 after the start of Riluzole.

Elevations of enzyme levels fell into mild and moderate range in 2/3 enrolled patients. A severe elevation of ALT (6 times the ULN) occurred in 1 patient, of AST (5.5 times the ULN) in another, and of GGT (7 times the ULN) in a third patient; all returned to normal at the 3- and 6-month follow-up examinations. There were no deaths among the 36 patients enrolled in the study.

#### **5.4.3 PK/PD Correlations of Riluzole**

Previous SCI clinical trial experience (Bracken MB et al., 1990 and 1997; Geisler FH et al., 2001) suggests that requiring the improvement of one or two ASIA grades over and above spontaneous recovery (e.g. AIS B to AIS C or AIS D), as a primary outcome end point (to document the benefit of a therapeutic intervention), may be too demanding a threshold (a relatively insensitive measure for a therapeutic effect). A candidate therapeutic with a very large effect size could be addressed with such a challenging clinical point. However, an intervention with a potentially smaller effect size might require a more sensitive outcome measure, such as a statistically significant changes in ASIA motor and sensory scores.

Both linear and logistic regressions were used to attempt the establishments of correlations between the changes of motor and sensory scores at different time intervals of follow-up examinations with Riluzole concentrations and/or AUC. We found that the changes of motor and sensory scores at 3-month follow-up examination could be correlated with  $AUC_{0-12}/kg$  on Day 3 within the range of 3.40-25.03 ng\*hr/ml/kg by linear regression.

In the ALS related literature, relationships between Riluzole serum levels and AUC/kg and aspartate aminotransferase (AST) and alanine aminotransferase (ALT) levels were determined with linear regression analysis (Groeneveld GJ et al., 2003). Therefore, we also used linear regression analysis to establish the correlations of the enzyme levels with Riluzole plasma concentrations and exposure (AUC). However, no relationship was established between the elevation of enzymes and  $AUC_{0-12}/kg$ . In other words, the systemic exposure of Riluzole in the range of 3.40-25.03 ng\*hr/ml/kg exhibited mild to moderate elevations of hepatic enzymes.

## **SUMMARY**

### **6.1 HPLC Assay**

A highly sensitive, reproducible and efficient HPLC assay method for the quantifications of Riluzole in rodent and human biomatrix samples was developed and validated.

The method had lower limit of quantification (LLOQ) of 7.8 ng/ml for plasma and CSF samples, and 31.25 ng/g for other biological matrixes (rat brain and spinal cord), using liquid-liquid extraction with coefficients of variation of < 4% for all samples. The assay was employed to quantify Riluzole concentrations in both preclinical and clinical studies.

### **6.2 Pharmacokinetics of Different Formulations**

The bioavailabilities of Riluzole in crushed tablet and paste alone groups were lower but comparable in rat model. Therefore, the bioavailabilities of Riluzole for patients taking oral tablet and nasogastric paste was not of a concern about the bioavailability variation. The clinical records of Riluzole administrations in acute SCI patients further confirmed that the Riluzole exposures ( $AUC_{0-12}$  and  $AUC_{0-\infty}$ ) for patients receiving oral tablet and nasogastric paste were comparable, with no statistical differences.

Oral suspension and solution had higher bioavailabilities and lower variabilities in the rat model. Since the suspension vehicle is commercially available, the oral suspension may

have potential use for the clinical patients in order to increase the compliance and achieve consistent dose administration and exposures.

### **6.3 Impacts of SCI on Riluzole Pharmacokinetics**

After a single I.P. dose, Riluzole exhibited higher concentrations in cervical and thoracic spinal cords in healthy rats, followed by in brain and plasma, the ratio of  $AUC_{0-\infty}$ , spinal cord/  $AUC_{0-\infty}$ , brain/  $AUC_{0-\infty}$ , plasma =8:4:1, providing the evidence that Riluzole may have therapeutic potential, due to favorable biodistribution to spinal cord, which is the site of action for SCI.

Acute spinal cord injury resulted in higher plasma, brain and spinal cord concentrations after multiple I.P. doses (2 and 6 doses), which was due to slower elimination caused by an impaired hepatic clearance resulting from the spinal cord injury.

Riluzole Concentrations in brain and spinal cord had good correlations with those in plasma, providing the rationale that human plasma samples collected in the clinical trial were sufficient since the plasma is an indicator of Riluzole exposures in brain and spinal cord.

Three compartment-model had good fitting using ADAPT II in all the compartments for both control and injured rats, except in brain compartment of the SCI rats due to insufficient data from brain samples. The simulation for multiple doses further validated

the model and suggested that spinal cord injury is a progressive disease, which affected the PK of Riluzole with different dynamics during the course of 3-day treatment.

## **6.4 Phase I Clinical Trial of Riluzole in Acute SCI**

### **Patients**

This is the first report of clinical pharmacokinetics of Riluzole in patients with SCI. The  $C_{max}$  and  $AUC_{0-12}$  achieved in SCI patients were lower than those in healthy subjects on the same dose basis, due to a higher clearance and larger volume of distribution in SCI patients. The finding in SCI patients of an increase in the clearance and distribution of Riluzole between the 3rd and 14th days after SCI, with a lower plasma concentration of Riluzole on the 14th day, stresses the importance of monitoring changes in drug metabolism after SCI in interpreting the safety and efficacy of therapeutic drugs that are used in clinical trials in SCI.

### **6.4.1 Distinct Alteration of Riluzole Pharmacokinetics in SCI**

#### **Patients**

The  $C_{max}$  (mean  $\pm$  SE) of Riluzole achieved with the 50 mg twice daily dose varied significantly among patients:  $128.8 \pm 13.8$  ng/ml (range 23.9 - 409.2 ng/ml) (n = 33) on Day 3 and  $76.2 \pm 13.7$  ng/ml (8.5 - 317.0 ng/ml) (n = 32) on Day 14. The  $C_{min}$  was of large inter-subject variability as well:  $45.6 \pm 6.8$  ng/ml (8.4-183.8 ng/ml) on Day 3 and  $19.1 \pm 2.5$  ng/ml (2.8-61.2 ng/ml) on Day 14. The declines of  $C_{max}$  and  $C_{min}$  on Day 14

from those of Day 3 were significant by nonparametric test ( $p < 0.05$ ), and they were consistently observed in individual patients from all clinical sites.

The systemic exposures of Riluzole from the treatment,  $AUC_{0-12}$  were  $982.03 \pm 111.18$  ng\*hr/ml and  $521.01 \pm 87.32$  ng\*hr/ml for Day 3 and Day 14, respectively, and exhibited the same trend of decline in  $C_{max}$  and  $C_{min}$  for Day 14 from Day 3 on the same dose basis.

#### **6.4.2 Individual and Population Pharmacokinetic Parameters**

The individual pharmacokinetic parameters were estimated using two concentration-time data on each day (Day 3 and Day 14) to obtain the elimination rate constant and other parameters using the standard PK equations.

The population pharmacokinetics model was best represented by a 1-compartment first-order absorption and elimination model that included inter-individual and intra-individual variability. The covariates that were introduced into the clearance and volume of distribution (sex, body weight, smoking status, age, and creatinine clearance ) did not significantly improve the fit of the basic model (objective function values  $> 7.8$ ,  $p < 0.005$ ).

The population mean parameter estimates were in good agreement with the parameters derived using individual estimation for CL/F (60.4 vs. 50.0 L/hr), V/F (663 vs. 557 L), and the derived half-life (7.29 vs. 11.91 hrs) on Day 3, as well as CL/F (148 vs. 106 L/hr), V/F

(2080 vs. 1300 L), and the derived half-life (9.76 vs. 10.61 hrs) on Day 14. The results suggested that the current sampling schedule (2 blood samples for peak and trough concentrations, respectively) was adequate to characterize the pharmacokinetics of Riluzole for future clinical trial in patients with SCI.

### **6.4.3 Safety**

There were no serious adverse events attributable to Riluzole. Medical complications common to patients with SCI occurred with incidences similar to those in a matched control group treated at NACTN hospitals. There was no mortality. Liver enzyme (ALT, AST) elevations were mild (<2.5x ULN) or moderate (2.5-5x ULN) in 2/3 of patients. A severe elevation of ALT (6x ULN) in one patient and of AST (5.5x ULN) in another and of GGT (7 times the ULN) in a third patient, all returned to normal at 3- and 6-month follow-up examinations. There was mild elevation of bilirubin in 4 patients and moderate in 1. No patient had an elevated bilirubin on day 14.

### **6.4.4 Efficacy Outcomes**

The first dosing time of Riluzole at any time within 12 hrs since injury had no effects on the efficacy outcomes (motor and sensory scores). So Riluzole did not need to be administered as early as possible during care of acute phase.

The changes of motor scores by the end of follow-up (3-month or 6-month) for the patients with AIS A were statistically lower than those of patients with AIS B and C. The

patients with cervical injury had better treatment outcomes compared to the ones with thoracic injury. The motor and sensory functions had been significantly improved at 3- and/or 6-month follow-ups after the 2-week Riluzole treatment.

#### **6.4.5 PK/PD Correlation**

The change of motor and sensory scores at 3-month follow-up had good correlations with Day 3 AUC/kg. The establishments of PK-PD correlation can help predict the PD outcomes in future clinical trials.

## Bibliography

1. Abbara C, Estournet B, Lacomblez L, Lelievre B, Ouslimani A, Lehmann B, et al: Riluzole pharmacokinetics in young patients with spinal muscular atrophy. **Br J Clin Pharmacol** **71**:403-410, 2011
2. Agrawal SK, Fehlings MG: Mechanisms of secondary injury to spinal cord axons in vitro: role of Na<sup>+</sup>, Na<sup>(+)</sup>-K<sup>(+)</sup>-ATPase, the Na<sup>(+)</sup>-H<sup>+</sup> exchanger, and the Na<sup>(+)</sup>-Ca<sup>2+</sup> exchanger. **J Neurosci** **16**:545-552, 1996
3. Aisen ML, Dietz MA, Rossi P, Cedarbaum JM, Kutt H: Clinical and pharmacokinetic aspects of high dose oral baclofen therapy. **J Am Paraplegia Soc** **15**:211-216, 1992
4. Ates O, Cayli SR, Gurses I, Turkoz Y, Tarim O, Cakir CO, et al: Comparative neuroprotective effect of sodium channel blockers after experimental spinal cord injury. **J Clin Neurosci** **14**:658-665, 2007
5. Bartanusz V, Jezova D, Alajajian B, Digicaylioglu M: The blood-spinal cord barrier: morphology and clinical implications. **Ann Neurol** **70**:194-206, 2011
6. Beattie MS, Hermann GE, Rogers RC, Bresnahan JC: Cell death in models of spinal cord injury. **Prog Brain Res** **137**:37-47, 2002
7. Bensimon G, Doble A: The tolerability of riluzole in the treatment of patients with amyotrophic lateral sclerosis. **Expert Opin Drug Saf** **3**:525-534, 2004
8. Bensimon G, Lacomblez L, Meininger V: A controlled trial of riluzole in amyotrophic lateral sclerosis. ALS/Riluzole Study Group. **N Engl J Med** **330**:585-591, 1994
9. Bracken MB, Collins WF, Freeman DF, Shepard MJ, Wagner FW, Silten RM, et al: Efficacy of methylprednisolone in acute spinal cord injury. **JAMA** **251**:45-52, 1984
10. Bracken MB, Shepard MJ, Collins WF, Holford TR, Young W, Baskin DS, et al: A randomized, controlled trial of methylprednisolone or naloxone in the treatment of acute spinal-cord injury. Results of the Second National Acute Spinal Cord Injury Study. **N Engl J Med** **322**:1405-1411, 1990
11. Bracken MB, Shepard MJ, Holford TR, Leo-Summers L, Aldrich EF, Fazl M, et al: Administration of methylprednisolone for 24 or 48 hours or tirilazad mesylate for 48 hours in the treatment of acute spinal cord injury. Results of the Third National

- Acute Spinal Cord Injury Randomized Controlled Trial. National Acute Spinal Cord Injury Study. **JAMA** **277**:1597-1604, 1997
12. Brunnemann SR, Segal JL: Amikacin serum protein binding in spinal cord injury. **Life Sci** **49**:PL1-5, 1991
  13. Bruno R, Vivier N, Montay G, Le Liboux A, Powe LK, Delumeau JC, et al: Population pharmacokinetics of riluzole in patients with amyotrophic lateral sclerosis. **Clin Pharmacol Ther** **62**:518-526, 1997
  14. Coleman MP, Perry VH: Axon pathology in neurological disease: a neglected therapeutic target. **Trends Neurosci** **25**:532-537, 2002
  15. Colovic M, Zennaro E, Caccia S: Liquid chromatographic assay for riluzole in mouse plasma and central nervous system tissues. **J Chromatogr B Analyt Technol Biomed Life Sci** **803**:305-309, 2004
  16. Crozier KS, Graziani V, Ditunno JF, Jr., Herbison GJ: Spinal cord injury: prognosis for ambulation based on sensory examination in patients who are initially motor complete. **Arch Phys Med Rehabil** **72**:119-121, 1991
  17. Cruz-Antonio L, Flores-Murrieta FJ, Garcia-Lopez P, Guizar-Sahagun G, Castaneda-Hernandez G: Understanding drug disposition alterations induced by acute spinal cord injury: role of injury level and route of administration for agents submitted to extensive liver metabolism. **J Neurotrauma** **23**:75-85, 2006
  18. Daniel PM, Lam DK, Pratt OE: Comparison of the vascular permeability of the brain and the spinal cord to mannitol and inulin in rats. **J Neurochem** **45**:647-649, 1985
  19. Ditunno JF, Little JW, Tessler A, Burns AS: Spinal shock revisited: a four-phase model. **Spinal Cord** **42**:383-395, 2004
  20. Donnelly DJ, Popovich PG: Inflammation and its role in neuroprotection, axonal regeneration and functional recovery after spinal cord injury. **Exp Neurol** **209**:378-388, 2008
  21. Ehlers MD: Deconstructing the axon: Wallerian degeneration and the ubiquitin-proteasome system. **Trends Neurosci** **27**:3-6, 2004
  22. Emery E, Aldana P, Bunge MB, Puckett W, Srinivasan A, Keane RW, et al: Apoptosis after traumatic human spinal cord injury. **J Neurosurg** **89**:911-920, 1998
  23. Fawcett JW, Curt A, Steeves JD, Coleman WP, Tuszynski MH, Lammertse D, et al: Guidelines for the conduct of clinical trials for spinal cord injury as developed

by the ICCP panel: spontaneous recovery after spinal cord injury and statistical power needed for therapeutic clinical trials. **Spinal Cord** **45**:190-205, 2007

24. Fealey RD, Szurszewski JH, Merritt JL, DiMagno EP: Effect of traumatic spinal cord transection on human upper gastrointestinal motility and gastric emptying. **Gastroenterology** **87**:69-75, 1984
25. Fehlings MG, Theodore N, Harrop J, Maurais G, Kuntz C, Shaffrey CI, et al: A phase I/IIa clinical trial of a recombinant Rho protein antagonist in acute spinal cord injury. **J Neurotrauma** **28**:787-796
26. Filippi M, Rocca MA: Magnetization transfer magnetic resonance imaging of the brain, spinal cord, and optic nerve. **Neurotherapeutics** **4**:401-413, 2007
27. Fuentes-Lara G, Guizar-Sahagun G, Garcia-Lopez P: Effect of experimental spinal cord injury on salicylate bioavailability after oral aspirin administration. **J Pharmacol Toxicol Methods** **42**:93-97, 1999
28. Garcia-Lopez P, Martinez-Cruz A, Guizar-Sahagun G, Castaneda-Hernandez G: Acute spinal cord injury changes the disposition of some, but not all drugs given intravenously. **Spinal Cord** **45**:603-608, 2007
29. Garcia-Lopez P, Perez-Urizar J, Ibarra A, Grijalva I, Madrazo I, Flores-Murrieta F, et al: Comparison between Sprague-Dawley and Wistar rats as an experimental model of pharmacokinetic alterations induced by spinal cord injury. **Arch Med Res** **27**:453-457, 1996
30. Garcia-Lopez P, Perez-Urizar J, Madrazo I, Guizar-Sahagun G, Castaneda-Hernandez G: Oral paracetamol bioavailability in rats subjected to experimental spinal cord injury. **Biopharm Drug Dispos** **18**:203-211, 1997
31. Garcia-Lopez P, Salas R: Bioavailability of diclofenac after intramuscular administration to rats with experimental spinal cord injury. **J Pharmacol Toxicol Methods** **42**:99-101, 1999
32. Ge S, Pachter JS: Isolation and culture of microvascular endothelial cells from murine spinal cord. **J Neuroimmunol** **177**:209-214, 2006
33. Geisler FH, Coleman WP, Grieco G, Poonian D: The Sygen multicenter acute spinal cord injury study. **Spine (Phila Pa 1976)** **26**:S87-98, 2001
34. Gilman TM, Segal JL, Brunnemann SR: Metoclopramide increases the bioavailability of dantrolene in spinal cord injury. **J Clin Pharmacol** **36**:64-71, 1996

35. GM W: Cardiac output, in **Kinetics and Dynamics of intravenous anesthetics**: Kluwer Academic, London, 1992, pp 188-226
36. Groeneveld GJ, Van Kan HJ, Kalmijn S, Veldink JH, Guchelaar HJ, Wokke JH, et al: Riluzole serum concentrations in patients with ALS: associations with side effects and symptoms. **Neurology** **61**:1141-1143, 2003
37. Guizar-Sahagun G, Castaneda-Hernandez G, Garcia-Lopez P, Franco-Bourland R, Grijalva I, Madrazo I: Pathophysiological mechanisms involved in systemic and metabolic alterations secondary to spinal cord injury. **Proc West Pharmacol Soc** **41**:237-240, 1998
38. Guizar-Sahagun G, Velasco-Hernandez L, Martinez-Cruz A, Castaneda-Hernandez G, Bravo G, Rojas G, et al: Systemic microcirculation after complete high and low thoracic spinal cord section in rats. **J Neurotrauma** **21**:1614-1623, 2004
39. Hadley MN, Walters BC, Grabb PA, Oyesiku NM, Przybylski GJ, Resnick DK, et al: Guidelines for the management of acute cervical spine and spinal cord injuries. **Clin Neurosurg** **49**:407-498, 2002
40. Harrop JS, Naroji S, Maltenfort MG, Ratliff JK, Tjoumakaris SI, Frank B, et al: Neurologic improvement after thoracic, thoracolumbar, and lumbar spinal cord (conus medullaris) injuries. **Spine (Phila Pa 1976)** **36**:21-25
41. Hawryluk GW, Rowland J, Kwon BK, Fehlings MG: Protection and repair of the injured spinal cord: a review of completed, ongoing, and planned clinical trials for acute spinal cord injury. **Neurosurg Focus** **25**:E14, 2008
42. Hayes KC, Potter PJ, Hansebout RR, Bugaresti JM, Hsieh JT, Nicosia S, et al: Pharmacokinetic studies of single and multiple oral doses of fampridine-SR (sustained-release 4-aminopyridine) in patients with chronic spinal cord injury. **Clin Neuropharmacol** **26**:185-192, 2003
43. Hayes KC, Potter PJ, Hsieh JT, Katz MA, Blight AR, Cohen R: Pharmacokinetics and safety of multiple oral doses of sustained-release 4-aminopyridine (Fampridine-SR) in subjects with chronic, incomplete spinal cord injury. **Arch Phys Med Rehabil** **85**:29-34, 2004
44. Heurteaux C, Laigle C, Blondeau N, Jarretou G, Lazdunski M: Alpha-linolenic acid and riluzole treatment confer cerebral protection and improve survival after focal brain ischemia. **Neuroscience** **137**:241-251, 2006
45. Hijazi Y, Bodonian C, Bolon M, Salord F, Bouliou R: Pharmacokinetics and haemodynamics of ketamine in intensive care patients with brain or spinal cord injury. **Br J Anaesth** **90**:155-160, 2003

46. Hill CE, Beattie MS, Bresnahan JC: Degeneration and sprouting of identified descending supraspinal axons after contusive spinal cord injury in the rat. **Exp Neurol** **171**:153-169, 2001
47. Ho CH, Wuermsler LA, Priebe MM, Chiodo AE, Scelza WM, Kirshblum SC: Spinal cord injury medicine. 1. Epidemiology and classification. **Arch Phys Med Rehabil** **88**:S49-54, 2007
48. Hugon J: Riluzole and ALS therapy. **Wien Med Wochenschr** **146**:185-187, 1996
49. Ibarra A, Guizar-Sahagun G, Correa D, Kretschmer R, Grijalva I, Flores-Murrieta FJ, et al: Alteration of cyclosporin-A pharmacokinetics after experimental spinal cord injury. **J Neurotrauma** **13**:267-272, 1996
50. Kakulas BA: Neuropathology: the foundation for new treatments in spinal cord injury. **Spinal Cord** **42**:549-563, 2004
51. Katoh S, Masry WS: Motor recovery of patients presenting with motor paralysis and sensory sparing following cervical spinal cord injuries. **Paraplegia** **33**:506-509, 1995
52. Keane RW, Kraydieh S, Lotocki G, Alonso OF, Aldana P, Dietrich WD: Apoptotic and antiapoptotic mechanisms after traumatic brain injury. **J Cereb Blood Flow Metab** **21**:1189-1198, 2001
53. Lacomblez L, Bensimon G, Leigh PN, Guillet P, Meininger V: Dose-ranging study of riluzole in amyotrophic lateral sclerosis. Amyotrophic Lateral Sclerosis/Riluzole Study Group II. **Lancet** **347**:1425-1431, 1996
54. Landwehrmeyer GB, Dubois B, de Yebenes JG, Kremer B, Gaus W, Kraus PH, et al: Riluzole in Huntington's disease: a 3-year, randomized controlled study. **Ann Neurol** **62**:262-272, 2007
55. Lang-Lazdunski L, Heurteaux C, Vaillant N, Widmann C, Lazdunski M: Riluzole prevents ischemic spinal cord injury caused by aortic crossclamping. **J Thorac Cardiovasc Surg** **117**:881-889, 1999
56. Lavezo LA, Davis RL: Vancomycin pharmacokinetics in spinal cord injured patients: a comparison with age-matched, able-bodied controls. **J Spinal Cord Med** **18**:233-235, 1995
57. Le Liboux A, Cachia JP, Kirkesseli S, Gautier JY, Guimart C, Montay G, et al: A comparison of the pharmacokinetics and tolerability of riluzole after repeat dose administration in healthy elderly and young volunteers. **J Clin Pharmacol** **39**:480-486, 1999

58. Le Liboux A, Lefebvre P, Le Roux Y, Truffinet P, Aubeneau M, Kirkesseli S, et al: Single- and multiple-dose pharmacokinetics of riluzole in white subjects. **J Clin Pharmacol** **37**:820-827, 1997
59. Lou J, Lenke LG, Ludwig FJ, O'Brien MF: Apoptosis as a mechanism of neuronal cell death following acute experimental spinal cord injury. **Spinal Cord** **36**:683-690, 1998
60. Maltese A, Maugeri F, Drago F, Bucolo C: Simple determination of riluzole in rat brain by high-performance liquid chromatography and spectrophotometric detection. **J Chromatogr B Analyt Technol Biomed Life Sci** **817**:331-334, 2005
61. Mann GE, Zlokovic BV, Yudilevich DL: Evidence for a lactate transport system in the sarcolemmal membrane of the perfused rabbit heart: kinetics of unidirectional influx, carrier specificity and effects of glucagon. **Biochim Biophys Acta** **819**:241-248, 1985
62. Marino RJ, Barros T, Biering-Sorensen F, Burns SP, Donovan WH, Graves DE, et al: International standards for neurological classification of spinal cord injury. **J Spinal Cord Med** **26 Suppl 1**:S50-56, 2003
63. Marino RJ, Graves DE: Metric properties of the ASIA motor score: subscales improve correlation with functional activities. **Arch Phys Med Rehabil** **85**:1804-1810, 2004
64. Mathias CJ, Naik RB, Warren DJ, Frankel HL: Autonomic neuropathy. **Arch Intern Med** **143**:1635, 1983
65. McDonald JW, Becker D, Sadowsky CL, Jane JA, Sr., Conturo TE, Schultz LM: Late recovery following spinal cord injury. Case report and review of the literature. **J Neurosurg** **97**:252-265, 2002
66. Mestre H, Alkon T, Salazar S, Ibarra A: Spinal cord injury sequelae alter drug pharmacokinetics: an overview. **Spinal Cord** **49**:955-960, 2011
67. Milane A, Fernandez C, Vautier S, Bensimon G, Meininger V, Farinotti R: Minocycline and riluzole brain disposition: interactions with p-glycoprotein at the blood-brain barrier. **J Neurochem** **103**:164-173, 2007
68. Milane A, Tortolano L, Fernandez C, Bensimon G, Meininger V, Farinotti R: Brain and plasma riluzole pharmacokinetics: effect of minocycline combination. **J Pharm Pharm Sci** **12**:209-217, 2009

69. Miller RG, Mitchell JD, Lyon M, Moore DH: Riluzole for amyotrophic lateral sclerosis (ALS)/motor neuron disease (MND). **Cochrane Database Syst Rev**:CD001447, 2007
70. Mu X, Azbill RD, Springer JE: Riluzole and methylprednisolone combined treatment improves functional recovery in traumatic spinal cord injury. **J Neurotrauma** **17**:773-780, 2000
71. Norenberg MD, Smith J, Marcillo A: The pathology of human spinal cord injury: defining the problems. **J Neurotrauma** **21**:429-440, 2004
72. Pan W, Banks WA, Kastin AJ: Permeability of the blood-brain and blood-spinal cord barriers to interferons. **J Neuroimmunol** **76**:105-111, 1997a
73. Pan W, Banks WA, Kastin AJ: Blood-brain barrier permeability to ebitatide and TNF in acute spinal cord injury. **Exp Neurol** **146**:367-373, 1997b
74. Park E, Velumian AA, Fehlings MG: The role of excitotoxicity in secondary mechanisms of spinal cord injury: a review with an emphasis on the implications for white matter degeneration. **J Neurotrauma** **21**:754-774, 2004
75. Perdiki M, Farooque M, Holtz A, Li GL, Olsson Y: Expression of endothelial barrier antigen immunoreactivity in blood vessels following compression trauma to rat spinal cord. Temporal evolution and relation to the degree of the impact. **Acta Neuropathol** **96**:8-12, 1998
76. Popovich PG, Wei P, Stokes BT: Cellular inflammatory response after spinal cord injury in Sprague-Dawley and Lewis rats. **J Comp Neurol** **377**:443-464, 1997
77. Potter PJ, Hayes KC, Hsieh JT, Delaney GA, Segal JL: Sustained improvements in neurological function in spinal cord injured patients treated with oral 4-aminopyridine: three cases. **Spinal Cord** **36**:147-155, 1998
78. Prockop LD, Naidu KA, Binard JE, Ransohoff J: Selective permeability of [3H]-D-mannitol and [14C]-carboxyl-inulin across the blood-brain barrier and blood-spinal cord barrier in the rabbit. **J Spinal Cord Med** **18**:221-226, 1995
79. Reihani-Kermani H, Ansari M, Karamousian S: The influence of experimental spinal cord injury on carbamazepine pharmacokinetics. **Arch Iran Med** **9**:231-235, 2006
80. Rosenberg LJ, Teng YD, Wrathall JR: Effects of the sodium channel blocker tetrodotoxin on acute white matter pathology after experimental contusive spinal cord injury. **J Neurosci** **19**:6122-6133, 1999

81. Rowland JW, Hawryluk GW, Kwon B, Fehlings MG: Current status of acute spinal cord injury pathophysiology and emerging therapies: promise on the horizon. **Neurosurg Focus** **25**:E2, 2008
82. Rowland M TT: Physiology concepts and kinetics, in **Clinical Pharmacokinetics Concepts and Applications**: Lea and Febiger, USA, 1989, pp 103-177
83. Schanne FA, Kane AB, Young EE, Farber JL: Calcium dependence of toxic cell death: a final common pathway. **Science** **206**:700-702, 1979
84. Schwartz G, Fehlings MG: Evaluation of the neuroprotective effects of sodium channel blockers after spinal cord injury: improved behavioral and neuroanatomical recovery with riluzole. **J Neurosurg** **94**:245-256, 2001
85. Schwartz G, Fehlings MG: Secondary injury mechanisms of spinal cord trauma: a novel therapeutic approach for the management of secondary pathophysiology with the sodium channel blocker riluzole. **Prog Brain Res** **137**:177-190, 2002
86. Segal JL, Brunnemann SR: Clinical pharmacokinetics in patients with spinal cord injuries. **Clin Pharmacokinet** **17**:109-129, 1989
87. Segal JL, Brunnemann SR, Eitorai IM, Vulpe M: Decreased systemic clearance of lorazepam in humans with spinal cord injury. **J Clin Pharmacol** **31**:651-656, 1991
88. Segal JL, Brunnemann SR, Gordon SK, Eitorai IM: The absolute bioavailability of oral theophylline in patients with spinal cord injury. **Pharmacotherapy** **6**:26-29, 1986
89. Segal JL, Gray DR, Gordon SK, Eitorai IM, Khonsari F, Patel J: Gentamicin disposition kinetics in humans with spinal cord injury. **Paraplegia** **23**:47-55, 1985
90. Segal JL, Hayes KC, Brunnemann SR, Hsieh JT, Potter PJ, Pathak MS, et al: Absorption characteristics of sustained-release 4-aminopyridine (fampridine SR) in patients with chronic spinal cord injury. **J Clin Pharmacol** **40**:402-409, 2000
91. Segal JL, Maltby BF, Langdorf MI, Jacobson R, Brunnemann SR, Jusko WJ: Methylprednisolone disposition kinetics in patients with acute spinal cord injury. **Pharmacotherapy** **18**:16-22, 1998
92. Sekhon LH, Fehlings MG: Epidemiology, demographics, and pathophysiology of acute spinal cord injury. **Spine (Phila Pa 1976)** **26**:S2-12, 2001
93. Shargel L W-PS, Yu A: in **Applied Biopharmaceutics and Pharmacokinetics**. Singapore McGraw-Hill, 2005, pp 107-130

94. Stone JM, Nino-Murcia M, Wolfe VA, Perlash I: Chronic gastrointestinal problems in spinal cord injury patients: a prospective analysis. **Am J Gastroenterol** **85**:1114-1119, 1990
95. Stys PK: White matter injury mechanisms. **Curr Mol Med** **4**:113-130, 2004
96. Tator CH, Fehlings MG: Review of the secondary injury theory of acute spinal cord trauma with emphasis on vascular mechanisms. **J Neurosurg** **75**:15-26, 1991
97. Tator CH: Update on the pathophysiology and pathology of acute spinal cord injury. **Brain Pathol** **5**:407-413, 1995
98. Tator CH, Koyanagi I: Vascular mechanisms in the pathophysiology of human spinal cord injury. **J Neurosurg** **86**:483-492, 1997
99. Tietze KJ, Putcha L: Factors affecting drug bioavailability in space. **J Clin Pharmacol** **34**:671-676, 1994
100. Van Kan HJ, Spieksma M, Groeneveld GJ, Torano JS, van den Berg LH, Guchelaar HJ: A validated HPLC assay to monitor riluzole plasma or serum concentrations in patients with amyotrophic lateral sclerosis. **Biomed Chromatogr** **18**:723-726, 2004
101. Vertiz-Hernandez A, Castaneda-Hernandez G, Martinez-Cruz A, Cruz-Antonio L, Grijalva I, Guizar-Sahagun G: L-arginine reverses alterations in drug disposition induced by spinal cord injury by increasing hepatic blood flow. **J Neurotrauma** **24**:1855-1862, 2007
102. Wang SJ, Wang KY, Wang WC: Mechanisms underlying the riluzole inhibition of glutamate release from rat cerebral cortex nerve terminals (synaptosomes). **Neuroscience** **125**:191-201, 2004
103. Winkler EA, Bell RD, Zlokovic BV: Central nervous system pericytes in health and disease. **Nat Neurosci** **14**:1398-1405, 2011
104. Wong YW, Tam S, So KF, Chen JY, Cheng WS, Luk KD, et al: A three-month, open-label, single-arm trial evaluating the safety and pharmacokinetics of oral lithium in patients with chronic spinal cord injury. **Spinal Cord** **49**:94-98, 2011
105. Xiong Y, Rabchevsky AG, Hall ED: Role of peroxynitrite in secondary oxidative damage after spinal cord injury. **J Neurochem** **100**:639-649, 2007
106. Yang ML, Li JJ, So KF, Chen JY, Cheng WS, Wu J, et al: Efficacy and safety of lithium carbonate treatment of chronic spinal cord injuries: a double-blind, randomized, placebo-controlled clinical trial. **Spinal Cord** **50**:141-146, 2012

107. Yong C, Arnold PM, Zoubine MN, Citron BA, Watanabe I, Berman NE, et al: Apoptosis in cellular compartments of rat spinal cord after severe contusion injury. **J Neurotrauma** **15**:459-472, 1998
108. Zlokovic BV, Apuzzo ML: Cellular and molecular neurosurgery: pathways from concept to reality--part I: target disorders and concept approaches to gene therapy of the central nervous system. **Neurosurgery** **40**:789-803; discussion 803-784, 1997
109. Zlokovic BV: The blood-brain barrier in health and chronic neurodegenerative disorders. **Neuron** **57**:178–201, 2008
110. Zlokovic BV: Neurovascular pathways to neurodegeneration in Alzheimer's disease and other disorders. **Nat Rev Neurosci** **12**:723-738, 2011